Annual Report
Jahresbericht

2017

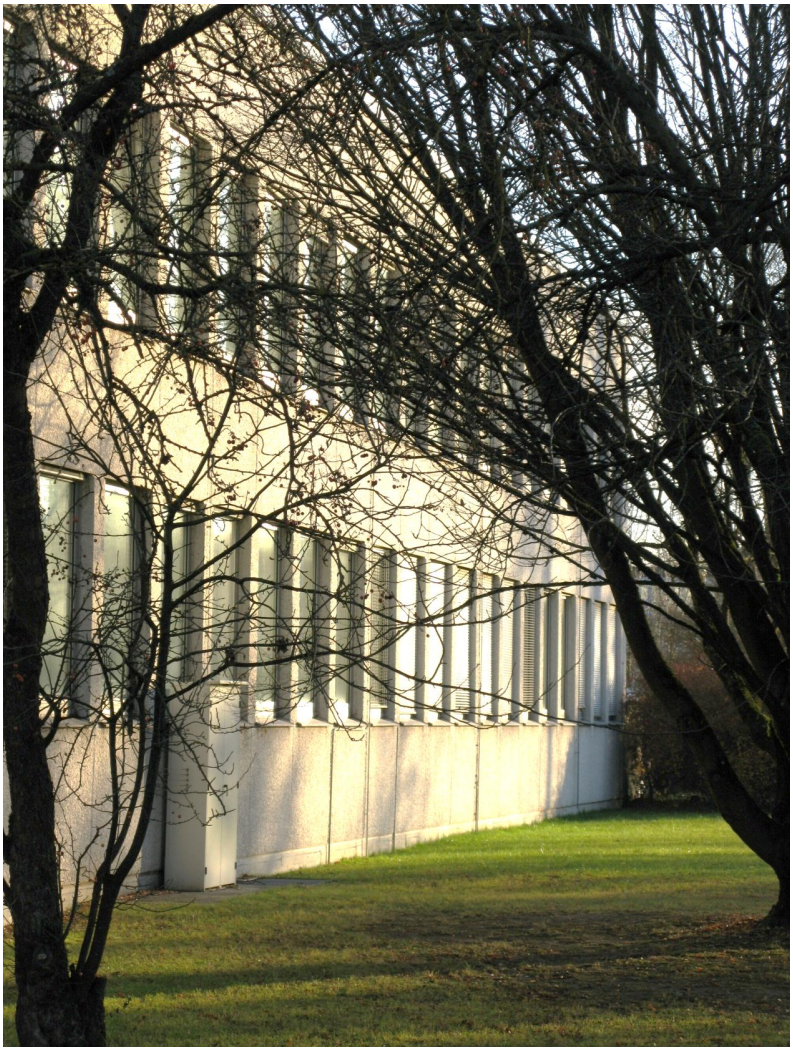

Walther–Meißner–Institut
für Tieftemperaturforschung

Bayerische Akademie der Wissenschaften

Contact:

Prof. Dr. Rudolf Gross
Walther–Meißner–Institut für Tieftemperaturforschung
Bayerische Akademie der Wissenschaften
and
Lehrstuhl für Technische Physik – E23
Technische Universität München

Address:

Walther–Meißner–Str. 8
D - 85748 Garching
GERMANY

Phone: +49 – (0)89 289 14201
Fax: +49 – (0)89 289 14206
e–mail: Rudolf.Gross@wmi.badw.de
www: http://www.wmi.badw.de

Secretary's Office and Administration:

Emel Dönertas

Phone: +49 – (0)89 289 14202
Fax: +49 – (0)89 289 14206
e–mail: Emel.Doenertas@wmi.badw.de
Sekretariat@wmi.badw.de

Ludwig Ossiander

Phone: +49 – (0)89 289 14205
Fax: +49 – (0)89 289 14206
e–mail: Ludwig.Ossiander@wmi.badw.de
Verwaltung@wmi.badw.de

Preface

Dear colleagues, friends, partners, and alumni of the Walther-Meißner-Institute for Low Temperature Research (WMI) of the Bavarian Academy of Sciences and Humanities (BAdW)! Our ***Annual Report 2017*** intends to provide you with an overview of our last year's scientific activities. It also contains some statistical data, an overview of our teaching and public outreach activities, and information on recent developments in infrastructure and experimental facilities.

The year 2017 was characterized by extensive construction work aiming at general redevelopment measures regarding the technical infrastructure, safety requirements and energy efficiency of the WMI building (see page 11–15). Although this construction work was quite perturbing, our research activities have been continued and resulted in a large number of high level publications (see page 93). We have also been successful in acquiring new extramural funding (see page 109) and continued our participation in several coordinated research programs and graduate schools on the European and national level (see page 109) as well as our fruitful collaborations with international research institutions and industry (see page 117). The high impact of our research work is documented by more than 2 000 citations of WMI publications in 2017 (ISI Web of Science) and a large number of invited conference, colloquium and seminar talks (see page 121). As in previous years, WMI was active in organizing symposia, workshops and conferences (see page 113).

An important activity in 2017 was the application for a new Cluster of Excellence within the ***German Excellence Strategy***, aiming at strengthening Germany's position as an outstanding place for research and further improving its international competitiveness. As the research activities on quantum nanoscience within Research Area 1 (coordinator: R. Gross) of the present Cluster of Excellence ***Nanosystems Initiative Munich (NIM)*** have been growing and broadening considerably and both Munich universities as well as the Max Planck Institute of Quantum Optics and WMI consider quantum science & technology strategic research fields, the application for a new Cluster of Excellence with this focus was mandatory (see page 19–23). WMI plays a key role in the application process of this cluster named ***Munich Center for Quantum Science and Technology (MCQST)*** with Rudolf Gross being one of the three spokespersons (together with Immanuel Bloch and Ignacio Cirac). A preproposal was submitted in March 2017 and has been positively evaluated by an international review panel. Presently, the full proposal (submission deadline: February 21, 2018) is prepared and a preliminary version already has been forwarded to the Boards of Management of LMU and TUM just before Christmas. The strong involvement of WMI in the MCQST is a natural continuation of its strong research focus on solid state-based quantum systems and its active participation in several projects related to quantum science & technology (see page 24–27). These include the ***«Munich Quantum Center» (MQC)***, the International Ph.D. School of Excellence ***«Exploring Quantum Matter» (ExQM)*** within the ***Elite-Netzwerk Bayern***, and the International Max Planck Research School ***«Quantum Science and Technology» (IMPRS-QST)***. Finally, WMI contributes to the structuring of the planned BMBF program ***«Quantentechnologie: Grundlagen und Anwendungen» (QUTEGA)*** with Rudolf Gross of WMI being member of the QUTEGA committee. QUTEGA will go hand in hand with the ***EU Quantum Technology Flagship*** which is presently in its ramp-up phase.

Beyond the already mentioned quantum science & technology related projects, WMI acquired third party funding in other research fields. The ***Transregional Collaborative Research Center «From Electronic Correlations to Functionality» (TRR 80)*** was reviewed in 2017 and was granted a third funding period from 01/2018 to 12/2021 (see page 28). Moreover, the new EU Collaborative Project ***«Magnetomechanical Platforms for Quantum Experiments and Quantum Enabled Sensing Technologies» (MaQSens)*** started in January 2017 and a new DFG Re-

search Project on ***Direct and Inverse Spin-Orbit Torques*** has been granted. Looking ahead, there are several research proposals in the pipeline. For example, WMI submitted two proposals within the new ***DFG Priority Program 2137 «Skyrmionics: Topological Spin Phenomena in Real-Space for Applications»*** which will be reviewed in January 2018.

The year 2017 was particularly successful regarding the improvement of the technological infrastructure. First, within the DFG Major Research Instrumentation Program WMI could buy a state-of-the-art UHV sputter deposition system for superconducting and magnetic materials (see page 67–70). Second, supported by the BMBF research network ***Quantum Communication (Q.com)*** a critical point dryer and a versatile laser writing systems could be acquired, considerably extending the WMI facilities for micro- and nano-patterning. Third, the Bavarian Ministry for Science and Arts granted more than 5 Mio. Euro to WMI for redevelopment measures, including the improvement and replacement of important technical infrastructure. This infrastructure project has been started in May 2017 and will hopefully be completed until summer 2018 (see page 11–15).

In 2017, the scientific, technical and administrative staff of WMI strongly suffered from noise and unforseen rearrangements related to the ongoing construction work. Nevertheless, due to the strong commitment and persistence of everybody most of our ambitious research programs could be implemented. In this context, I would like to thank all members of WMI for the inexhaustible patience, understanding and support! Moreover, despite the unfavorable circumstances, 10 bachelor, 15 master and 3 PhD theses were completed, while 16 master and 16 PhD students as well as 3 habilitation candidates are still ongoing with their work (see page 101). The research program of WMI relies on the continuous support by various funding agencies. To this end, we gratefully acknowledge financial support from the BAdW, the DFG, the Bavarian Ministry for Science and Arts, the BMBF and the EU. An important key to success is the recruitment of outstanding, scientifically independent group leaders with complementary research interests and technical expertise. This process is monitored by the Scientific Advisory Board of WMI which has a strong commitment to support and promote young scientists in their career.

Finally, I would like to thank all colleagues, guests, students, postdocs and cooperating partners, who contributed to our research and teaching activities within the past year, and last but not least all our friends and sponsors for their interest, trust and continuous support. I hope that our Annual Report 2017 inspires your interest in WMI.

Garching, December 2017

Rudolf Gross

Contents

The Walther–Meißner–Institute

General Information

The ***Walther-Meißner-Institute for Low Temperature Research (WMI)*** was originally operated by the Commission for Low Temperature Research of the ***Bavarian Academy of Sciences and Humanities (BAdW)***. Between 2013 and 2015, the Bavarian Academy of Sciences and Humanities with its more than 300 employees was reorganized. With the passing of the new statutes in October 2015, the 36 Commissions (Research Groups) of the Academy — they were originally set up in order to carry out long-term projects, which are too ambitious for the lifetime or capacity of any single researcher, or which require the collaboration of specialists in various disciplines — were abolished. The research program of BAdW is now implemented in Academy Institutes (such as the Walther-Meißner-Institute or the Leibniz Supercomputing Center) and Academy Projects. The Academy Institutes and Projects are managed by the Institute and Project Committees and supervised by the Institute and Project Advisory Boards, respectively. In this way a clear separation between the managing bodies of the institutes/projects (responsible for the implementation of the research programs) and the corresponding supervisory bodies (responsible for the quality control) was established. To this end, also the Commission for Low Temperature Research was dissolved and replaced by the WMI Committee and the WMI Advisory Board in 2015.

The historical roots of WMI go back to ***Walther Meißner***. He founded the Commission for Low Temperature Research in 1946 when he was president of BAdW (1946 – 1950). The first research activities then were started in 1946 in the Herrsching barracks. After the retirement of Walther Meißner in 1952, Heinz Maier-Leibnitz, who followed Walther Meißner on the Chair for Technical Physics of the Technische Universität München, became the new head of the Commission for Low Temperature Research. In 1967, the commission moved to the Garching research campus after the construction of the new "Zentralinstitut für Tieftemperaturforschung (ZTTF)" was completed (director: Prof. Heinz Maier-Leibnitz, technical director: Prof. Franz Xaver Eder). Until 1972, the theory group of the Institute Laue Langevin was hosted at the ZTTF with prominent members such as Peter Fulde. In 1980, Prof. Dr. Klaus Andres became the new director of the ZTTF again associated with the Chair for Technical Physics (E23) at the Technical University of Munich (TUM), followed by Prof. Dr. Rudolf Gross in 2000. In 1982, the ZTTF was renamed into Walther-Meißner-Institute for Low Temperature Research (WMI) on the occasion of Walther Meißner's 100. birthday.

Starting from 2000, the so far unused basement of the WMI building was made available for technical infrastructure (airconditioning, particulate airfilters, pure water system etc. for clean room) and additional laboratory space. Fortunately, in 2008 WMI succeeded in getting extra money from the state government within the so-called "Konjunkturpaket II". This money has been used to establish the new "WMI Quantum Science Laboratory" in the basement of the building, providing about 150 m^2 additional laboratory space particularly suited for low temperature facilities and ultra-sensitive studies on solid state quantum systems. The WMI Quantum Science Laboratory was fully operational early in 2011 and meanwhile hosts three new mK systems and sophisticated experimental techniques for the study of solid state based quantum systems and circuits.

As already mentioned, it is a long tradition that WMI hosts the Chair for Technical Physics (E 23) of TUM with the director of the WMI being a full professor at the Faculty of Physics of TUM. However, there are also close ties with the Ludwig-Maximilians-University (LMU). Between 2004 and 2010, WMI hosted a scanning probe division with the head of this division being a professor at LMU. In this way a tight collaboration has been established between WMI and research groups of both Munich universities, joining technological and human resources

in the fields of experimental and theoretical solid-state and condensed matter physics, low temperature techniques, materials science as well as thin film and nanotechnology. Noteworthy, the WMI supplies liquid helium to more than 25 research groups at both Munich universities and provides the technological basis for low temperature research. In 2016, the Bavarian Ministry for Science and Arts granted more than 5 Mio. Euro for redevelopment measures regarding the technical infrastructure, safety requirements and energy efficiency. An important part of the building project is the reconstruction of the entrance area, providing then direct access to the new WMI Quantum Laboratories in the basement of the WMI building and additional meeting rooms. Moreover, it includes the replacement of all windows, the upgrade of the technical infrastructure for cooling water, air conditioning, liquid nitrogen and helium storage, as well as various safety measures.

Research Activities

The research activities of the Walther-Meißner-Institute are focused on low temperature condensed matter physics (see reports below). The research program is devoted to both **fundamental** and **applied research** and also addresses **materials science, thin film and nanotechnology** aspects. With respect to **basic research** the main focus of the WMI is on

- superconductivity and superfluidity,
- magnetism, including spin transport, spin dynamics, spin mechanics and spin caloritronics,
- quantum phenomena and quantum coherence in mesoscopic systems and solid state nanostructures,
- circuit quantum electrodynamics and circuit electro-nanomechanics,
- ordering and emergent phenomena in correlated quantum matter,
- and the general properties of metallic systems at low and very low temperatures.

The WMI also conducts **applied research** in the fields of

- solid-state quantum information processing systems,
- superconducting and spintronic devices,
- oxide electronics,
- multi-functional and multiferroic materials,
- and the development of low and ultra-low temperature systems and techniques.

With respect to **materials science, thin film and nanotechnology** the research program is focused on

- the synthesis of superconducting and magnetic materials,
- the single crystal growth of oxide materials,
- the thin film technology of complex superconducting and magnetic heterostructures, including multi-functional and multi-ferroic material systems,
- and the fabrication of superconducting, magnetic and hybrid nanostructures.

The WMI also develops and operates systems and techniques for low and ultra–low temperature experiments. A successful development have been dry mK-systems that can be operated without liquid helium by using a pulse-tube refrigerator for precooling. In the early 2000s, these systems have been successfully commercialized by the company VeriCold Technologies GmbH at Ismaning, Germany, which was taken over by Oxford Instruments in 2007. As a further typical example we mention very flexible dilution refrigerator inserts for temperatures down to about 20 mK fitting into a 2 inch bore. These systems have been engineered and fabricated at WMI. Within the last years, several dilution refrigerators have been provided to other research groups for various low temperature experiments. WMI also operates a helium

liquifier with an annual capacity of above 180.000 liters and supplies both Munich universities with liquid helium. To optimize the transfer of liquid helium into transport containers, WMI has developed a pumping system for liquid helium that is commercialized in collaboration with a company.

To a large extent the research activities of WMI are integrated into national and international research projects such as Clusters of Excellence, Collaborative Research Centers, Research Units, or EU projects. The individual research groups of WMI offer a wide range of attractive research opportunities for bachelor and master students, Ph.D. students and postdoctoral fellows.

Experimental Facilities and Resources

The WMI is equipped with state of the art facilities for the preparation and characterization of superconducting and magnetic materials as well as for various low and ultra–low temperature experiments. The main experimental and technological resources of WMI are listed in the following.

Materials Preparation and Fabrication of Nanostructures

- Laser Molecular Beam Epitaxy (L-MBE) system for oxide heterostructures (equipped with in–situ RHEED, Omicron AFM/STM system, atomic oxygen/nitrogen source, infrared-laser heating system, metallization)
- molecular beam epitaxy (MBE) system for metals
- UHV magnetron sputtering systems for metals (e.g. Nb, Al, NiPd, ...)
- UHV cluster tools consisting of two magnetron sputter deposition systems for superconducting and magnetic heterostructures and a load lock
- reactive ion etching (RIE) system, Plasmalab 80 Plus with ICP plasma source, Oxford Instruments Plasma Technology
- ion beam etching (IBE) system equipped with a LN_2 cooled sample holder
- automated critical point dryer Leica EM CPD 300
- polishing machine for substrate preparation
- ultrasonic bonding machine
- 50 m^2 class 1000 clean room facility
- maskless lithography UV Direct Laser Writer, SPS PicoMaster 200 UV
- 100 kV nB5 Electron Beam Lithography System by NanoBeam Limited, UK, with 6 inch laser stage
- optical lithography (Süss maskaligner MJB 3 and projection lithography)
- four-mirror image furnace for crystal growth

Characterization

- 2–circle x–ray diffractometer (Bruker D8 Advance, sample temperature up to 1 600°C)
- high resolution 4–circle x–ray diffractometer with Göbel mirror and Ge monochromator (Bruker D8 Discover)
- Philips XL 30 SFEG scanning electron microscope with EDX analysis
- UHV room temperature AFM/STM system
- two Raman spectroscopy systems (1.5 to 300 K, in-situ sample preparation)
- tip-enhanced Raman spectroscopy (TERS) system
- SQUID magnetometer (Quantum Design, 1.5 to 700 K, up to 7 T)
- several high field magnet systems (up to 17 T Tesla) with variable temperature inserts

- 7 T split coil magnet systems with optical access and variable temperature insert
- 3D vector magnet (2/2/6 Tesla) with variable temperature inserts
- experimental set–ups for the measurement of noise including low noise SQUID amplifiers and signal analyzers
- high-frequency network analyzers (up to 40 GHz) and various microwave components (sources, mixers, circulators, attenuators) for the determination of high frequency parameters
- ultra-sensitive microwave receiver for state tomography of quantum microwaves (dual path method with FPGA signal processing)
- high-frequency cryogenic probing station (up to 20 GHz, $T > 4$ K)
- magnetooptical Kerr effect (MOKE) system
- broadband ferromagnetic resonance (FMR) system

Low temperature systems and techniques

- several ^{3}He/^{4}He dilution refrigerator inserts for temperatures down to 10 mK
- "dry" mK-cooler based on a dilution refrigerator with pulse-tube precooling and equipped with a large number of microwave lines and cold electronics (e.g. amplifiers, circulators, attenuators, directional couplers) for ultra-sensitive experiments on solid state quantum systems
- "dry" dilution refrigerator with a base temperature of about 10 mK equipped with a 3D vector magnet (1/1/6 Tesla)
- "wet" mK-cooler based on a dilution refrigerator liquid helium precooling and equipped with a large number of microwave lines and cold electronics (e.g. amplifiers, circulators, attenuators, beam splitters) for time-domain microwave experiments on solid state quantum systems
- experimental set–ups for the measurement of specific heat, magnetization, thermal expansion as well as electrical and thermal transport properties as a function of temperature, magnetic field and pressure

Building Projects

General Redevelopment of the Technical Infrastructure

Rudolf Gross

The Bavarian Ministry for Science and Arts granted 5.8 Mio. Euro to the Walther-Meißner-Institute (WMI) for general redevelopment measures regarding the technical infrastructure, safety requirements and energy efficiency. The planning stage of this building project was completed late in 2016 and the construction work started in May 2017. The building project includes the following specific measures:

- extension of the main staircase of the WMI building to the basement and redesignment of the front entrance
- replacement of all windows and office/laboratory doors
- equipping the WMI laboratories with air conditioning systems
- installation of a new chemical laboratory
- redevelopment and replacement of the helium recovery system and the liquid nitrogen tank
- installation of a new transformer station for increasing the power handling capability of the electric power system.

The initial plan was to finish the building project until Christmas 2017. However, due to a significant lack in coordination, missing professionalism of the involved companies and unforseen delays due to technical reasons, a total delay of more than five months has been accumulated so far. This is quite unfortunate for the WMI research activities, as laboratory rooms could not be used for an extended period and our experiments have been often perturbed by the ongoing construction work. Although this is nerve-shattering for everybody at present, the ongoing building project will have a large future benefit for WMI and therefore it was mandatory to tackle it.

Historical Context

The first redevelopment of the WMI building which has been established in 1967 took place between 2000 and 2003. At that time besides the general renovation of most office and laboratory rooms the key measures have been

- the installation of the WMI clean room and thin film laboratories
- the installation of the WMI crystal growth laboratory
- the redevelopment of the WMI seminar and library rooms
- the replacement of the electrical power system
- the installation of a glas fibre network.

Starting from 2000, the so far unused basement of the WMI building was made available for technical infrastructure (airconditioning, particulate airfilters, pure water system etc. for clean room) and additional laboratory space. However, the extension to the full basement was not possible due to the limited budget.

Fortunately, in 2008 WMI succeeded in getting extra money from the state government within the so-called «Konjunkturpaket II». This money has been used to establish the new «WMI Quantum Science Laboratory» in the basement of the building, providing about 150 m^2 additional laboratory space particularly suited for low temperature facilities and ultra-sensitive studies on solid state quantum systems. The WMI Quantum Science Laboratory was fully operational early in 2011 and meanwhile hosts three new mK systems and sophisticated experimental techniques for the study of solid state based quantum systems and circuits.

Although the basement of the WMI was fully usable already in 2011, the access to the basement via the main staircase at the north side of the WMI building was not possible. A temporary access was established via the safety exits at the east and west side of the building. This severe drawback will now be removed by the extension of the main staircase to basement.

Extension of the Main Staircase and Redesignment of the Front Entrance

Since the completion of the «WMI Quantum Science Laboratory» in 2011, the basement of the WMI building hosts a lot of laboratory space. Therefore, the extension of the main staircase down to the basement is urgently required. Since for the implementation of this measure the old staircase tower had to be torn down and replaced by a new structure, it was decided to combine the staircase extension with a general redesignment of the front entrance. As shown in Fig. 1 and 2 , this redesignment is accompanied by a change of the fire rescue path, allowing to make better use of the wide cross-aisles in the ground and first floor. A particular benefit will be new meeting rooms/areas on the ground floor level which have been urgently lacking and new changing room with showers for the technical staff. In addition, the aisles along the long side of the building receive new safety exits directly to the Walther-Meißner street and the main entrance is raised to avoid stairs inside the building.

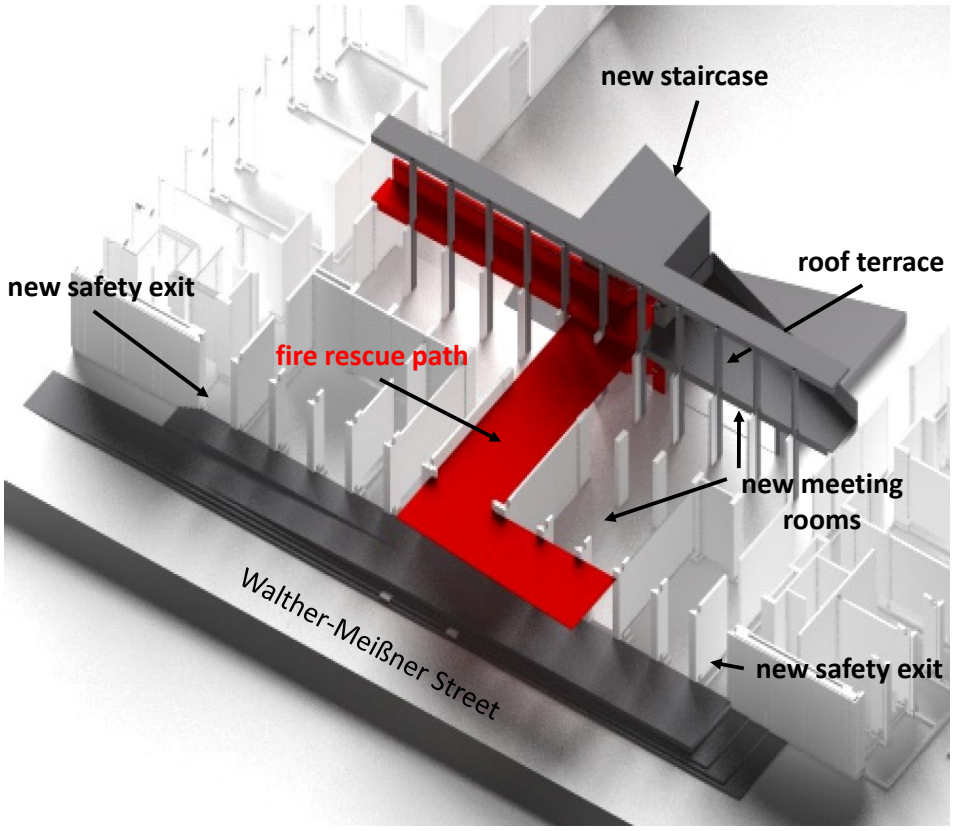

Figure 1: North end of the WMI building with the new front entrance and main staircase. The red area marks the fire rescue path which does no longer include the main aisles in the ground and first floor running parallel to the Walther-Meißner street. Therefore, in future these aisles can be used for sitting areas and meeting points. The ground floor aisles running perpendicular to the Walther-Meißner street obtain additional safety exits. The entrance level will be elevated to avoid stairs inside the building and make the main entrance suitable for the needs of people with disabilities.

Replacement of the Windows and Office/Laboratory Doors

The replacement of all windows in the WMI building has been almost completed in 2017. Only the aisle windows to the inner courtyard are missing. Besides a better thermal insulation the new windows have integrated venetian blinds and a small window part allowing for a permanent ventilation (e.g. during the night) what is particularly important in the hot

Figure 2: Top left: An artists view of the new main staircase of the WMI building. Top right: Cross-sectional view of the new main staircase. Bottom: View of the cross-aisle and the new stairway as seen from the inner courtyard.

summer period. The replacement of the doors of the laboratory and office rooms has been completed. However, cosmetic repair work still has to be done.

Airconditioning Systems for the Laboratory Rooms

The laboratory rooms of WMI have been equipped with airconditioning systems. This measure was urgently required and has been mostly completed until the end of 2017. First, the increased installed electrical power in some laboratories resulted in intolerable temperatures over the summer period. Second, an increasing number of sensitive experiments requires temperature stabilization.

For supplying the required cooling power, in spring 2018 a new refrigerating compressor will be installed in the basement at the south end of the WMI building. For this purpose the respective part of the basement has been redone and a new outside door has been introduced, which allows for an easy access to the basement area. This is particularly useful for the installation of the refrigerating compressor and other big machines. Moreover, new chillers will be installed on the roof of the WMI building. The reinforcement of the roof construction is already completed.

Installation of a New Chemical Laboratory

The chemical laboratory in the ground floor of the WMI building has been newly laid out (see Fig. 3) and rebuilt from scratch. Unfortunately, the involved engineers and companies did a bad job and the laboratory has not been completed as expected from the technical drawings.

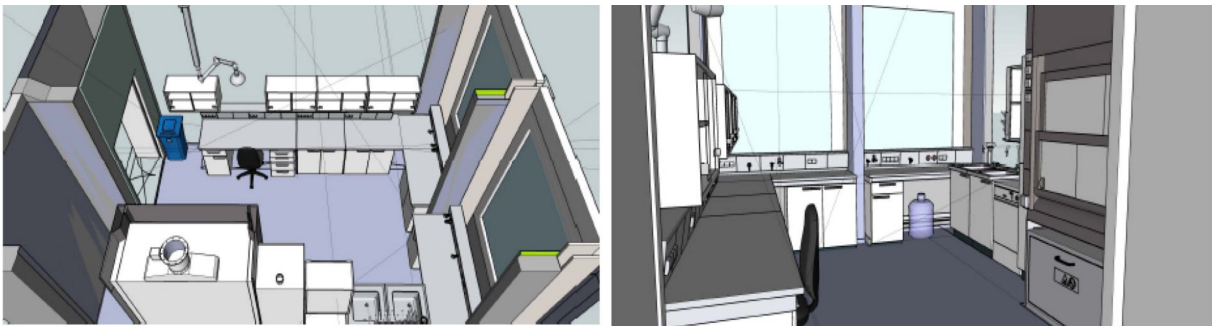

Figure 3: Technical drawing of the new chemical laboratory.

Replacement of the Helium Recovery System and the Liquid Nitrogen Tank

The replacement of the high pressure storage containers for the recovered helium gas and the liquid nitrogen tank has been completed and both systems are already in operation. Furthermore, new storage vessels for ultra-pure helium gas needed for the starting phase of the liquifier have been installed and are also in use. Due to the competent company taking care about this part, this measure was completed in time without significantly perturbing the helium liquefaction.

Installation of a New Transformer Station

The installation of a new transformer station for increasing the power handling capability of the WMI electric power system has been postponed until spring 2018. The change from a low to medium voltage connection will reduce the required cross-sectional area of the underground cable considerably and remove the problem of missing space in the cable duct.

Renovation and Modernization of the Mechanical Workshop

Rudolf Gross

The Mechanical Workshop of the Walther-Meißner-Institute has not been renovated since the completion of the WMI building in 1967. Therefore, it was high time to start redevelopment and modernization measures. Fortunately, the Bavarian Ministry for Science and Arts granted 400 kEuro for 2018/19 within a so-called «Kleine Baumaßnahme» to implement this plan. Key parts are

- the replacement of the workshop floor
- the replacement of the electrical power installation
- the movement of the stockroom into the basement
- the rearrangement of the machine park and the office of the workshop manager
- the partial replacement of the furnishings

Meanwhile, the planning of this measure has been almost completed. It also includes the replacement of the floor in the aisle in front of the workshop area. According to the present schedule, the complete measure will be implemented between February and May 2018.

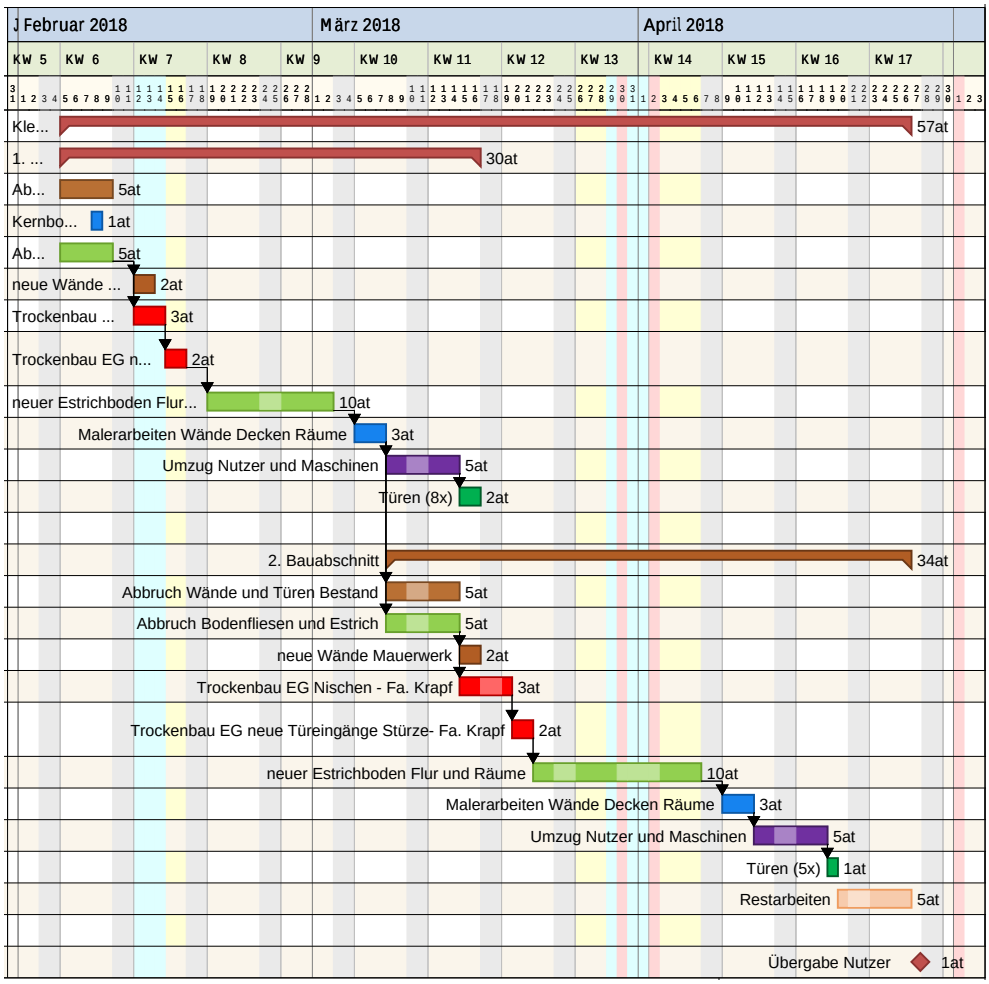

Figure 1: Schedule of the renovation and modernization measure of the mechanical workshop of WMI.

Joint Research Projects

Clusters of Excellence

Rudolf Gross

The past years were considerably influenced by the discussion of new proposals for Clusters of Excellence within the ***German Excellence Strategy***, which aims to strengthen Germany's position as an outstanding place for research and to further improve its international competitiveness. The *Excellence Strategy* is designed to continue the development of German universities successfully begun with the *Excellence Initiative* in 2005 by supporting research of the highest standard, enhancing research profiles, and facilitating cooperation in the research system. On the basis of the administrative agreement reached by the federal and state governments on 16 June 2016, the DFG and the German Council of Science and Humanities implements the Excellence Strategy in two funding lines:

1. **Clusters of Excellence** for project-based funding in internationally competitive fields of research at universities or university consortia,
2. **Universities of Excellence** to strengthen universities as individual institutions or as university consortia in the long term and further develop their leading international role on the basis of successful Clusters of Excellence.

A. The Cluster of Excellence «Nanosystems Initiative Munich» (NIM)

The Walther-Meißner-Institute (WMI) is a founding member of the Cluster of Excellence ***«Nanosystems Initiative Munich» (NIM)*** which was established in 2006 within the ***German Excellence Initiative***. After a successful first funding period (10/2006 – 09/2012), a second five-year funding period (10/2012 – 09/2017) was granted. Recently, this second funding period has been extended until December 2018 to guarantee a smooth transition to the new program named ***«Excellence Strategy»*** starting from 2019.

Regarding the future of the present Cluster of Excellence ***«Nanosystems Initiative Munich» (NIM)*** there have been two possible options for the upcoming Excellence Strategy: (i) applying for a third funding period of NIM with an updated research strategy or (ii) applying for a new Cluster of Excellence with new research directions having overlap with particularly strong research areas of NIM. As WMI is a very active player in NIM, it was strongly involved in the planning of successor clusters. On the one hand, NIM was and still is highly successful making the application for a third funding period a promising option. However, on the other hand NIM became so big and so broad that the NIM Executive Board decided not to apply for a follow-up cluster. Instead, it was decided to support the creation of three new and much more focussed cluster initiatives out of the NIM Research Area 1, 3 and 4, focusing on quantum science & technology, energy conversion, and synthetic biology, respectively. As the coordinator of the NIM Research Area I on *Quantum Nanophysics*, Rudolf Gross submitted an extended proposal for a new excellence cluster on *Quantum Science, Technology & Matter* to the university board of TUM already in August 2015. Finally, after a lengthy selection procedure all three cluster initiatives created

out of NIM were considered promising by the university boards of both Munich universities and letters of intent for joint initiatives have been submitted to the German Research Foundation in November 2016. Finally, the following draft proposals were emerging out of the NIM Research Areas 1, 3 and 4 and have been submitted to the DFG Head Office until the cut-off date of 3 April 2017:

1. **Munich Center for Quantum Science and Technology**
2. **e-conversion**
3. **BioDesign**.

In total, 195 draft proposals for Clusters of Excellence (Munich: 3 TUM, 5 LMU, 5 joint TUM/LMU proposals) have been submitted and reviewed by panels with relevant expertise. The comparative assessment of the review results formed the basis for the decisions made by a Committee of Experts in September 2017 as to which 88 projects (Munich: 1 TUM, 1 LMU, 4 joint TUM/LMU proposals) have been invited to submit full proposals. Fortunately, two of the tree NIM-emerging proposals made it to the next round. Only the proposal «Biodesign» failed. This means that NIM was contributing to one third of the successful clusters proposals of the two Munich universities.

Although the nanoscience oriented excellence cluster «Nanosystems Initiative Munich» will be discontinued at the end of 2018, there is still strong interest in nanoscience and nanotechnology and the NIM research activities have been continued with great success also in 2017. In the following, a few activities directly related to WMI are mentioned:

NIM Seed Funding

Also in 2017, WMI was very successful in attracting NIM seed funding for high-risk projects. All NIM seed funding proposals are reviewed by the NIM Scientific Advisory Board.

Within the project ***Highly coherent flux qubits with capacitive shunt for coherent quantum annealing*** (Gross, Deppe) we develop the capacitively shunted version of the flux qubit. These devices are known to exhibit coherence times up to several tens of microseconds and will be the work horse for our future efforts towards coherent quantum annealing. To this end, we implement parallel on-chip capacitors in either parallel-plate (multilayer) or interdigital (single-layer) configuration. Within the short time scale of a seed funding project, we aim at achieving coherence times above 10 μs for the capacitively shunted flux qubits. Nevertheless, building on our experience with flux-based tunable couplers, we will also design and fabricate first samples containing unit cells with 4 to 8 of these qubits in a highly-interconnected manner. In this way, we get started on our path towards the experimental exploration of a platform for coherent quantum annealing with coherent qubits in Germany. At the same time, our work will be a fundamental prerequisite for the scalability of our circuits towards order of ten coupled and controlled coherent quantum devices. Besides the interesting scientific aspects, a key goal of the seed funding project is to perform proof-of-principle experiments with a new type of highly coherent superconducting qubits and to provide the technological basis for their controlled fabrication. This is an important prerequisite for the successful participation in the upcoming national and international projects on quantum technology such as the planned Quantum Technology Flagship of EU and the QUTEGA (Quantentechnologie: Grundlagen und Anwendungen) program of the Federal Ministry of Education and Research (BMBF).

In a second seed funding project ***Multi-photon scattering tomography with propagating quantum microwaves*** (Deppe, Gross) we proposed to extend the experimental work on quantum scatterers. So far all experiments on quantum scatterers are well described by resonant

(single photon) scattering theory. In our seed funding project we will move beyond such simple scenarios and towards fundamentally novel grounds: The investigation of multi-photon scattering at a quantum system, where each photon is strongly off-resonant. Specifically, we aim at the experimentally relevant challenge of determining multi-photon scattering matrix elements using only coherent states as inputs and simple quadrature measurements at the outputs. To this end, we plan to combine already existing platforms and techniques, namely our superconducting on-chip interferometer with our correlation-based dual-path detector. In the simplest case, the scatterer placed in one of the interferometer arms can be a single transmon qubit. In such a scenario, theory predicts that one can directly measure the two-photon scattering matrix element, essentially by recording the first-order-correlation function between the two interferometer outputs. It is a key goal of the seed funding project to measure such scattering matrix element for the first time.

Finally, in a third seed funding project ***Quantum sounds on nanostrings*** (Hübl, Gross) we plan to combine a circuit QED setup with a nano-mechanical, doubly-clamped string resonator to (i) swap non-classical photonic states to the nano-string resonator, (ii) store complex phononic quantum states in the mechanical element, and (iii) determine the mechanical lifetime of the phononic quantum state by swapping it back to the microwave domain. Realizing this approach represents a major step towards generating/storing quantum states in mechanical elements and will have an important impact for the realization of quantum-enhanced mechanical sensing applications. A key requirement for implementing this approach is to establish strong coupling between the mechanical and the circuit QED subsystems, allowing for fast state swapping. It is the key goal of this seed-funding project to establish such strong coupling and thereby pave the way to a variety of interesting quantum experiments and sensing applications.

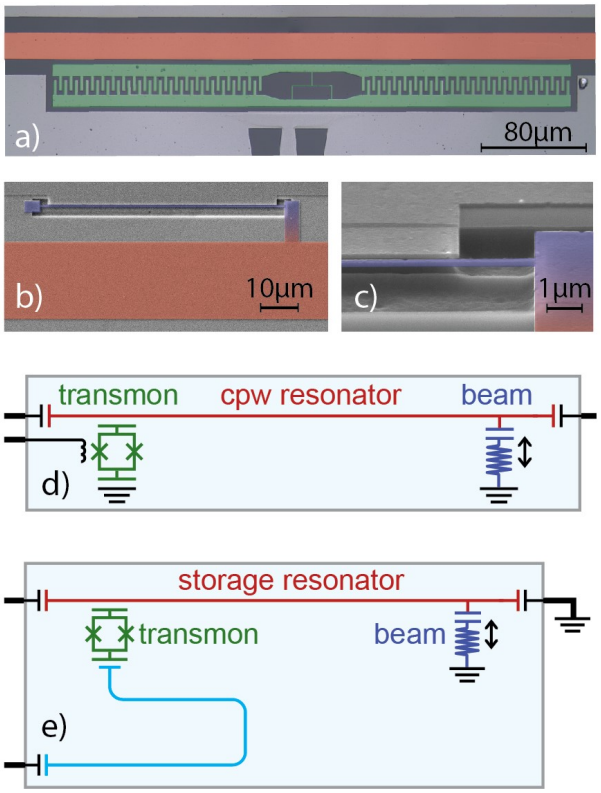

Figure 1: False-colored scanning electron micrographs of a quantum mechanical hybrid device and circuit schemes for enabling microwave quantum state preparation, swapping and readout. Panel (a) shows the transmon qubit located at the voltage antinode of the coplanar waveguide resonator, while panel (b) and (c) show the freely suspended aluminum nano-string resonator. (d) Sketch of the existing device configuration, which is compatible with the quantum state preparation. In panel (e), an additional readout resonator coupled to the transmon qubit is used to enable higher readout fidelity and the generation of microwave cat-states.

NIM Research Conferences

Following the recommendation of its Scientific Advisory Board, NIM started the ***NIM Research Conferences*** in 2015. These conferences aim to bring together leading international experts to discuss and explore emerging new fields, as well as to bridge different communities to share, pursue and diffuse the benefits of collaborations. In 2017, Rudolf Gross, Jonathan Finley and Gerhard Rempe organized the NIM Conference ***R-QED 2017*** at the Kardinal-Wendel-Haus in Schwabing (for more details, see page 114. It was a continuation of the highly successful EU-supported R-QED 2013 and the NIM supported R-QED 2015 conferences, all organized by Gross, Finley and Rempe and also taking place at Munich.

Research Activities

As in previous years, also in 2017 the WMI research activities strongly profited from NIM. Some of our recent results are presented in several contribution to this Annual Report. They range from the field of superconducting quantum circuits, hybrid quantum systems, electro-nanomechanical systems, to spin dynamics, spin caloritronics and the study of physics related to pure spin currents.

B. The Cluster Proposal «Munich Center for Quantum Science and Technology»

Over the past two years WMI contributed to the application of a new Cluster of Excellence within the ***German Excellence Strategy***. The cluster proposal is named ***Munich Center for Quantum Science and Technology*** and coordinated by the three spokesmen Immanuel Bloch (LMU Munich and MPQ), Ignacio Cirac (MPQ and TUM) and Rudolf Gross (TUM and BAdW). A draft proposal was submitted to the German Research Foundation jointly by LMU Munich and TUM on 3 April 2017. After a positive review by an expert panel and a comparative assessment by the Committee of Experts appointed by the Joint Science Conference (GWK) the preparation of the full proposal was started early in October 2017.

The rationale for a cluster initiative focussing on quantum science and technology is straightforward. Although quantum information science was first developed to describe the working principles of future quantum computers, it meanwhile

emerged into a powerful description of our physical world, with wide ranging relevance for fields such as quantum materials, quantum chemistry or even quantum cosmology. At the core of this description is the notion of entanglement. In fact, understanding and controlling entanglement on different length and time scales is a key objective of the new cluster initiative and is considered a key prerequisite for numerous technological revolutions. The ***Munich Center for Quantum Science and Technology*** intends to combine multidisciplinary research across physics, mathematics, computer science, materials science, chemistry, and cosmology. This promises extraordinary applications ranging from inherently secure communications and processing of information, to ultrasensitive sensors and transducers for precision metrology, as well as providing new insights into the behavior of quantum many-body systems and quantum phases of matter and allowing the design of novel materials.

Meanwhile, a preliminary version of the full proposal has been completed and forwarded to the Management Boards of LMU and TUM just before Christmas 2017. The final version has to be submitted to the DFG Head Office until the cut-off date of 21 February 2018.

Coordinated Projects in Quantum Science and Technology

Rudolf Gross

The Walther-Meißner-Institute (WMI) participates in several coordinated research programs, centers, graduate schools and initiatives in the field of Quantum Science and Technology (QST). Besides the already existing Cluster of Excellence ***«Nanosystems Initiative Munich»*** with its Research Area 1 on Quantum Nanophysics and the proposed new cluster ***«Munich Center for Quantum Science and Technology»*** (see page 19–23) these are:

- **The Munich Quantum Center (MQC)**
- **The Ph.D. School of Excellence «Exploring Quantum Matter» (ExQM)**
- **The International Max Planck Research School «Quantum Science and Technology» (IMPRS-QST)**
- **The EU Collaborative Project «Magnetomechanical Platforms for Quantum Experiments and Quantum Enabled Sensing Technologies»**.

Within these mid and long-term projects WMI continues its ambitious research program in QST which started already in 2003 with the Collaborative Research Center 631 «Solid State Quantum Information Processing Systems». The focus of these projects and their present status is briefly summarized below.

The Munich Quantum Center (MQC)

The ***Munich Quantum Center (MQC)*** was founded in 2014. Meanwhile, it gathers more than 40 research groups of TUM, LMU, MPQ and WMI. The members and PIs of the MQC research groups meet up regularly at common workshops and seminars to create a very interactive ambience for quantum science in Munich. In this way, MQC aims at communicating recent advances and developments in the field of QST. Furthermore, MQC is a successful platform to enhance the outside visibility of the Munich research activities in the field of QST. To this end, MQC is very successful in organizing workshops and schools as well as in stimulating new coordinated research projects.

The MQC member institutions cover a large variety of topics ranging from mathematical foundations, quantum information, computational methods, quantum nanosystems, quantum optics, and quantum many-body physics to superconducting devices. In MQC, theoretical and experimental physicists, chemists, mathematicians and engineers analyze physical systems exhibiting intriguing quantum mechanical properties. They also design new methods for leveraging and controlling such systems, thus paving the way for the development of quantum technologies.

The Graduate School of Excellence «Exploring Quantum Matter» (ExQM)

The International Graduate School of Excellence (IDK) entitled ***«Exploring Quantum Matter»*** was founded within the «Elite-Netzwerk Bayern» in June 2014. It passed a very positive intermediate evaluation in November 2016 and was extended until May 2022. At present, one of the WMI Ph.D. students, Michael Fischer, gets a scholarship from ExQM. He works on ***Scalable Networks of Solid-state Quantum Circuits***.

The key goal of ExQM is to unite the unique competence in quantum physics in Munich and to integrate it into an ***international excellence network of doctoral training centres*** with partners at the Austrian Academy of Sciences in Vienna and Innsbruck, at ETH Zurich, ICFO Barcelona, Imperial College London, Caltech, and Harvard. The participating institutions are the Technical University of Munich (TUM, spokesman: Steffen Glaser), the Ludwig-Maximilians University Munich (LMU), the Max Planck Institute of Quantum Optics (MPQ), and the Walther-Meißner-Institute of BAdW. The research topics of ExQM include seven primary research areas between the broader field of quantum optics, numerical tensor networks methods and theoretical quantum information. The individual focus areas are:

I: Ultracold Atoms in Optical Lattices
II: Scalable Networks of Solid-State Quantum Circuits
III: Density-Matrix Renormalization Group Methods (DMRG) and Matrix-Product State Approaches
IV: Interfacing Light and Matter
V: All-Optical Quantum Simulation
VI: Exploring Open Quantum Systems
VII: Polariton Condensation in Emergent Nanomaterials

The training of PhD students is supported by the development of new-media tools tailored to research requirements (e.g. visualization, outreach, interaction with partners).

In 2017, ExQM was organizing a large number of seminar talks and events. Examples are the *IAS Symposion on Quantum Control: Mathematical Aspects and Physical Applications*, 3-5 April 2017, the Munich Quantum Days on 26 May and 13 October 2017, or the block course by Prof. Michael Keyl (FU Berlin) on *Mathematical Aspects of Quantum Field Theory*, 9-12 October 2017. The latter was jointly organized with International Max Planck Research School on Quantum Science and Technology.

The Int. Max Planck Research School «Quantum Science and Technology» (IMPRS-QST)

The IMPRS ***«Quantum Science and Technology»*** (spokesman: Ignacio Cirac, MPQ) started in 2016. It provides the opportunity of a common research and teaching platform to unite the competences of leading research groups in Munich in an interdisciplinary, professional and coherent manner. The IMPRS-QST particularly exploits the synergies between MPQ, WMI and the Munich universities of excellence LMU and TUM.

The PhD students of IMPRS-QST profit from an exceptionally broad, yet focussed, international training at the highest level that combines theoretical, experimental and communication skills in a vibrant field pertinent to new technologies. PhD students who join the IMPRS-QST are part of a large community, establish networks, and have their thesis work complemented by an educational program. The curriculum consists of:

- Two basic courses (1st year of PhD)
- Two advanced courses (2nd year of PhD)
- Annual Summer School (every year)
- Regular seminars (organized by students)
- Tutoring and discussion groups
- Soft-skills and interdisciplinary training
- International research stay: 1-3 months

WMI contributes to the educational program with the courses (i) Superconductivity and Low Temperature Physics 1, (ii) Applied Superconductivity, and (iii) Superconductivity and Low Temperature Physics 2.

Important events of the IMPRS-QST in 2017 have been the *Workshop on Condensed Matter, Quantum Technology and Quantum Materials*, 3-7 April 2017, jointly organized by IMPRS-QST and MPI-PKS Dresden, and the IMPRS-QST/TopMath Spring School 2017 on *Quantum Entropy and its Use*, 29-31 March 2017, taking place at Abtei Frauenwörth, Chiemsee.

The EU-Project «Magnetomechanical Platforms for Quantum Experiments and Quantum Enabled Sensing Technologies» (MaQSens)

The EU-Project ***MagQSens***[1] (coordinator: Markus Aspelmeyer, University of Vienna) started in January 2017. Within this project, WMI collaborates with partners from the University of Vienna, the Technical University of Vienna, the Austrian Academy of Sciences, and the Universitat Autonòma de Barcelona as well as the industry partners Airbus DS GmbH and attocube systems AG.

MaQSens seeks to establish a radically new technology platform for experiments in macroscopic quantum physics and for quantum enabled sensing. It exploits magnetic coupling between superconducting quantum circuits and superconducting mechanical resonators – both levitated and suspended – to enter a hitherto inaccessible parameter regime of both unprecedented force sensitivity and full quantum control of massive, macroscopic objects. The approach followed by MaQSens combines, in a new way, techniques from different research areas (magnetic levitation, superconducting circuits, atom-chip technology, cavity opto-mechanics and quantum optics) and is set up as a joint collaborative effort between expert European teams from academia and industry. The technology developed in MaQSens will enable quantum experiments of otherwise unachievable coherence times and masses, which has immediate implications for testing fundamental physical questions, for performing hybrid quantum information processing and, on the applied side, for ultrasensitive force sensing applications.

In 2017, WMI organized the MagQSens Workshop «Science Meets Industry: Ultra-Low Vibration Cryogenic Platforms», taking place at the Munich Residence (see 113).

Upcoming Coordinated Research Projects in QST

A: The BMBF Project «Quantentechnologie – Grundlagen und Anwendungen»(QUTEGA)

The Federal Ministry of Education and Research (BMBF) decided to set up the national initiative ***Quantentechnologie – Grundlagen und Anwendungen (QUTEGA)*** to promote quantum technologies in Germany and to prepare for the EU Quantum Technology Flagship. Following a suggestion from the scientific community, Gerd Leuchs (Max Planck Institute for the Science of Light, Erlangen) has been assigned the coordination of QUTEGA. He is supported by the ***QUTEGA Committee***. Rudolf Gross of WMI is member of this expert committee which is working out the research strategy and funding structure for QUTEGA.

[1] This project has received funding from the European Union's Horizon 2020 research and innovation programme under grant agreement No. 736943, and from the European Research Council (ERC) under the European Union's Horizon 2020 research and innovation programme under grant agreement No. 649008.

Early in 2017, a strategic paper named *«Quantentechnologie: Grundlagen und Anwendungen»* has been completed by the QUTEGA Committee. It describes the different research topics to be addressed by the national QUTEGA initiative and also contains recommendations for the funding structure of the QUTEGA program. Meanwhile, the BMBF already has launched three *«Pilotprojekte»* in 2017, providing an early boost for QUTEGA. Furthermore, the program *«Schlüsselkomponenten für Quantentechnologien»* has been announced within the funding scheme *«Photonik Forschung Deutschland»*. Unfortunately, due to the election in Germany and the delay in forming a new government, the official announcement of further QUTEGA-related programs will be most likely delayed until the second half of 2018.

B: The EU Quantum Technology Flagship

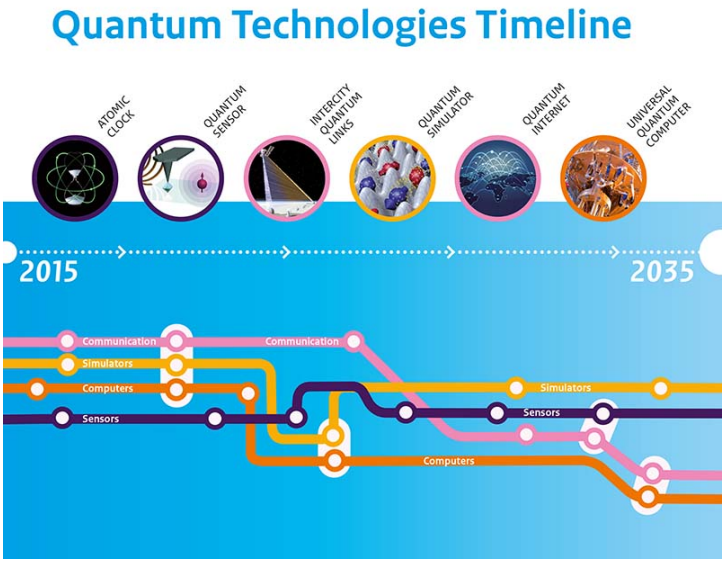

The European Commission has proposed making a billion euros available to establish a *«Quantum Technology Flagship»*, a large-scale European research program that will see European researchers, industry and requesting parties come together through a common ambition and roadmap, and to take the development of quantum mechanics closer to the market. The Quantum Flagship is part of the so called «Technology Package», a broad package of measures to strengthen the digital economy of Europe. It will provide an ambitious, coordinated and long-term strategy needed to support joint science, engineering and application oriented research & development in the field of quantum science and technology, including IPR, standardization, market development, training and public procurement.

Following a series of dialogues initiated by the European Commission with industry and other stakeholders, a *Quantum Manifesto* has been published already in 2016 with the support of more than 3 000 representatives from academia, industry as well as governmental and funding institutions. The roadmap presented in the Quantum Manifesto calls for an ambitious strategy to set the bases of a world-class quantum industry in Europe that will unlock the full potential of quantum technologies and bring commercial products to public and private markets, combining education, science, engineering and entrepreneurship. In September 2017, the *Quantum Technologies Flagship Final Report* of the High Level Steering Committee on Quantum Technologies has been published. This document completes the intermediate report which was published in February 2017. The final report expands the section dedicated on the implementation and includes a proposal for the governance structure of the QT flagship.

The Quantum Technology Flagship will be managed as part of the *Future and Emerging Technologies (FET)* program. It is expected to be a large-scale initiative similar in size, timescale and ambition to the two ongoing FET flagships, the Graphene Flagship and the Human Brain Project. The flagship will be partly financed from H2020 and from different other sources at EU and national level. The additional sources for its financial support, its leadership and governance will be defined as part of the flagship preparation process.

Third Funding Period for the Transregional Collaborative Research Center TRR 80 "From Correlations to Functionality"

R. Hackl [1]

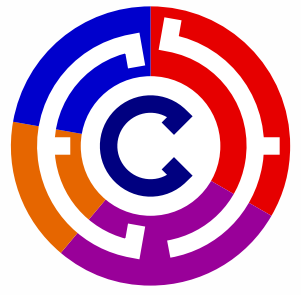

On November 27, 2017 the German Research Foundation (DFG) decided to support the Transregional Collaborative Research Center TRR 80 "From Correlations to Functionality" for another four year funding period from 01/2018 to 12/2021. The last funding period of TRR 80 is a collaboration between the University Augsburg (UA) as the coordinating institution, the Technical University Munich (TUM), the University Duisburg-Essen, and the Walther-Meißner-Institute (WMI). The first two funding periods (2010–2017) were very successful and productive, yielding more than 500 publications.

The objective of TRR 80 is to find new materials having electronic correlations and offering opportunities for functionalities. Important examples are interfaces of materials having properties entirely different from those of the constituents. Similarly, the introduction of defects and other inhomogeneities into correlated metals or metal oxides often yields new and unexpected properties that can be used for future applications. The situation is comparable to that of semiconductor research some 50 years ago. Since then a wealth of applications emerged from the observation of new properties and the intelligent modification of materials.

The TRR 80 is a collaboration between materials scientists, experimentalists, and theorists. It is planned to exploit the enormous possibilities of materials engineering, proceeding from single crystal growth and thin film deposition to heteroepitaxy and atomically precise structures. Many of the properties are not understood yet and need in-depth experimental studies and theoretical modeling. The projects of the TRR 80 comprise state-of-the-art preparation techniques, a large variety of innovative experimental tools, and various theory projects covering analytical and the most advanced numerical techniques.

The WMI contributes with a spectroscopy project which is intended to improve the spatial resolution of light scattering experiments and to combine single- and two-particle spectroscopies *in situ*. The spatial resolution of a light scattering experiment can in fact be improved by more than an order of magnitude, thus bridging the gap between the diffraction limit of visible light and scanning tunneling techniques. The improvement is achieved by exploiting the near-field (lightening-rod) effect of a metallic tip with a typical apex radius of 5 nm. The tip is placed into the focus of the laser and brought close to the sample surface. The highly enhanced electric field around the tip is confined to a volume determined by the apex radius. In this way the interaction volume is reduced by three to six orders of magnitude and the intensity of the scattered light per unit volume is amplified by a similar or larger factor, yielding an overall enhancement in spite of the smaller volume probed. As will be described in more detail in the contribution "Off-axis parabolic mirror optics for near-field Raman spectroscopy" (this volume), it is intended to study lattice, electronic, and transport properties on length scales of order 10 nm relevant for most of the new materials of interest for TRR 80.

[1] The work is supported by the DFG via the Transregional Collaborative Research Center TRR 80.

Basic Research

Towards remote state preparation with propagating quantum microwaves

S. Pogorzalek, K. G. Fedorov, B. Ghaffari, P. Eder, M. Fischer, E. Xie, A. Marx, F. Deppe, R. Gross [1]

In quantum communication protocols one achieves an efficient transfer of quantum information by utilizing quantum correlations between two communicating parties. Remote state preparation (RSP) is such a protocol, where the aim is to prepare a target quantum state at a distant location, using classical communication and previously shared nonclassical correlations. Compared to a purely classical protocol, RSP exhibits a quantum advantage in terms of a lower amount of classical information required to achieve its goal. For a general RSP protocol shown in Fig. 1(a), one of the two parties (Alice) performs a measurement on her part of the quantum correlated state and creates a feedback signal depending on the measurement outcome and the target state. This signal is subsequently sent to the other party (Bob) via a classical communication channel. There, Bob performs a local operation conditioned on the received information, which will prepare the target state on Bob's side.

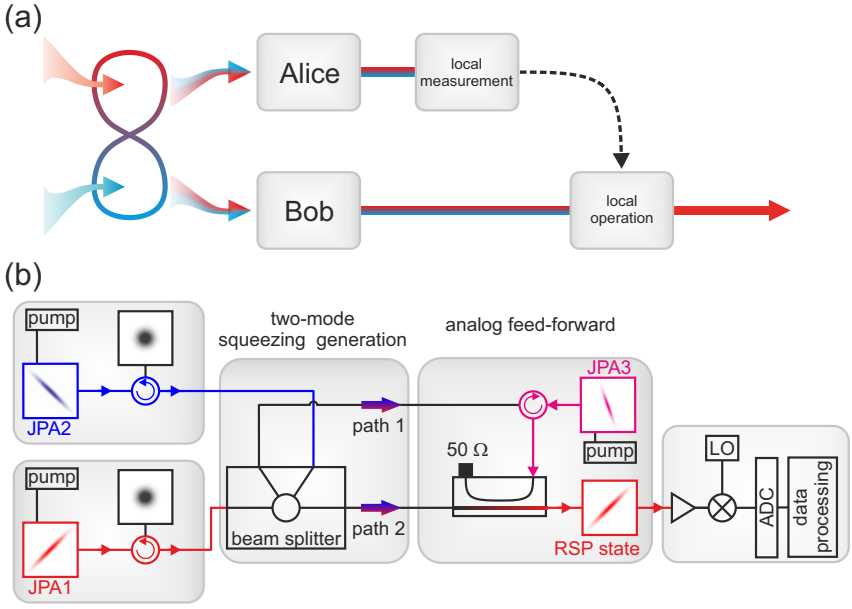

Figure 1: **(a)** Concept of RSP using an entangled resource and feed-forward with a local measurement, classical communication, and a local operation. **(b)** Schematic experimental setup using two JPAs and a beam splitter for the entanglement generation. A third JPA together with a directional coupler implements an analog feed-forward.

We present an experimental implementation of the RSP protocol with an analog feed-forward in the microwave regime utilizing two-mode squeezed (TMS) states as a quantum resource and show that it is possible to remotely prepare a limited set of different squeezed states. A schematic experimental setup is shown in Fig. 1(b). We use multiple flux-driven Josephson parametric amplifiers (JPAs) consisting of a $\lambda/4$ coplanar waveguide resonator shunted by a dc-SQUID [1] in order to generate single-mode squeezed states or perform phase-sensitive amplification. The JPAs are placed inside magnetically shielded sample holders in a dry dilution refrigerator and are operated at $f_0 = 5.43\,\mathrm{GHz}$ at a temperature of 50 mK. JPA1 and JPA2 are used to generate orthogonal single-mode squeezed states with an average squeezing level of 7.7 dB below the vacuum limit. The single-mode squeezed states are superimposed by a microwave beam splitter in order to generate an entangled TMS state [2], which serves as a quantum resource in the RSP protocol. We use an analog feed-forward scheme, where the

[1] The authors acknowledge support from the German Research Foundation through FE 1564/1-1, the doctorate program ExQM of the Elite Network of Bavaria, the IMPRS 'Quantum Science and Technology', and the German Excellence Initiative via the 'Nanosystems Initiative Munich' (NIM). We also acknowledge the productive collaboration with Prof. Y. Nakamura and Prof. E. Solano.

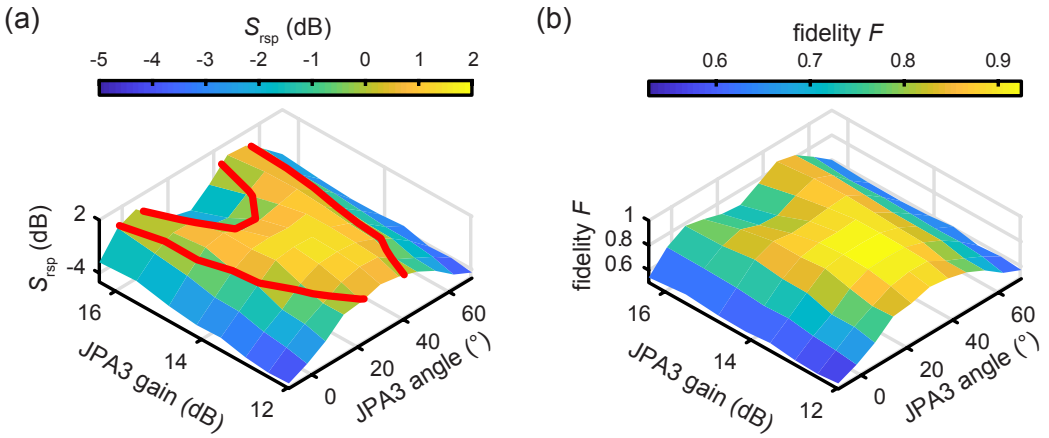

Figure 2: (a) Squeezing level S_{rsp} of the prepared state as a function of the phase-sensitive gain G_d and amplification angle γ of JPA3. The threshold for squeezing below the vacuum limit (positive S_{rsp}) is indicated by the red line. **(b)** Fidelity F of the analog feed-forward as a function of the parameters of JPA3.

signal of one path of the TMS state is phase-sensitively amplified by a third JPA and subsequently superimposed with the signal of the other path by a microwave directional coupler with a designed coupling of 15 dB. The directional coupler implements a local displacement operation [3] with the displacement amplitude provided by the feed-forward signal. The resulting state is reconstructed with a reference state method.

For the presented scheme, JPA3 acts as a control knob for the preparation of different squeezed states on Bob's side. We first investigate how the squeezing level S_{rsp} of the prepared state depends on the phase-sensitive gain G_d and amplification angle γ of JPA3, as shown in Fig. 2(a). Around $G_d \simeq 13.5\,\mathrm{dB}$ and $\gamma \simeq 30°$ one observes a region where the RSP protocol yields squeezed states with maximum squeezing levels up to $S_{\mathrm{rsp}} = 1.7\,\mathrm{dB}$. A deviation from this optimal region leads to a degradation of S_{rsp}. Furthermore, a splitting occurs for $G_d > 15\,\mathrm{dB}$ where there are two narrow regions of γ with squeezing levels below the vacuum limit. In order to quantify the quality of the analog feed-forward, we use a fidelity criterion for Gaussian states and compare the experimentally measured state with the state one expects from the used imperfect TMS states and a perfect feed-forward operation. The obtained fidelity F is shown in Fig. 2(b) and reaches values above 0.9 for the region with the highest squeezing levels S_{rsp} and exhibits a similar splitting for increasing G_d.

To conclude, we have successfully demonstrated the first RSP protocol in the microwave regime and explored the influence of different parameters of the used JPA for the analog feed-forward. We have obtained a highest squeezing level of $S_{\mathrm{rsp}} = 1.7\,\mathrm{dB}$ below the vacuum limit, showing that the protocol fundamentally works. The optimal fidelity of the analog feed-forward of $F = 0.93$ confirms that propagating quantum microwaves are suitable for quantum communication tasks.

References

[1] S. Pogorzalek, K. G. Fedorov, L. Zhong, J. Goetz, F. Wulschner, M. Fischer, P. Eder, E. Xie, K. Inomata, T. Yamamoto, Y. Nakamura, A. Marx, F. Deppe, and R. Gross, Phys. Rev. Appl. **8**, 024012 (2017).

[2] K. G. Fedorov, S. Pogorzalek, U. L. Heras, M. Sanz, P. Yard, P. Eder, M. Fischer, J. Goetz, E. Xie, K. Inomata, Y. Nakamura, R. Di Candia, E. Solano, A. Marx, F. Deppe, and R. Gross, submitted for publication, arXiv:1703.05138 (2017).

[3] K. G. Fedorov, L. Zhong, S. Pogorzalek, P. Eder, M. Fischer, J. Goetz, E. Xie, F. Wulschner, K. Inomata, T. Yamamoto, Y. Nakamura, R. Di Candia, U. Las Heras, M. Sanz, E. Solano, E. P. Menzel, F. Deppe, A. Marx, and R. Gross, Phys. Rev. Lett. **117**, 020502 (2016).

Temporal matching in propagating two-mode squeezed microwaves

K. G. Fedorov, S. Pogorzalek, P. Yard, P. Eder, M. Fischer, J. Goetz, E. Xie, F. Deppe, A. Marx, R. Gross [1]

Propagating quantum microwave signals in the form of squeezed states are natural candidates for quantum communication and quantum information processing with continuous variables. This assessment stems from the fact that they belong to the same frequency range and are generated using the same material technology as quantum information processing platforms based on superconducting circuits. Utilizing propagating quantum microwaves, one can potentially realize quantum illumination protocols, hybrid computation schemes with continuous variables, and a high-fidelity seamless connection between distant superconducting quantum computers [1]. In two-mode squeezed microwave states, entanglement is expressed in strong correlations between two nonlocal field quadratures. The physical limits of this entanglement are of broad interest regarding both quantum information theory and applications. In this context, finite-time properties of propagating two-mode squeezed states provide an important information about the entanglement tolerance to a temporal mismatch τ.

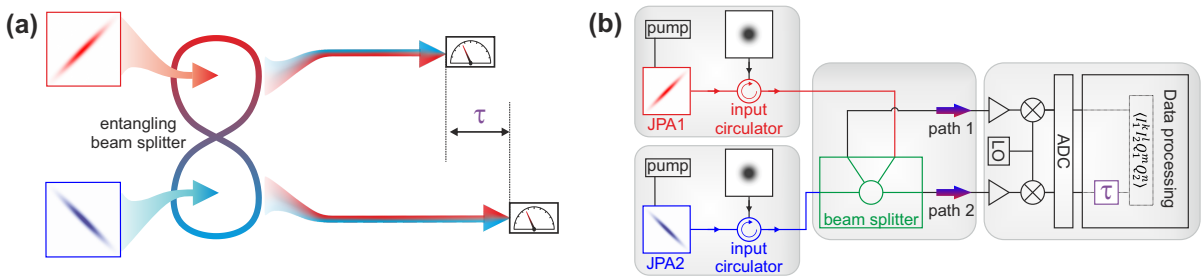

Figure 1: **(a)** Concept of entanglement measurements between temporally mismatched two-mode squeezed microwave states. **(b)** Schematic experimental layout. Symmetric two-mode squeezing is produced by two orthogonal squeezers (JPAs) and a microwave beam splitter. The temporal mismatch is introduced by a digital time delay in the data processing chain.

We use two superconducting flux-driven Josephson parametric amplifiers (JPAs) operated at $f_0 = 5.323\,\mathrm{GHz}$ for the generation of squeezed microwave states. The task of each JPA is to perform a squeezing operation on the incident vacuum state [2, 3]. We conveniently characterize the degree of squeezing of the quantum state in decibels as $S = -10\log_{10}[(1+2n)\exp(-2r)]$, where n reflects the number of added noise photons due to JPA imperfections and r is the squeezing factor. Generation of symmetric two-mode squeezed states is achieved with a microwave beam splitter superimposing two orthogonally squeezed microwave states (see Fig. 1). The final state tomography is based on cross-correlation measurements of the entangled signals and provides a covariance matrix of the entangled beams as a result [2, 3].

In general, the amount of bipartite entanglement in Gaussian states can be assessed using the negativity $\mathcal{N}$. It is defined as $\mathcal{N} \equiv \max\{0, N_k\}$, where the negativity kernel $N_k(\tau)$ is a function of the covariance matrix of the investigated state. The condition $N_k > 0$ implies the presence of entanglement. Here, we introduce a maximally acceptable delay τ_d which still allows for the existence of entanglement in a propagating two-mode squeezed (TMS) state. This condition is given by $N_k(\tau_d) = 0$ for a monotonically decreasing $N_k(\tau)$. Assuming all other system properties to be equal, a large τ_d is beneficial in quantum communication. The

[1] The authors acknowledge support from the German Research Foundation through FE 1564/1-1, the doctorate program ExQM of the Elite Network of Bavaria, the IMPRS 'Quantum Science and Technology', and the German Excellence Initiative via the 'Nanosystems Initiative Munich' (NIM). We also acknowledge the productive collaboration with the groups of Prof. Y. Nakamura and Prof. E. Solano.

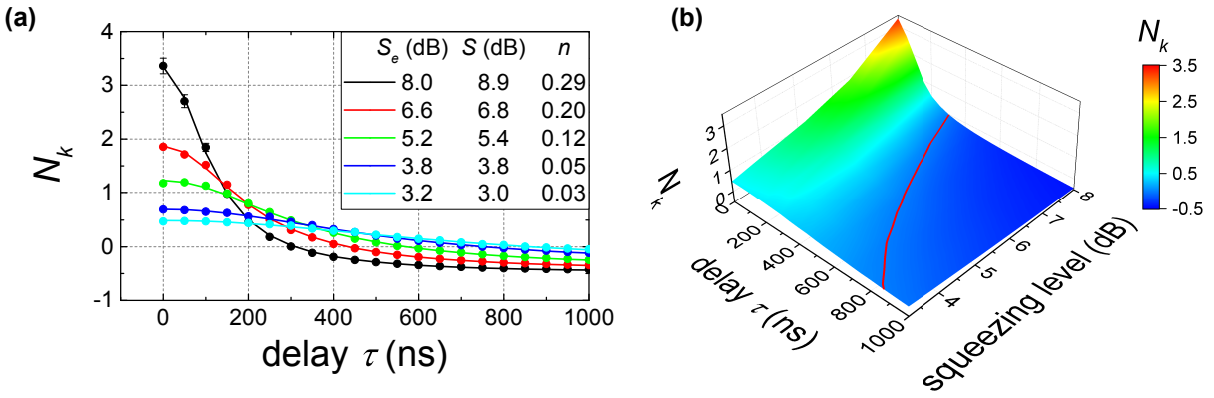

Figure 2: Entanglement decay in temporally mismatched propagating TMS states. **(a)** Experimental data (circles) measured with the filter bandwidth $\Omega = 430$ kHz and the corresponding theory fits (solid lines) according to Eq. (1). S_e values in the inset represent the experimental squeezing levels for both JPA1 and JPA2, S values denote the fitted squeezing levels, and n denotes the noise photon number. **(b)** 3D color plot illustrating the same data, where the red line marks the boundary between the entangled ($N_k > 0$) and classical ($N_k < 0$) regions.

expression for the negativity kernel $N_k(\tau)$ for an arbitrary two-mode squeezed state produced by two independent JPAs is given by [3]

$$N_k(\tau) = -0.5 + 0.5\left[(n_1 - n_2)^2 + \tilde{n}C + (\tilde{n}C - (n_1 + n_2 + 1)^2)\mathrm{sinc}^2\,\Omega\tau - \tilde{n}D|\mathrm{sinc}\,\Omega\tau|\right]^{-0.5}, \quad (1)$$

where Ω is the width of a measurement bandpass filter centered at f_0, $\tilde{n} \equiv (1+2n_1)(1+2n_2)$, $C \equiv \cosh^2(r_1 + r_2)$, $D \equiv \sinh(2r_1 + 2r_2)$; r_1 (r_2) and n_1 (n_2) are the squeezing factor and number of noise photons of JPA1 (JPA2), respectively. The negativity kernel N_k depends on the squeezing level S and the corresponding values of r since the delay τ_d decreases with increasing S as it can be clearly seen from the experimental data fitted with Eq. (1) shown in Fig. 2.

In conclusion, we have uncovered that, for propagating microwave TMS states, the entanglement quantified via $N_k(\tau)$ survives for considerable temporal mismatches τ. We found an analytic expression for the negativity kernel $N_k(\tau)$ as a function of the squeezing level S and the noise photon number n in addition to Ω. This function is given by Eq. (1) and accurately describes the experimental results. High squeezing levels and accompanying large noise photon numbers additionally reduce the entanglement for finite delays between the paths. With respect to applications, a key result of this work is the observation of the characteristic temporal matching timescale τ_d for two-mode squeezed microwaves, which can be longer than 1 μs for squeezing levels $S \simeq 3$ dB. This result confirms that propagating TMS microwave states are suitable for the remote preparation of squeezed states and short-to-medium distance quantum teleportation.

References

[1] R. Di Candia, K. G. Fedorov, L. Zhong, S. Felicetti, E. P. Menzel, M. Sanz, F. Deppe, A. Marx, R. Gross, and E. Solano, EPJ Quantum Technol. **2**, 25 (2015).

[2] E. P. Menzel, R. Di Candia, F. Deppe, P. Eder, L. Zhong, M. Ihmig, M. Haeberlein, A. Baust, E. Hoffmann, D. Ballester, K. Inomata, T. Yamamoto, Y. Nakamura, E. Solano, A. Marx, and R. Gross, Phys. Rev. Lett. **109**, 250502 (2012).

[3] K. G. Fedorov, S. Pogorzalek, U. Las Heras, M. Sanz, P. Yard, P. Eder, M. Fischer, J. Goetz, E. Xie, K. Inomata, Y. Nakamura, R. Di Candia, E. Solano, A. Marx, F. Deppe, and R. Gross. Finite-time quantum correlations of propagating squeezed microwaves. Submitted for publication, arXiv:1703.05138 (2017).

Artificial atom with dipole and quadrupole moments

F. Deppe, J. Goetz K.G. Fedorov, P. Eder, M. Fischer, S. Pogorzalek, E. Xie, A. Marx, R. Gross [1]

Superconducting circuits for quantum science and technology are typically divided into two types. Linear or harmonic circuits are often used as quantum memories storing microwave light, quantum buses, or quantum state readout devices. In contrast, anharmonic superconducting circuits are interpreted as artificial atoms, typically in a two-level approximation. Interestingly, the analogy between artificial and natural atoms not only exists in the rather abstract quantized scenario, where ladder operators are used to describe the system, but also extends to real space. Just as their natural counterparts, artificial atoms can interact with electromagnetic radiation via an actual, not at all artificial, dipole moment produced by either a capacitance (electric) or a loop inductance (magnetic). The latter has been used to study selection rules and their breakdown [1] using a superconducting loop interrupted by three nanoscale Josephson junctions forming a quantum mechanical two-level system, a flux qubit. In terms of the Pauli operators σ_x and σ_z, the effective Hamiltonian of such a qubit becomes $H_{\mathrm{dip}} = (\epsilon\sigma_z + \Delta\sigma_x)/2$. Here, the dipole moment enters into the flux-tunable energy bias ϵ and Δ is a constant energy determined by certain junction parameters [1]. As a consequence, such a qubit couples to an electromagnetic drive via the σ_z term, which translates to transversal coupling in the energy eigenbasis.

Here, we take the analogy between artificial and natural atoms one step further by investigating a gradiometric flux qubit [2] shown in Fig. 1. For this layout, ϵ is controlled via the flux gradient in the gradiometer loop. Furthermore, *in-situ* control over Δ is achieved by implementing one of the Josephson junctions in the dc SQUID geometry. In this way, we construct an artificial two-level atom with a magnetic dipole and a magnetic quadrupole moment. By means of a suitably arranged pair of antennas, we resonantly excite the atom with microwave fields whose spatial amplitude distribution is either symmetric, antisymmetric, or does not posses a well defined symmetry. As a consequence, the drive couples either transversally, longitudinally, or as a mixture of both to the artificial atom. As discussed in detail in Ref. [3], we perfrom spectroscopy experiments and observe dipole and quadrupole selection rules as well as longitudinally-induced transparency. In the latter case, the symmetry of the qubit potential is broken, which usually results in an absence of selection rules [1]. However, when we break the symmetry of the driving field in the same way, we observe a restoration of selection rules.

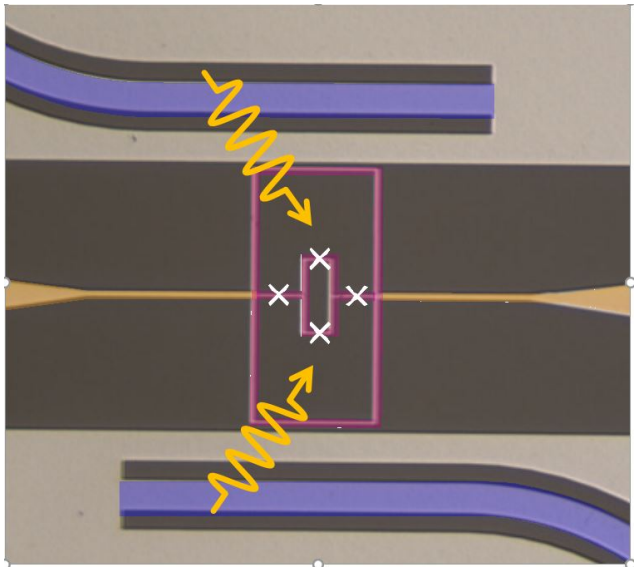

Figure 1: Artificial atom with gradiometer loop and dc SQUID (violet) coupled to the center conductor of a coplanar waveguide resonator (yellow). Microwave fields (wiggly arrows) of suitable symmetry can be applied via a pair of on-chip antennas (blue). White crosses: $\mathrm{Al/AlO}_x\mathrm{/Al}$ Josephson junctions.

[1] The authors acknowledge support from German Research Foundation through FE 1564/1-1 and the excellence cluster 'Nanosystems Initiative Munich (NIM)', the doctorate program ExQM of the Elite Network of Bavaria and the IMPRS 'Quantum Science and Technology'.

Finally, we exploit the fact that our artificial atom is coupled to a superconducting resonator, giving rise to an artificial orbital momentum. The direct qubit transition along with the red and blue sideband transitions to the resonator qualitatively reproduce the behavior of the lowest three transitions in the potassium atom. In contrast to the pure qubit, this artificial potassium atom allows us to investigate selection rules for transitions between states of the same parity. Again, a detailed discussion of the experimentally verified selection rules is given in Ref. [3].

In conclusion, we have constructed an artificial atom, where we could extend the analogy to natural atoms from a mere dipole moment to a quadrupole moment and, to some extent, to the orbital momentum. We expect that our approach will open novel perspectives for quantum chemistry simulations, where a decomposition into two-level atoms would require a large number of qubits to solve real-world problems. In such a situation, the 'analog' construction of larger building blocks, i.e., of more complex artificial atoms as shown here, can help to drastically reduce the required resources.

References

[1] F. Deppe, M. Mariantoni, E. Menzel, A. Marx, S. Saito, K. Kakuyanagi, H. Tanaka, T. Meno, K. Semba, H. Takayanagi, E. Solano, and R. Gross, Nature Physics **4**, 686–691 (2008).
[2] M. J. Schwarz, J. Goetz, Z. Jiang, T. Niemczyk, F. Deppe, A. Marx, and R. Gross, New J. Phys. **15**, 045001 (2013).
[3] J. Goetz, F. Deppe, K. G. Fedorov, P. Eder, M. Fischer, S. Pogorzalek, E. Xie, A. Marx, and R. Gross. Parity-engineered light-matter interaction. arXiv:1708.06405 (2017).

Effect of π-d exchange interaction on quantum oscillations in the layered antiferromagnetic superconductor κ-(BETS)$_2$FeBr$_4$

M. Kartsovnik, M. Kunz, F. Kollmansberger, W. Biberacher, [1]
H. Fujiwara [2]

Molecular conductors based on the organic donor bis(ethylenedithio)tetraselenafulvalene (BETS) and containing transition metal ions like Fe^{3+}, Mn^{2+}, Cu^{2+}, etc. are natural multi-layered structures with conducting and magnetic systems alternating on a single-molecular scale. The charge transport in these materials is provided by itinerant π-electrons in the layers of fractionally charged BETS donors, whereas magnetic properties are dominated by localized d-electron spins in the insulating anionic layers. While the latter often undergo antiferromagnetic ordering at low temperatures, the ground state of the π-electron system is determined by a subtle balance between different instabilities of the normal metallic state and is very sensitive to the interlayer π-d exchange interaction, see, e.g., [1].

Magnetic quantum oscillations have been proposed to be used as a tool for a quantitative analysis of this interaction [2]. When a strong magnetic field B is applied to such a material, the saturated d-electron spins in the insulating layers impose an effective exchange field,

$$B_J = \frac{J_{\pi d} S_d}{g\mu_B}, \tag{1}$$

on the spins of the itinerant π electrons in the molecular layers. Here, $J_{\pi d}$ is the π-d exchange energy, S_d the d-electron spin, g the Landé g-factor, and μ_B the Bohr magneton. As a result, the usually constant spin damping factor in the expression for the amplitude of the quantum oscillations acquires a field dependence [2, 3]:

$$R_s = \cos\left[\frac{\pi}{2}\frac{g m_0^*}{\cos\theta}\left(1 - \frac{|B_J|}{B}\right)\right], \tag{2}$$

where θ is the angle between the magnetic field and the normal to the layers, $m_0^* = m^*(0^\circ)/m_e$ is the cyclotron mass of charge carriers normalized to the free electron mass, and the sign "$-$" corresponds to an antiferromagnetic exchange.

To test the theoretical proposal, we have carried out a systematic study of quantum oscillations of magnetoresistance, known as the Shubnikov-de Haas (SdH) effect, in the antiferromagnetic superconductor κ-(BETS)$_2$FeBr$_4$. At $B > 5\,\mathrm{T}$ and $T \lesssim 1.5\,\mathrm{K}$, this compound is a paramagnetic metal [4] with the localized Fe^{3+} spins saturated along the field direction. Two fundamental SdH frequencies are generally observed, corresponding to the classical cyclotron orbit α on the cylindrical Fermi surface and to the magnetic breakdown orbit β [5].

Figure 1(a) shows the β-oscillation component of magnetoresistance measured at different polar angles θ. One clearly sees beats with θ-dependent positions of nodes and antinodes. Considering the beats as coming from the field-dependent spin factor, one should expect from Eq. (2) that at $B = |B_J|$ the oscillation amplitude is always maximum, independent of the angle. Indeed, at sufficiently high tilt angles the oscillations in Fig. 1(a) display a maximum amplitude at $B \approx 13\,\mathrm{T}$, independent of θ. This value is in good agreement with the exchange field estimated from the position of the re-entrant superconductivity region on the phase diagram [4]. A detailed analysis of the beat positions, using Eqs. (1) and (2), yields $g = 1.98 \pm 0.06$ and $J_{\pi d} = (0.60 \pm 0.015)\mathrm{meV}$.

[1] The work was supported by the German Research Foundation via grant KA 1652/4-1
[2] Osaka Prefecture University, 5998531 Osaka, Japan

However, for small tilt angles, $-20° < \theta < 20°$, the beats become more complex. Not only some of the beat nodes become much less pronounced, but also their positions shift in an apparently irregular manner. For example, at $\theta \approx -9°$ and $+8°$ a minimum in the amplitude is found around $B = 13\,\mathrm{T}$, where the θ-independent maximum should be expected. At present we do not have a satisfactory explanation of this anomalous behaviour. One might appeal to other possible mechanisms of beating of the SdH oscillations, such as weak warping of the cylindrical Fermi surface in the interlayer direction [6] or mosaicity of the crystal.

The α oscillations corresponding to the smaller, classical cyclotron orbit on the Fermi surface should also be modulated by the field-dependent spin factor according to Eq. (2). However, we have found no modulation at tilt angles below $15-20°$, i.e. in the range where the beat behaviour of the β oscillations is anomalous. In Fig. 1(b) we show the evolution of the α-oscillating component at $\theta \geq 20°$. The weak modulation observed at 20° develops gradually into full beating with periodic nodes. However, the node positions are still inconsistent with those found on the β oscillations. As shown in Fig. 1(b), apparently only every second expected node shows up in the experiment. According to Eq. (2), this would imply that the g-factor on the α orbit is only one half of that on the β orbit. This would be highly surprising, especially since the latter does incorporate the α orbit as a part. Thus, further angle-resolved studies are needed to clarify the situation.

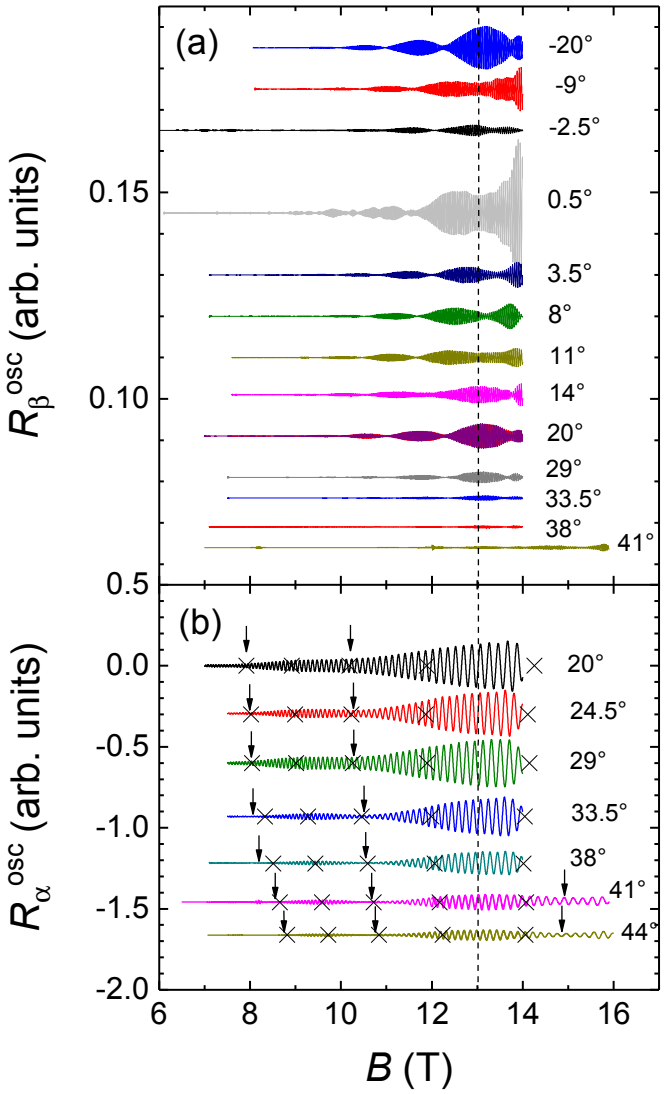

Figure 1: SdH oscillations in κ-$(BETS)_2FeBr_4$ corresponding to (a) the magnetic breakdown orbit β and (b) the classical cyclotron orbit α, obtained at different angles θ, $T = 0.45\,\mathrm{K}$. The curves are vertically shifted for clarity. The vertical line indicates the field $B = -B_J$, at which the high-angle oscillations show a maximum. Crosses in (b) indicate the positions of the amplitude minima for the α oscillations expected from the analysis of the β oscillations; arrows point to the actual minima positions.

References

[1] H. Kobayashi, H. Cui, and A. Kobayashi, Chem. Rev. **104**, 5265 (2004).
[2] O. Cépas, R. H. McKenzie, and J. Merino, Phys. Rev. B **65**, 100502 (2002).
[3] D. Shoenberg. *Magnetic Oscillations in Metals* (Cambridge University Press, Cambridge, 1984).
[4] T. Konoike, S. Uji, T. Terashima, M. Nishimura, S. Yasuzuka, K. Enomoto, H. Fujiwara, B. Zhang, and H. Kobayashi, Phys. Rev. B **70**, 094514 (2004).
[5] T. Konoike, S. Uji, T. Terashima, M. Nishimura, S. Yasuzuka, K. Enomoto, H. Fujiwara, E. Fujiwara, B. Zhang, and H. Kobayashi, Phys. Rev. B **72**, 094517 (2005).
[6] M. V. Kartsovnik, Chem. Rev. **104**, 5737 (2004).

On the degeneracy transition in Fermi liquids

D. Einzel

Introduction

In this contribution I consider many-body systems of N fermions of mass m, energy dispersion $\epsilon_{\mathbf{k}} = \hbar^2\mathbf{k}^2/2m$, in a volume V and density $n = N/V$. In the spirit of Landau's theory of Fermi liquids, interaction effects can be incorporated by the simple replacement $m \to m^* = m(1 + F_1^s/3)$ [1], with F_1^s being a dimensionless Landau parameter. Classical vs. degenerate behavior of such Fermi systems can in general be associated with the size of the thermal de Broglie wavelength $\lambda_T = h/\sqrt{2\pi m^* k_B T}$. While classical behavior occurs for $n\lambda_T^3 \ll 1$, degenerate behavior sets in when $n\lambda_T^3$ becomes large, the degeneracy transition occuring for $n\lambda_{T^*}^3 = O(1)$ at the temperature T^*. While the degeneracy temperature T^* of electrons in metals lies above the melting temperature of the metal, degeneracy phenomena in the neutral Fermi liquid ^{3}He are known to set in at temperatures $T^* = \mathcal{O}(1\mathrm{K})$ [1] and are therefore experimentally accessible easily [2]. The aim of this contribution is an *analytic* study of the degeneracy transition of (i) the density response function χ_n^0, (ii) the spin susceptibility $\chi_s^0 = \mu_B^2\chi_n^0$ (μ_B is the Bohr magneton), (iii) the internal energy u, (iv) the entropy σ and (v) the specific heat capacity c_V of Fermi liquids. For an analytic description of Fermi liquids the reduced chemical potential $\alpha = \mu(T)/k_BT$ [with $\mu(T)$ being the chemical potential] or equivalently, the *fugacity* $z = e^\alpha$ is of central importance. Close to the classical limit (high temperatures) one may take resort to a *fugacity expansion* ($z \to 0$, $\alpha \to -\infty$), whereas in the low temperature limit one may perform a *Sommerfeld expansion* ($\beta = \alpha^{-1} \to 0$). The degeneracy transition can be associated with the sign change of α at T^*.

Important definitions and relations

The temperature dependence of all relevant observables can be described by the *Jonquière function* or *polylogarithm* [3], which is a universal function of the variable α:

$$\mathrm{Li}_x^{(\theta)}(\alpha) = \frac{1}{\Gamma(x)}\int_0^\infty \frac{dt\, t^{x-1}}{e^{t-\alpha} - \theta} = \sum_{\nu=1}^\infty \frac{\theta^{\nu+1}e^{\nu\alpha}}{\nu^x}\,. \tag{1}$$

Here the statistical parameter $\theta = \pm 1$ allows for the distinction between Bose– and Fermi many-body systems. In the Fermion case ($\theta = -1$) one finds the following asymptotic expansion for the Jonquière function:

$$\lim_{\alpha\to\infty} \mathrm{Li}_x^{(-)}(\alpha) \;=\; \frac{\alpha^x S_m(x)}{\Gamma(x+1)} \;;\; S_m(x) = 1 + 2\sum_{\nu=1}^m \eta(2\nu)\frac{a_\nu(x)}{\alpha^{2\nu}}\,, \tag{2}$$

in which the sum $S_m(x)$ provides one possible origin for what may be referred to as the *Sommerfeld expansion* [4]. In Eq. (2) $a_\nu(x) = \Gamma(x+1)/\Gamma(x+1-2\nu)$ with Γ the Euler Γ function [5] and η the Dirichlet η function [5]. Restricting to the Fermi case in what follows, the total density n of a Fermi liquid may be written in the form $n = 2\mathrm{Li}_{3/2}^{(-)}(z)/\lambda_T^3$. Introducing the Fermi temperature through $k_BT_F = \mu(0) = \hbar^2k_F^2/2m^*$ [with $k_F = (3\pi^2 n)^{1/3}$ being the Fermi wavenumber, one obtains the following condition for the reduced temperature $r(\alpha) = T(\alpha)/T_F$:

$$r(\alpha) = \frac{T(\alpha)}{T_F} = \left[\Gamma\left(\frac{5}{2}\right)\frac{n\lambda_T^3}{2}\right]^{-\frac{2}{3}} = \left[\Gamma\left(\frac{5}{2}\right)\mathrm{Li}_{\frac{3}{2}}^{(-)}(\alpha)\right]^{-\frac{2}{3}}\,, \tag{3}$$

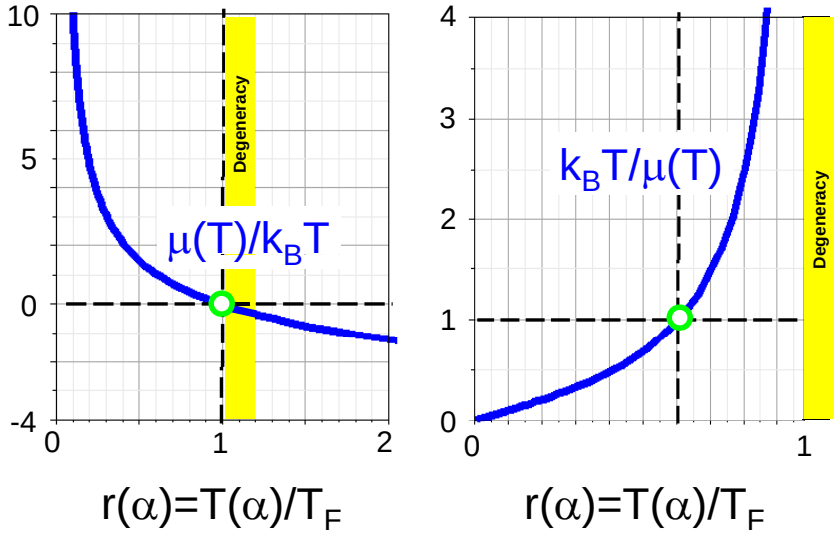

Figure 1: The conversion from the α– to the $r(\alpha)$– scale.

which allows for a conversion of the α–scale into the T/T_F–scale. Note that the degeneracy temperature,

$$T^* = 2\pi\frac{\hbar^2}{mk_B}\left(\frac{n}{2\eta\left(\frac{3}{2}\right)}\right)^{\frac{2}{3}} = \frac{T_F}{\left[\Gamma\left(\frac{5}{2}\right)\eta\left(\frac{3}{2}\right)\right]^{\frac{2}{3}}} = 0.9887335\cdots\cdot T_F\,, \tag{4}$$

associated with the condition $\alpha = 0$ (or $z = 1$), is slightly different from the traditional Fermi temperature T_F. The chemical potential, normalized to $k_B T_F$, can trivially be written as $\mu(T)/\mu(0) = \alpha r(\alpha)$. The degeneracy transition can be shown to be entirely described by only two *transition functions*:

$$t_n(\alpha) \;=\; \frac{\mathrm{Li}^{(-)}_{\frac{1}{2}}(\alpha)}{\mathrm{Li}^{(-)}_{\frac{3}{2}}(\alpha)} \overset{\alpha\to-\infty}{=} 1\;;\quad t_u(\alpha) = \frac{\mathrm{Li}^{(-)}_{\frac{5}{2}}(\alpha)}{\mathrm{Li}^{(-)}_{\frac{3}{2}}(\alpha)} \overset{\alpha\to-\infty}{=} 1\;. \tag{5}$$

Results

- The density response function $\chi^0_n(\alpha)$ $[N_F = 3n/2\mu(0)]$:

$$\begin{aligned}\chi^0_n(\alpha) &\overset{\text{exact}}{=} \frac{\partial n}{\partial\mu} = \frac{n}{k_B T}t_n(\alpha)\,;\\ \frac{\chi^0_n(\alpha)}{N_F} &\overset{\text{exact}}{=} \frac{2t_n(\alpha)}{3r(\alpha)} \overset{\text{Sommerfeld}}{\approx} 1 - \frac{\pi^2 r^2(\alpha)}{12} - \frac{11\pi^4 r^4(\alpha)}{360} - \cdots\end{aligned} \tag{6}$$

- The internal energy $u(\alpha)$ $[\delta u^0(\alpha) = N_F\pi^2 r^2(\alpha)/6]$:

$$\begin{aligned}u(\alpha) &\overset{\text{exact}}{=} \frac{3}{2}nk_B T t_u(\alpha)\,;\\ \frac{u(\alpha)-u(\infty)}{\delta u^0(\alpha)} &\overset{\text{exact}}{=} \frac{6}{\pi^2}\frac{r(\alpha)t_u(\alpha)-\frac{2}{5}}{r^2(\alpha)} \overset{\text{Sommerfeld}}{\approx} 1 - \frac{3\pi^2 r^2(\alpha)}{20} - \frac{247\pi^4 r^4(\alpha)}{3024} - \cdots\end{aligned} \tag{7}$$

- The entropy density $\sigma(\alpha)$ $[\sigma^0(\alpha) = N_F\pi^2 k_B^2 T/3]$:

$$\begin{aligned}\sigma(\alpha) &\overset{\text{exact}}{=} nk_B\left[\frac{5}{2}t_u(\alpha) - \alpha\right]\,;\\ \frac{\sigma(\alpha)}{\sigma^0(\alpha)} &\overset{\text{exact}}{=} \frac{2}{\pi^2}\frac{\frac{5}{2}t_u(\alpha)-\alpha}{r(\alpha)} \overset{\text{Sommerfeld}}{\approx} 1 - \frac{\pi^2 r^2(\alpha)}{10} - \frac{247\pi^4 r^4(\alpha)}{5040} - \cdots\end{aligned} \tag{8}$$

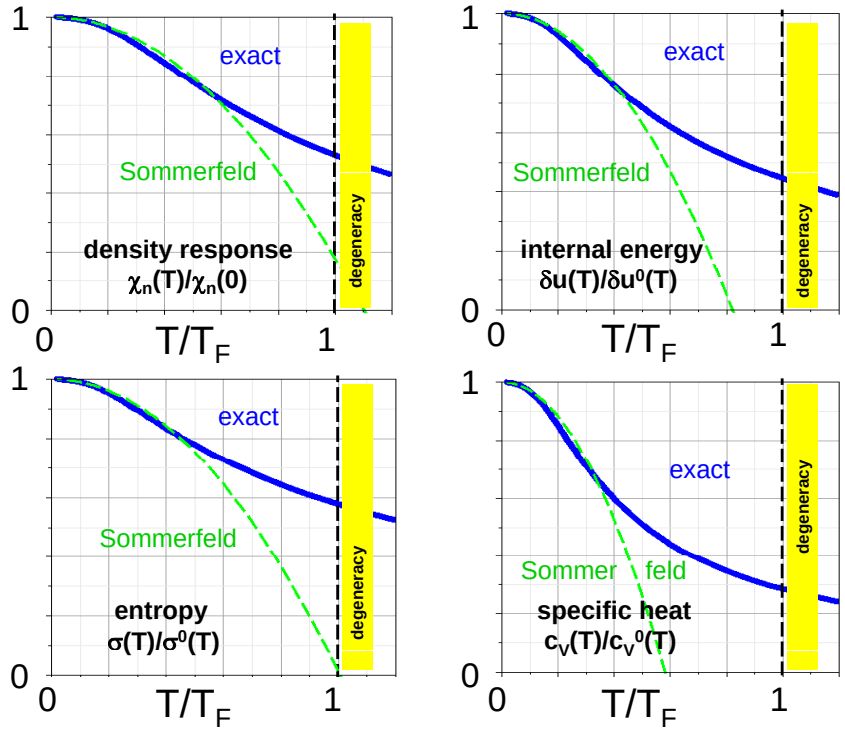

Figure 2: The degeneracy transition in Fermi liquids.

- The specific heat $c_V(\alpha)$ $[c_V^0(\alpha) = N_F \pi^2 k_B^2 T/3]$:

$$c_V(\alpha) \overset{\text{exact}}{=} \frac{3}{2} n k_B \left[\frac{5}{2} t_u(\alpha) - \frac{3}{2 t_n(\alpha)} \right] ;$$
$$\frac{c_V(\alpha)}{c_V^0(\alpha)} \overset{\text{exact}}{=} \frac{3}{\pi^2} \frac{\frac{5}{2} t_u(\alpha) - \frac{3}{2 t_n(\alpha)}}{r(\alpha)} \overset{\text{Sommerfeld}}{\approx} 1 - \frac{3\pi^2 r^2(\alpha)}{10} - \frac{247 \pi^4 r^4(\alpha)}{1008} - \cdots \qquad (9)$$

The classical counterparts of Eqs. (6)-(9) emerge in the limit as $t_n(\alpha \to -\infty) = t_u(\alpha \to -\infty) = 1$. It is worth noting that the derivation of the analytic form for $c_V(\alpha)$ involves an awkward term $\tilde{\mu} = \mu - T(d\mu/dT)$, which can, fortunately, be eliminated in favor of the more elegant expression $\tilde{\mu} = 3k_B T/2t_n$.

Conclusions

In summary, I have presented a rigorous analytic treatment of the degeneracy transition of relevant macroscopic observables like charge susceptibility $\chi_n^0(T)$, spin susceptibility $\chi_s^0(T)$, internal energy $u(T)$, entropy density $\sigma(T)$ and specific heat capacity $c_V(T)$ in Fermi liquids in terms of the tabulated polylogarithm functions $\mathrm{Li}_x^{(-)}(e^\alpha)$. Degeneracy is traditionally connected with the Fermi temperature $T_F = \mu(T=0)/k_B$ but, like in Bose many-body systems, it should rather be associated with the temperature T^*, at which the chemical potential $\mu(T^*) = 0$ changes sign. It turns out that only two transition functions $t_n(\alpha)$ and $t_u(\alpha)$ are capable to describe the degeneracy transition. The textbook results for the classical limit and the degenerate limit of these observables emerge in the limit as $\alpha \to -\infty$ $(z \to 0)$ and $\alpha \to \infty$ $(z \to \infty)$, respectively. These results show that the traditional low–T *Sommerfeld expansions* can be replaced by analytic forms involving the reduced temperature $r(\alpha)$ together with the transition functions $t_n(\alpha)$ and $t_u(\alpha)$ for each relevant observable. It should be noted, that in the degenerate regime there are further Fermi liquid corrections, which lead to renormalizations of the charge $[\chi_n = \chi_n^0/(1+F_0^s)]$ and spin $[\chi_s = \chi_s^0/(1+F_0^a)]$ responses, where

$F_0^{s,a}$ denote the dimensionless spin–symmetric and –antisymmetric ($\ell = 0$)–Landau parameters, respectively [1]. Strictly speaking, the Landau treatment of interaction effects through an expansion w.r.t. the dimensionless Landau parameters $F_\ell^{s,a}$ is valid only deeply in the degenerate regime. The question arises whether the physical meaning of these parameters may be thought to perpetuate into the regime of temperatures close to T_F, i.e. across the degeneracy transition.

References

[1] D. Vollhardt, and P. Wölfle (eds.) *The Superfluid Phases of Helium 3* (Taylor and Francis, London, 1990).
[2] D. Fairbank, D. B. S., C. W. F. Everitt, and P. F. Michelson (eds.) *Near Zero* (W. H. Freeman and Co., New York, 1988).
[3] A. Jonquière, Bulletin de la S. M. F. **17**, 142–152 (1889).
[4] R. Gross, A. Marx, and D. Einzel (eds.) *Festkörperphysik. Aufgaben und Lösungen* (De Gruyter, München, 2014).
[5] M. Abramowitz, and I. A. Stegun (eds.) *Handbook of Mathematical Functions* (Taylor and Francis, London, 1990).

Magnetism and stripe fluctuations in FeSe

A. Baum, T. Böhm, R. Hackl [1]
N. Lazarević, Z. V. Popović [2,3]
H. N. Ruiz, Yao Wang, B. Moritz, T. P. Devereaux [4,5]
P. Adelmann, T. Wolf [6]

Iron pnictides and chalcogenides are characterized by the proximity of various phases including magnetism and superconductivity. The magnetism of Fe-based systems does not directly follow from the Fe valence or changes in the Fermi surface topology [3, 4]. Some systems have nearly ordered localized moments, whereas FeSe does not order down to the lowest temperatures [5]. AFe$_2$As$_2$-based compounds (A = Ba, Sr, Eu or Ca) display aspects of itinerant spin-density-wave (SDW) magnetism with a gap in the electronic excitation spectrum. The material specific differences are a matter of intense discussion and low- and high-energy electronic as well as structural properties may contribute [3, 6, 7].

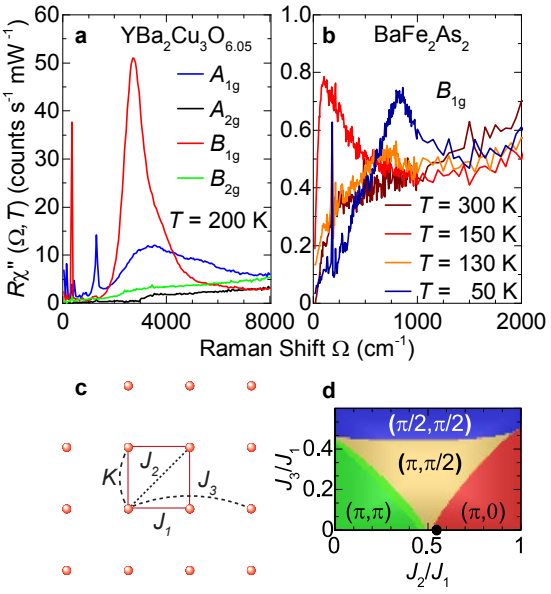

Figure 1: Localized and itinerant magnets. (**a**) Raman spectra of $YBa_2Cu_3O_{6.05}$ at all four accessible symmetries. From Ref. [1]. (**b**) B_{1g} spectra of $BaFe_2As_2$ at four characteristic temperatures. (**c**) A 4×4 cluster used for the simulations. Each Fe atom (red spheres) carries a localized spin $\mathbf{S}_i$, with $S = 1$. The dashed lines represent the exchange interactions, where K is the coefficient of a biquadratic term proportional to $(\mathbf{S}_i \cdot \mathbf{S}_j)^2$. (**d**) $J_2 - J_3$ phase diagram as obtained from our simulations at $T = 0$. The black point shows the parameters at which temperature-dependent simulations [2] have been performed.

Prototypical examples for the response of localized and itinerant magnetism are the Raman spectra of $YBa_2Cu_3O_{6.05}$ (YBCO) and of $BaFe_2As_2$ as shown in Fig. 1 (a) and (b), respectively. In YBCO [Fig. 1 (a)] a well-defined peak is observed in B_{1g} ($x^2 - y^2$) symmetry at approximately $2.84\,J_1$ as predicted theoretically on the basis of the Heisenberg model [8]. The response in the other symmetries is weaker. The temperature dependence of the B_{1g} peak is continuous [9]. In $BaFe_2As_2$ [Fig. 1 (b)] abrupt changes are observed in B_{1g} symmetry upon entering the SDW state: the fluctuation peak below $100\,\mathrm{cm}^{-1}$

[1]The project was funded by the German Research Foundation (DFG) via the Transregional Collaborative Research Center TRR 80 and the Priority Program SPP 1458 (grant-no. HA 2071/7). The collaborations with Stanford University and University of Belgrade were supported, respectively, by the Bavarian Californian Technology Center BaCaTeC (grant-no. A5 [2012-2]) and by the German Academic Exchange Service (DAAD) through the bilateral project between Serbia and Germany (grant-nos. 57142964 and 57335339).

[2]Center for Solid State Physics and New Materials, Institute of Physics Belgrade, University of Belgrade, Pregrevica 118, 11080 Belgrade, Serbia

[3]Serbian Academy of Sciences and Arts, Knez Mihailova 35, 11000 Belgrade, Serbia. Work was funded by the Serbian Ministry of Education, Science and Technological Development under Projects ON171032 and III45018.

[4]Stanford Institute for Materials and Energy Sciences, SLAC National Accelerator Laboratory, 2575 Sand Hill Road, Menlo Park, CA 94025, USA. Work in the SIMES at Stanford University and SLAC was supported by the U.S. Department of Energy, Office of Basic Energy Sciences, Division of Materials Sciences and Engineering, under Contract No. DE-AC02-76SF00515. Computational work was performed using the resources of the National Energy Research Scientific Computing Center supported by the U.S. Department of Energy, Office of Science, under Contract No. DE-AC02-05CH11231.

[5]Geballe Laboratory for Advanced Materials & Dept. of Applied Physics, Stanford University, CA 94305, USA.

[6]Karlsruher Institut für Technologie, Institut für Festkörperphysik, 76021 Karlsruhe, Germany

vanishes and the intensity is redistributed from low to high energies [10, 11]. This behavior is typical for an SDW or charge-density-wave (CDW) system [12].

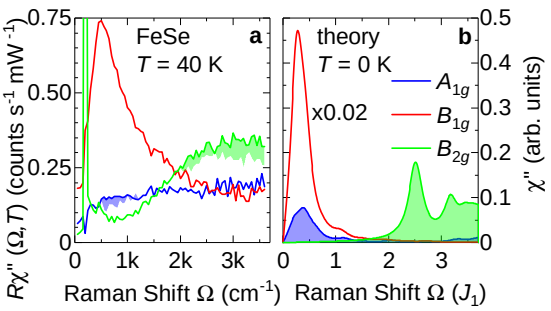

Figure 2: Experimental vs. theoretical Raman spectra of FeSe at low temperature and symmetries as indicated. From Ref. [2]. (**a**) The B_{1g} response dominates by far. In A_{1g} and B_{2g} symmetries the magnetic contribution (blue and green shaded areas at approximately 700 and 3 000 cm^{-1}, respectively) to the cross-section is very weak and can only be separated from the particle-hole continuum by comparing low and high-temperature spectra. (**b**) Simulation of the Raman spectra using exact diagonalization on a 4×4 cluster [see Fig. 1 (**c**)].

As shown in Fig. 2 (a), the response in FeSe is rather different from that in $BaFe_2As_2$: (i) The maximum in B_{1g} symmetry is found at a very low energy given that the exchange coupling J_1 is similarly large as in YBCO [7]. (ii) The peak does not vanish even at room temperature, and the variation with temperature is continuous [2]. These observations motivated a simulation of the magnetism in FeSe in terms of a (localized) J_1-J_2-J_3-K Heisenberg model [7] rather than an SDW. Using the exact diagonalization for a spin-1 system on a 4×4 cluster [Fig. 1 (c)], we have derived the phase diagram, hosting different types of spin order [Fig. 1 (d)], and the Raman response. The parameters are similar to those of Ref. [7], $J_1 = 123\,\mathrm{meV}$, $J_2/J_1 = 0.528$ and $J_3 = 0$, but we set $K/J_1 = 0.1 > 0$ (repulsive) in order to suppress a long range order. The result is shown in Fig. 2 (b). Since $J_2/J_1 = 0.528$ is very close to the frustration point between the Néel, dimer, and stripe orders [black point in Fig. 1 (d)], the B_{1g} maximum appears at an energy much smaller than J_1, in agreement with experiment, reflecting the fact that the energy for flipping two neighboring spins is very small. In addition, the positions and relative intensities of the A_{1g} and B_{2g} spectra are qualitatively reproduced. Similarly, the temperature dependence of the B_{1g} maximum and the shift from the Néel (π, π) to stripe $(\pi, 0)$ order upon cooling, as observed by neutron scattering [13], is properly reproduced. Detailed information is available in Ref. [2].

References

[1] N. Chelwani, A. Baum, T. Böhm, M. Opel, F. Venturini, A. Erb, H. Berger, L. Forró, and R. Hackl, ArXiv e-prints (2017). arXiv:1705.01496.

[2] A. Baum, H. N. Ruiz, N. Lazarević, Y. Wang, T. Böhm, R. Hosseinian Ahangharnejhad, P. Adelmann, T. Wolf, Z. V. Popović, B. Moritz, T. P. Devereaux, and R. Hackl, ArXiv e-prints (2017). arXiv:1709.08998.

[3] Z. P. Yin, K. Haule, and G. Kotliar, Nature Mater. **10**, 932–935 (2011).

[4] Q. Si, R. Yu, and E. Abrahams, Nat. Rev. Mater. **1**, 16017 (2016).

[5] S.-H. Baek, D. V. Efremov, J. M. Ok, J. S. Kim, J. van den Brink, and B. Büchner, Nature Mater. **14**, 210–214 (2014).

[6] I. I. Mazin, and M. D. Johannes, Nature Phys. **5**, 141 (2009).

[7] J. K. Glasbrenner, I. I. Mazin, H. O. Jeschke, P. J. Hirschfeld, R. M. Fernandes, and R. Valentí, Nature Phys. **11**, 953–958 (2015).

[8] S. A. Weidinger, and W. Zwerger, Eur. Phys. B **88**, 237 (2015).

[9] P. Knoll, C. Thomsen, M. Cardona, and P. Murugaraj, Phys. Rev. B **42**, 4842–4845 (1990).

[10] L. Chauvière, Y. Gallais, M. Cazayous, M. A. Méasson, A. Sacuto, D. Colson, and A. Forget, Phys. Rev. B **82**, 180521 (2010).

[11] S. Sugai, Y. Mizuno, R. Watanabe, T. Kawaguchi, K. Takenaka, H. Ikuta, Y. Takayanagi, N. Hayamizu, and Y. Sone, J. Phys. Soc. Japan **81**, 024718 (2012).

[12] H.-M. Eiter, M. Lavagnini, R. Hackl, E. A. Nowadnick, A. F. Kemper, T. P. Devereaux, J.-H. Chu, J. G. Analytis, I. R. Fisher, and L. Degiorgi, Proc. Nat. Acad. Sciences **110**, 64–69 (2013).

[13] Q. Wang, Y. Shen, B. Pan, X. Zhang, K. Ikeuchi, K. Iida, A. D. Christianson, H. C. Walker, D. T. Adroja, M. Abdel-Hafiez, X. Chen, D. A. Chareev, A. N. Vasiliev, and J. Zhao, Nature Commun. **7**, 12182 (2016).

Observation of the spin Nernst effect

M. Althammer, S. Meyer, S. Geprägs, H. Huebl, R. Gross [1]
S.T.B. Goennenwein [2,3]

Over the last years our WMI research had a particular focus on pure spin current physics, i.e. the flow of (spin) angular momentum. The spin Hall effect and the inverse spin Hall effect (ISHE) are the key ingredients for most experimental work on pure spin current phenomena, as they allow to transform a charge current into a spin current and vice versa. However, since in spin-orbit coupled electrical conductors the charge carriers transporting charge and spin also transport heat, not only a longitudinal charge current can generate a transverse pure spin current, but also a longitudinal heat current. The resulting spin-thermo-electric effect is called the spin Nernst effect (SNE). In a collaboration with the theory groups of G.E.W. Bauer and H. Ebert we were able to observe the SNE for the first time in heterostructures consisting of yttrium iron garnet (YIG) and platinum. This observation has been published recently in Nature Materials [1].

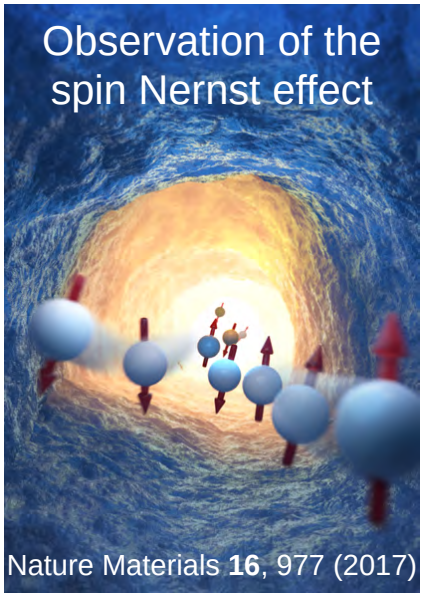

Figure 1: This artistic illustration of the spin Nernst effect was intended as the cover art for the publication in Nature Materials (©Christoph Hohmann, Nanosystems Initiative Munich, 2017).

In more detail, we utilize YIG/Pt heterostructures grown at the WMI to provide the first experimental evidence for the spin Nernst effect in Pt. These heterostructures enable us to modulate the spin current transport across the YIG/Pt interface by changing the orientation of the magnetization direction in the YIG and to detect the spin accumulation induced by the spin Nernst effect (SNE) in the charge channel, via the ISHE as a thermopower signal. This spin Nernst magneto-thermopower (SMT) is present in any electrical conductor with spin-orbit coupling, and can be experimentally discerned from the conventional Seebeck effect by selectively changing the spin current transport across the YIG/Pt interface.

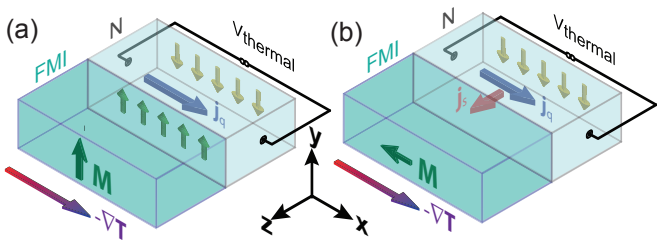

Figure 2: Boundary conditions for the spin Nernst magneto-thermopower (SMT): (a) For $\mathbf{M} \parallel \mathbf{y}$ the SNE generated spin current is compensated by the spin accumulation in the N and no SMT is detected. (b) For $\mathbf{M} \parallel -\mathbf{x}$, a finite pure spin current $\mathbf{j}_s$ flows across the FMI/N interface. Via the ISHE $\mathbf{j}_s$ generates an additional charge current in N and thus a finite SMT.

This concept is illustrated in Fig. 2(a) and (b). A paramagnetic metal film (N) is exposed to a temperature gradient $-\nabla T||\mathbf{x}$. Through the Seebeck effect, a thermopower arises along $\mathbf{x}$. Furthermore, because of the SNE, a transverse spin current is flowing along $\mathbf{z}$ with spin polarization along $\mathbf{y}$, resulting in a spin accumulation at the metal film boundaries, as sketched in Fig. 2(a). If $\mathbf{s}$ and $\mathbf{M}$ in the ferromagnetic insulator (FMI) are collinear (either parallel or antiparallel), there is no interfacial spin current and the ensuing spin accumulation in turn

[1]Financial support via the DFG Priority Program 1538 "Spin-Caloric Transport" (projects GO 944/4 and GR 1132/18) and the Nanosystems Initiative Munich (NIM) is gratefully acknowledged.
[2]Institut für Festkörperphysik, TU, 01062 Dresden, Germany.
[3]Center for Transport and Devices of Emergent Materials, TU Dresden, 01062 Dresden, Germany.

drives a diffusive spin current compensating the SNE spin current. In the steady state, the net transverse spin current flow vanishes and thus no SMT is measured. In contrast, when **s** and **M** enclose a finite angle, a finite spin current $\mathbf{j}_s$ flows across the interface, becoming maximal for **s** orthogonal to **M** [Fig. 2(b)], and an additional SMT signal contributes to the thermopower. In the experiment, we control the transverse spin current boundary conditions by systematically changing the orientation of the magnetization in the FMI layer, and record the ensuing spin-Nernst driven changes in the thermopower, i.e., the SMT. The phenomenology of the SMT is similar to the recently established spin Hall magnetoresistance (SMR) [2].

For our experiments, we used a YIG/Pt bilayer sample ($t_{YIG} = 40\,nm / t_{Pt} = 4.1\,nm$) and patterned it into a Hall bar as shown in Fig. 3(a). An additional YIG|Pt strip extending along **y** served as an on-chip heater. We generated a temperature difference $\Delta T = 18.0\,K$ by applying a constant power of 286 mW to the on-chip heater, while maintaining an average sample temperature $T_{sample} \approx 255\,K$. We then measured the thermopower $V_{thermal}$ along **x** [cf. Fig. 3(a)] while rotating the external magnetic field in the (**x**, **y**) plane.

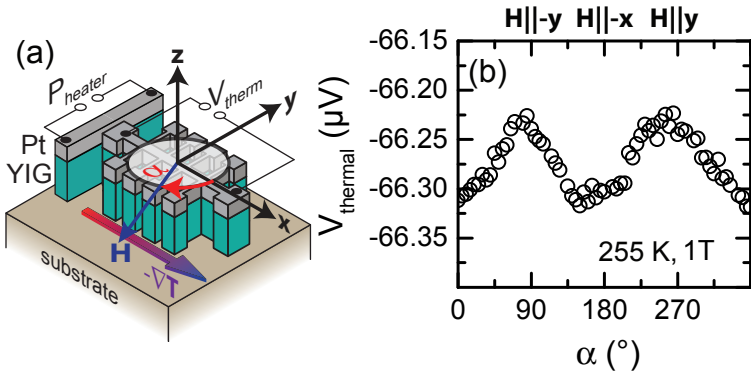

Figure 3: Setup of the SMT experiments. (a) A YIG|Pt Hall bar and an additional heater strip along **y** are defined by lithography. By applying an electric current with power P_{heater} to the heater strip, one end of the Hall bar is hotter than the other end that is connected to a heat sink provided by the sample holder, leading to a temperature gradient $-\nabla T$ along **x**. The magnetization vector **M** of the YIG layer is rotated by an external magnetic field $\mu_0 H = 1\,T$ in the rotation plane spanned by (**x**, **y**). The measured thermal voltage $V_{thermal}$ for this geometry is depicted in panel (b).

The external magnetic field $\mu_0 H = 1\,T$ is much larger than the demagnetization and anisotropy fields of YIG, such that $\mathbf{M} \parallel \mathbf{H}$. Then, $\mathbf{H} \parallel \mathbf{y}$ corresponds to $\mathbf{M} \parallel \mathbf{s}$ and thus open boundary conditions (no spin current flow across the interface), while for $\mathbf{H}||\mathbf{x}$ and $\mathbf{H}||\mathbf{z}$ the ferrimagnet represents an efficient spin current sink resulting in maximum spin current flow across the interface.

Our measurements confirm this expectation: For open boundary conditions, $V_{thermal} = -66.225\,\mu V$ is about $\Delta V_{thermal} = 100\,nV$ larger than for short-circuit conditions, with a relative signal amplitude of $|\Delta V_{thermal}/V_{thermal}| = (1.5 \pm 0.3) \times 10^{-3}$, see Fig. 3(b). We reproduced this behavior for full 360° rotations of the applied field in the sample plane spanned by **x** and **y**, leading to a $\sin^2 \alpha$ behavior of $V_{thermal}$ with minima for no interfacial spin current flow ($\alpha = 0°, 180°$), and maxima for a maximum interfacial spin current flow ($\alpha = 90°, 270°$). From these experiments we extract a spin Nernst angle of $\theta_{SN} = -0.20$ for Pt, which is in fair agreement to first-principles calculations [1].

This first experimental observation of the spin Nernst effect opens up new avenues for the thermal generation of pure spin currents and completes the experimental picture of spin-thermo-electric effects.

References

[1] S. Meyer, Y.-T. Chen, S. Wimmer, M. Althammer, T. Wimmer, R. Schlitz, S. Geprägs, H. Huebl, D. Ködderitzsch, H. Ebert, G. E. W. Bauer, R. Gross, and S. T. B. Goennenwein, Nat. Mater. **16**, 977 (2017).

[2] M. Althammer, S. Meyer, H. Nakayama, M. Schreier, S. Altmannshofer, M. Weiler, H. Huebl, S. Geprägs, M. Opel, R. Gross, D. Meier, C. Klewe, T. Kuschel, J.-M. Schmalhorst, G. Reiss, L. Shen, A. Gupta, Y.-T. Chen, G. E. W. Bauer, E. Saitoh, and S. T. B. Goennenwein, Phys. Rev. B **87**, 224401 (2013).

Spin Hall magnetoresistance in antiferromagnet/normal metal heterostructures

J. Fischer, K. Ganzhorn, N. Vlietstra, M. Althammer, H. Huebl, M. Opel, R. Gross, S. Geprägs [1] *O. Gomonay* [2] *R. Schlitz, S.T.B. Goennenwein* [3]

Spintronic devices integrating ferromagnetic materials and normal metals in multilayer hybrid structures represent well established basic elements in the field of data storage. For future spintronic applications, *anti*ferromagnetic materials have come into the focus of interest. They promise robustness against external magnetic field perturbations as well as faster magnetization dynamics compared to simple ferromagnets, paving the way to ultrafast information processing. For integration in data storage devices, a robust detection scheme for their magnetization state is required. The spin Hall magnetoresistance (SMR) [1] could serve as a sensitive probe in this regard. It originates from the interplay of charge and spin currents at the interface between a magnetic insulator and a metal with strong spin-orbit coupling. Here, we focus on the SMR in antiferromagnetic insulator/heavy metal (AFI/HM)) thin film bilayers using NiO as the AFI and Pt as the HM layer.

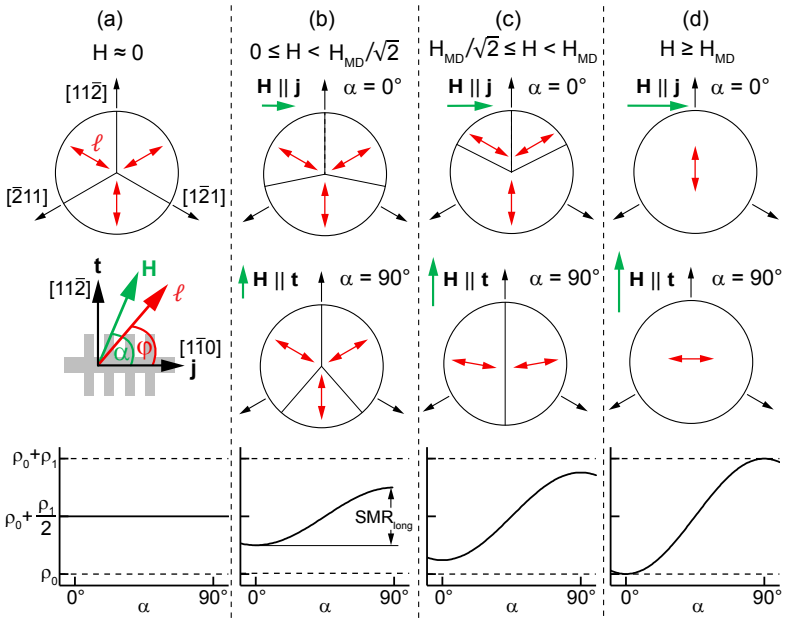

Figure 1: Magnetic configurations in the magnetically easy (111) plane of NiO for an in-plane rotation of the magnetic field **H** with α representing the angle between **H** and the current density direction **j** for (a) $H \approx 0$, (b) $0 < H < H_{\mathrm{MD}}/\sqrt{2}$, (c) $H_{\mathrm{MD}}/\sqrt{2} \leq H < H_{\mathrm{MD}}$, and (d) $H \geq H_{\mathrm{MD}}$ with the monodomainization field H_{MD}. Top: Evolution of the antiferromagnetic multi-domain state in NiO with the Néel vector $\boldsymbol{\ell}^{(k)}$ of each domain k (red double arrows) for an applied magnetic field along **j** ($\alpha = 0°$). Middle: Same for **H** along **t** ($\alpha = 90°$). Bottom: Expected angular dependence of the resistivity ρ_{long} of a NiO/Pt Hall bar within the SMR theory. The inset shows the orientation of the Pt Hall bar, the magnetic field **H**, and the Néel vector $\boldsymbol{\ell}$ with respect to the NiO in-plane directions.

Below the Néel temperature of NiO (523 K), the Néel vector $\boldsymbol{\ell}$ is aligned along the $\langle 11\bar{2} \rangle$ easy axes at zero magnetic field, resulting in three types ($k = 1, 2, 3$) of physically distinguishable antiferromagnetic domains [cf. Fig. 1(a)]. A finite applied magnetic field **H** splits the degeneracy of the energetically equivalent domains and creates an effective (ponderomotive) force able to push the domain walls towards the energetically unfavourable domains. This leads to a domain redistribution at low magnetic field magnitudes, while a coherent rotation of $\boldsymbol{\ell}$ perpendicular to **H** starts at higher magnetic field values when most of the unfavourable domains are removed. This process is schematically shown in Fig. 1(b-d).

While the external magnetic field triggers domain redistribution, another mechanism, based on magneto-elastic interactions, is responsible for restoring the domain structure after

[1] This work is financially supported by the German Research Foundation via the Priority Program SPP 1538 (projects GO 944/4 and GR 1132/18), and a Laura-Bassi stipend of the Technical University of Munich.

[2] Institut für Physik, Johannes Gutenberg Universität Mainz.

[3] Institut für Festkörper- und Materialphysik, Technische Universität Dresden.

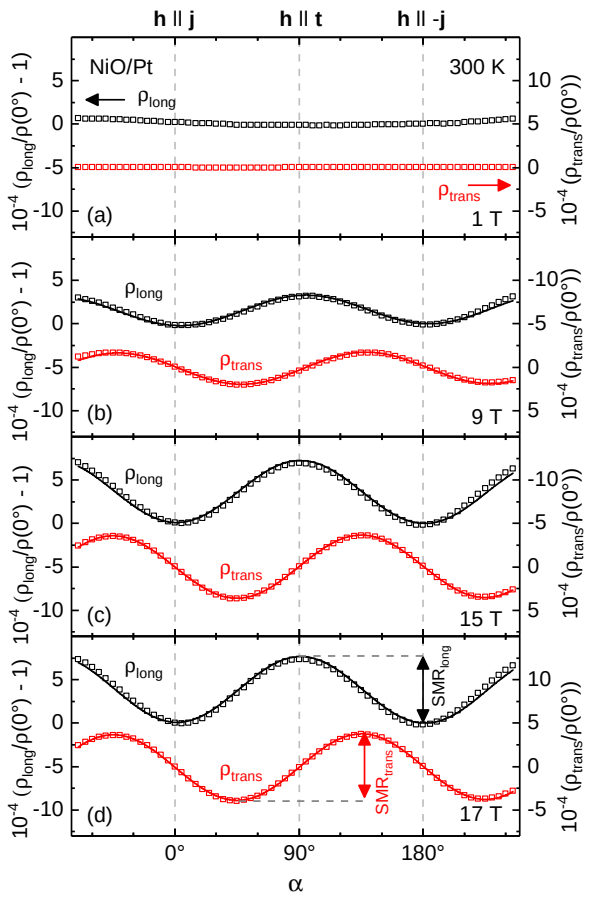

Figure 2: ADMR of a NiO(111)/Pt thin film heterostructure, measured at 300 K with in-plane external magnetic field magnitudes of (a) 1 T, (b) 9 T, (c) 15 T, (d) 17 T. Normalized longitudinal resistivity ρ_{long} (black symbols) and transverse resistivity ρ_{trans} (red symbols) as a function of the magnetic field orientation α. The lines are fits to the data using $\cos 2\alpha$ and $\sin 2\alpha$ functions [cf. Eqs. (1)].

the magnetic field is removed. In antiferromagnets with pronounced magneto-elastic coupling this mechanism is based on strain release effects (destressing effects), which is an elastic analogue to the demagnetization phenomenon in ferromagnets. Therefore, the domain structure in the presence of an external magnetic field **H** can be calculated by minimizing the sum of the Zeeman energy, the magnetic anisotropy, and the destressing energy. With the obtained domain fractions, the component of the resistivtiy tensor of the Pt layer $\boldsymbol{\rho}$ along the current direction **j** (**t**), coinciding with the longitudinal (transverse) resistivity ρ_{long} (ρ_{trans}) can be calculated within the SMR theory [2] by averaging over the Pt resistance contributions from individual NiO domains to

$$\begin{aligned} \rho_{\mathrm{long}} &= \rho_0 + \frac{\rho_1}{2}\left(1 - \frac{H^2}{H_{\mathrm{MD}}^2}\cos 2\alpha\right) , \\ \rho_{\mathrm{trans}} &= -\frac{\rho_3}{2}\frac{H^2}{H_{\mathrm{MD}}^2}\sin 2\alpha , \end{aligned} \tag{1}$$

where ρ_0 is approximately equal to the normal resistivity of the Pt layer [3] and ρ_1 (ρ_3) represents the SMR coefficient with $\rho_1(\rho_3) \ll \rho_0$. H_{MD} can be identified as the monodomainization field and is given by the destressing field H_{dest} and the exchange field H_{ex} as $2\sqrt{H_{\mathrm{dest}}H_{\mathrm{ex}}}$. The longitudinal resistivity ρ_{long} thus oscillates around $\rho_0 + \rho_1/2$ as schematically shown in Fig. 1. The SMR amplitudes are then given by

$$\begin{aligned} \mathrm{SMR}_{\mathrm{long}} &\approx \frac{\rho_1}{\rho_0}\frac{H^2}{H_{\mathrm{MD}}^2} , \\ \mathrm{SMR}_{\mathrm{trans}} &\approx \frac{\rho_3}{\rho_0}\frac{H^2}{H_{\mathrm{MD}}^2} , \end{aligned} \tag{2}$$

increasing quadratically with the external magnetic field magnitude H.

To corroborate this model, we fabricated a 120 nm thick, epitaxial, (111)-oriented NiO thin film on a (0001)-oriented Al_2O_3 substrate via pulsed laser deposition. Subsequently, the NiO thin film was covered by a 3.5 nm thin Pt layer by electron-beam evaporation *in-situ*, without breaking the vacuum. To measure the SMR in NiO/Pt, we use angular-dependent magnetoresistance (ADMR) measurements, rotating the magnetic field with a constant magnitude in the easy (111)-plane of NiO. For the ADMR measurements, the sample is patterned into a Hall bar mesa structure via optical lithography and Ar ion milling. The longitudinal (ρ_{long}) and transverse resistivities (ρ_{trans}) are calculated from the longitudinal and the transverse voltages V_{long} and V_{trans}, measured with a standard four-probe technique.

The data obtained from the ADMR measurements at different magnetic field magnitudes are shown in Fig. 2. The predicted $\cos 2\alpha$ dependence of ρ_{long} as well as the $-\sin 2\alpha$-dependence

of ρ_{trans} with increasing amplitudes as a function of the applied magnetic field strength are clearly observed for $\mu_0 H > 1\,T$. The angular dependence is shifted by 90° with respect to previous experiments in Pt on collinear ferrimagnets [1]. This provides evidence that we are indeed sensitive to ℓ in the antiferromagnetic NiO. To evaluate the field dependence of the modulation of ρ_{long} and ρ_{trans} as well as the SMR amplitudes SMR_{long} and SMR_{trans}, we fit our data according to Eqs. (1) using $\cos 2\alpha$ and $\sin 2\alpha$ functions, respectively. The fits are shown as solid lines in Fig. 2(b-d).

The SMR amplitudes obtained in this way are depicted in Fig. 3 as a function of the external magnetic field H. As expected from Eq. (2), we observe a quadratic dependence of the SMR amplitudes on H for small magnetic fields. At higher fields, the SMR amplitudes start to saturate. To determine H_{MD}, we fit the SMR amplitudes according to Eqs. (2). The best fit was obtained for $\mu_0 H_{MD}^{film} = 13.4\,T$ (cf. green line in Fig. 3). H_{MD} is highly dependent on the specific sample used for the experiment. This is further evidenced by evaluating the data published by Hoogeboom and coworkers using a NiO/Pt sample based on a NiO single crystal [4]. For this sample we derive a significantly lower value of $\mu_0 H_{MD}^{cryst} = 4.1\,T$.

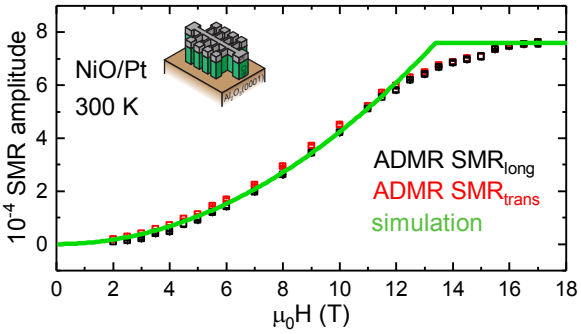

Figure 3: SMR amplitude of the NiO(111)/Pt thin film bilayer obtained from ADMR measurements at 300 K at different applied magnetic fields (cf. Fig. 2) for the longitudinal (black symbols) and transverse (red symbols) resistivities. The data are compared to the analytical model based on a magnetic field induced domain redistribution in NiO (green line).

In addition, the destressing field $H_{dest} = H_{MD}^2/(4H_{ex})$, which is a measure of the local internal stress fields created by the antiferromagnetic ordering, can be determined by using $\mu_0 H_{ex} = 968.4\,T$. We obtain $\mu_0 H_{dest}^{film} = 46\,mT$ for our NiO/Pt thin film sample and $\mu_0 H_{dest}^{cryst} = 4\,mT$ for the bulk NiO/Pt sample of Ref. [4]. Thus, H_{dest} is one order of magnitude larger in our NiO/Pt thin film heterostructure than in NiO/Pt hybrids using NiO single crystals. This is mainly caused by the elastic clamping of the NiO thin film on the Al_2O_3 substrate.

In summary, our study of the field dependence of the SMR amplitude and the comparison to simulations provides conclusive evidence for magnetic field induced domain redistribution due to movable antiferromagnetic domain walls as the dominant effect for the field dependence of the SMR in NiO/Pt heterostructures. We further demonstrate that the SMR is a versatile tool to investigate not only the magnetic spin structure, but also local magnetoelastic effects in antiferromagnetic materials. More details on this work can be found in Ref. [5].

References

[1] M. Althammer, S. Meyer, H. Nakayama, M. Schreier, S. Altmannshofer, M. Weiler, H. Huebl, S. Geprägs, M. Opel, R. Gross, D. Meier, C. Klewe, T. Kuschel, J.-M. Schmalhorst, G. Reiss, L. Shen, A. Gupta, Y.-T. Chen, G. E. W. Bauer, E. Saitoh, and S. T. B. Goennenwein, Phys. Rev. B **87**, 224401 (2013).

[2] K. Ganzhorn, J. Barker, R. Schlitz, B. A. Piot, K. Ollefs, F. Guillou, F. Wilhelm, A. Rogalev, M. Opel, M. Althammer, S. Geprägs, H. Huebl, R. Gross, G. E. W. Bauer, and S. T. B. Goennenwein, Phys. Rev. B **94**, 094401 (2016).

[3] Y.-T. Chen, S. Takahashi, H. Nakayama, M. Althammer, S. T. B. Goennenwein, E. Saitoh, and G. E. W. Bauer, Phys. Rev. B **87**, 144411 (2013).

[4] G. R. Hoogeboom, A. Aqeel, T. Kuschel, T. T. M. Palstra, and B. J. van Wees, Appl. Phys. Lett. **111**, 052409 (2017).

[5] J. Fischer, O. Gomonay, R. Schlitz, K. Ganzhorn, N. Vlietstra, M. Althammer, H. Huebl, M. Opel, R. Gross, S. T. B. Goennenwein, and S. Geprägs, ArXiv e-prints (2017). arXiv:1709.04158 [cond-mat.mes-hall].

Application–Oriented Research

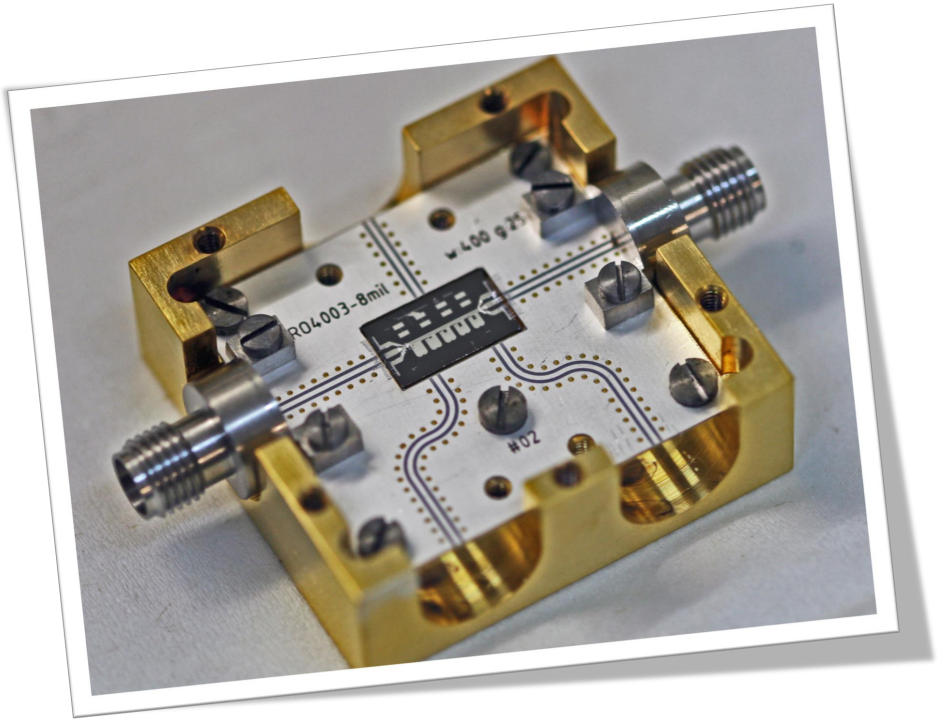

Sample box with printed circuit board and superconducting quantum circuit chip.

Frequency control and coherent excitation transfer in a nanostring resonator network

D. Schwienbacher, M. Pernpeintner, P. Schmidt, R. Gross, H. Huebl [1]

The coupling, synchronization, and non-linear dynamics of resonator modes are omnipresent in nature [1] and highly relevant for a multitude of applications, like lasers, Josephson arrays and spin torque oscillators. Nanomechanical resonators are ideal candidates to study these effects on a fundamental level [2] as well as to realize all-mechanical platforms for information processing [3] and storage [4]. For larger resonator networks, however, this requires the ability to tune the mode frequencies selectively and to operate the resonators in the strong coupling regime. We present a proof-of-principle realization of a resonator network consisting of two high-quality silicon-nitride nanostring resonators (in the following referred to as resonator A and B, respectively), coupled mechanically by a shared support. We demonstrate that we can control the fundamental mode frequencies of both nanostrings independently by a strong drive tone resonant with one of the higher harmonics of the network. The tuning mechanism relies on an effective increase of the pre-stress in a highly excited nanostring, known as geometric nonlinearity. Using this selective frequency control of the individual nanomechanical resonators, we investigate the coherent dynamics of the resonator network.

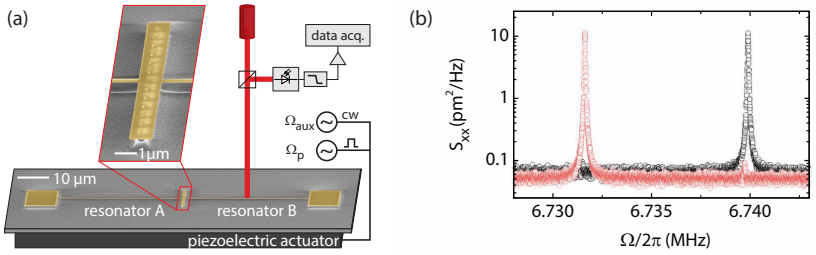

Figure 1: *Experimental setup and thermal motion spectra.* (a) False-colored scanning electron microscope image of the sample and schematic illustration of the experimental setup. (b) Thermal motion spectra of both nanostrings (A and B).

The experimental setup is sketched in Fig. 1(a). The sample is mounted in vacuum to prevent air damping of the string motion and all experiments are performed at room temperature. Both nanostrings can be excited and frequency controlled with a global external mechanical drive provided by a piezoelectric actuator. For readout of the mechanical motion, we use laser interferometry and analyze the signal with a spectrum analyzer or a digitizer card. Hereby, we gain access to the nanostring's thermal motion spectrum as well as the dynamic evolution of the coupled system. Figure 1(b) displays the measured thermal motion spectra when probing nanostring A (red circles) and B (black circles) without any applied drive.

To demonstrate that the frequency of the nanostrings can be tuned utilizing the geometric nonlinearity, we employ a strong auxiliary drive via the piezoelectric actuator exciting the second-order

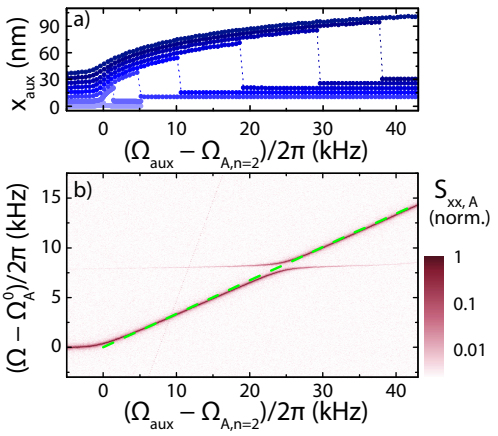

Figure 2: *Frequency tuning and mode splitting.* (a) Amplitude spectrum of the second-order mode (*auxiliary mode*) of nanostring A for different drive amplitudes. (b) Thermal motion spectrum of nanostring A as a function of the auxiliary drive frequency demonstrating frequency tunability.

[1] The authors acknowledge support from the German Excellence Initiative via the Nanosystems Initiative Munich (NIM).

mode (*auxiliary mode*) of nanostring A. Figure 2(a) shows the amplitude spectrum of the auxiliary mode for a strong coherent drive. As expected for a Duffing oscillator with positive cubic nonlinearity, we observe an increase of the effective resonance frequency for strong drive amplitudes. More importantly, the excitation amplitude of the auxiliary mode is related to the drive frequency. We use this well-known behavior to tune the eigenfrequency of the fundamental mode. To this end, we measure the thermal motion spectrum of the fundamental out-of-plane mode of nanostring A as a function of the auxiliary drive frequency Ω_{aux}, as shown in Fig. 2(b) (see also Ref. [5]). We use a constant auxiliary drive amplitude and gradually increase the frequency Ω_{aux}. The tuning effect is clearly visible once the auxiliary mode enters the nonlinear regime. Here, the fundamental mode frequency quantitatively follows our model depicted as the green dashed line in Fig. 2(b) (see also Ref. [5]). Around $\Omega_{\mathrm{aux}} - \Omega_{\mathrm{A},n=2} \approx 2\pi \times 25\,\mathrm{kHz}$, we observe an avoided crossing of the two fundamental out-of-plane modes of nanostrings A and B, with a mode splitting of 830 Hz, well exceeding the mechanical linewidth, $\approx 42\,\mathrm{Hz}$, and therefore placing the system in the strong coupling regime.

We start with the coherent oscillatory exchange of excitations between the fundamental out-of-plane modes of nanostrings A and B, the classical analog of Rabi oscillations in a quantum two-level system (see also Refs. [6, 7]). We initialize the system by exciting the lower mode resonantly with a short pulse of duration t_{p} and amplitude V_{p} as sketched in Fig.3(a). In a single-shot experiment, we measure the displacement of nanostring A as a function of time, followed by digital down-conversion and low-pass filtering. Hereby, we study the time evolution of the energy stored in this resonator, which is proportional to the square of its motional amplitude.

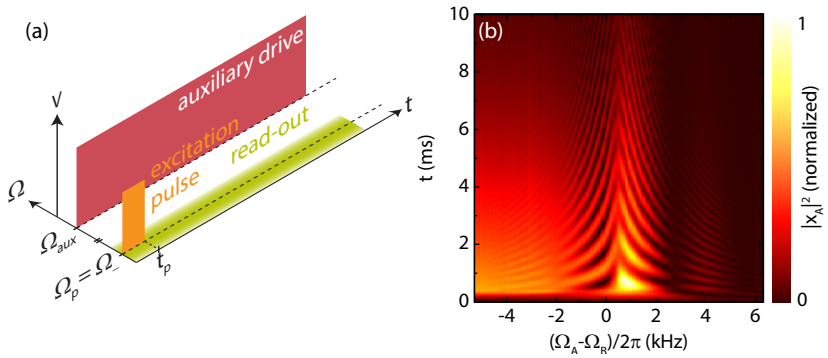

Figure 3: *Rabi oscillations.* (a) Measurement scheme: After a short excitation pulse at the lower mode's frequency Ω_-, the displacement of nanostring A is measured as a function of time. A constant drive tone at the auxiliary frequency Ω_{aux} is used to control the eigenfrequency of nanostring A. (b) Squared displacement amplitude of the fundamental mode of nanostring A as a function of time t and detuning.

In summary, we demonstrate individual frequency control of resonators on a single chip without using local control gates. Our work opens the path towards targeted transfer of excitations in phonon networks. Further details and results are given in Ref. [5].

References

[1] A. Pikovsky, M. Rosenblum, and J. Kurths. *Synchronization: A Universal Concept in Nonlinear Sciences* (Cambridge University Press, 2003).
[2] S.-B. Shim, M. Imboden, and P. Mohanty, Science **316**, 95 (2007).
[3] D. Hatanaka, I. Mahboob, K. Onomitsu, and H. Yamaguchi, Appl. Phys. Lett. **102**, 213102 (2013).
[4] A. D. O'Connell, M. Hofheinz, M. Ansmann, R. C. Bialczak, M. Lenander, E. Lucero, M. Neeley, D. Sank, H. Wang, M. Weides, J. Wenner, J. M. Martinis, and A. N. Cleland, Nature **464**, 697 (2010).
[5] M. Pernpeintner, P. Schmidt, D. Schwienbacher, R. Gross, and H. Huebl. Frequency control and coherent excitation transfer in a nanostring resonator network. arXiv:1612.07511 (2016).
[6] T. Faust, J. Rieger, M. J. Seitner, P. Krenn, J. P. Kotthaus, and E. M. Weig, Phys. Rev. Lett. **109**, 037205 (2012).
[7] T. Faust, J. Rieger, M. J. Seitner, J. P. Kotthaus, and E. M. Weig, Nat. Phys. **9**, 485 (2013).

Towards a scalable 3D quantum memory

E. Xie, F. Deppe, D. Repp, P. Eder, M. Fischer, J. Goetz, S. Pogorzalek, K. G. Fedorov, A. Marx, R. Gross [1]

For superconducting quantum bits dispersively coupled to three-dimensional (3D) microwave cavities, both T_1- and T_2-times in excess of 100 µs have been achieved [1]. Moreover, due to the small losses of superconducting materials intrinsic photon lifetimes of the order of 10 ms have been demonstrated recently for 3D microwave cavities [2]. This makes them attractive for the realization of a quantum memory, allowing to store quantum information on 10 ms time scales. There are two particular drawbacks with such memories. First, the 3D cavity architecture is bulky in comparison to its (less coherent) 2D counterpart. Second, the huge quality factors Q of the 3D microwave cavities result in a long cavity ring down and, in turn, in long readout times.

A more scalable device with fast readout can be built by exploiting the multi-mode structure of the 3D cavity. In such configuration one high-Q mode can be used for storage, while another low-Q mode can be used for readout. Here, we present an experimental study on such a device: a transmon qubit capacitively coupled to two distinct modes of a single 3D microwave cavity. Our device offers a fast readout capability simultaneously with a cavity enhanced coherence time. To obtain two modes with high and low Q, we engineer the fundamental and the first harmonic modes of a single cavity in such a way that the former (low-Q mode) couples well to the external feedline, whereas the latter (high-Q mode) has negligible coupling to the feedline and is limited only by the internal quality factor of the superconducting cavity. The qubit is dispersively coupled to both modes with the rate $g/2\pi \simeq 60\,\mathrm{MHz}$. In the experimentally studied device, the low-Q readout mode has a resonant frequency of $\omega_{\mathrm{RO}}/2\pi = 5.518\,\mathrm{GHz}$ and a decay rate of $\kappa_{\mathrm{RO}}/2\pi = 4 \times 10^6\,\mathrm{s}^{-1}$. The high-$Q$ storage mode has a resonant frequency of $\omega_{\mathrm{s}}/2\pi = 8.707\,546\,\mathrm{GHz}$ and a decay rate of $\kappa_{\mathrm{s}}/2\pi = 2.47 \times 10^4\,\mathrm{s}^{-1}$. That is, the decay rate of the readout mode is by more than two orders of magnitude larger than that of the storage mode, allowing for fast readout of the quantum information stored in the storage mode with very small decay rate.

With respect to the results presented in [3], two major improvements are implemented in the current design of our devices. Both aim at a reduced decay rate and hence increased lifetime of the storage mode without sacrificing the fast readout enabled by a high decay rate of the readout mode. First, in order to reduce the coupling rate of the storage mode to the antenna of the feedline, the latter has to be precisely positioned at a node of the electric field and be as thin as possible. Precise positioning requires to keep the electric field distribution of the storage mode symmetric with regard to the antenna position. This is achieved by additionally inserting a bare silicon (dummy) chip positioned completely symmetric to the qubit chip [cf. Fig. 1 (a)]. This avoids any distortion of the electric field distribution by an asymmetrically positioned dielectric material. Second, the diameter of the antenna used to couple to the readout mode is reduced to 0.1 mm. Together with the precise positioning this results in a significantly enhanced external quality factor of the storage mode.

With the second-order coupling sequence introduced in [3, 4], we observe a memory lifetime of $T_1^{\mathrm{mem}} \approx 8.0\,\mu\mathrm{s}$ and $T_2^{\mathrm{mem}} \approx 15.5\,\mu\mathrm{s}$ [cf. Fig. 1(b)]. These values constitute an enhancement by a factor of 6 as compared to the corresponding timescales of the bare qubit. Furthermore, the ratio between the storage time and the readout time accounts to 100, exceeding that found in the previous experiments [4–6]. Realistic simulations show that these values are currently

[1] The authors acknowledge support from the German Research Foundation through FE 1564/1-1, the doctorate program ExQM of the Elite Network of Bavaria, the IMPRS 'Quantum Science and Technology', and the German Excellence Initiative via the 'Nanosystems Initiative Munich' (NIM).

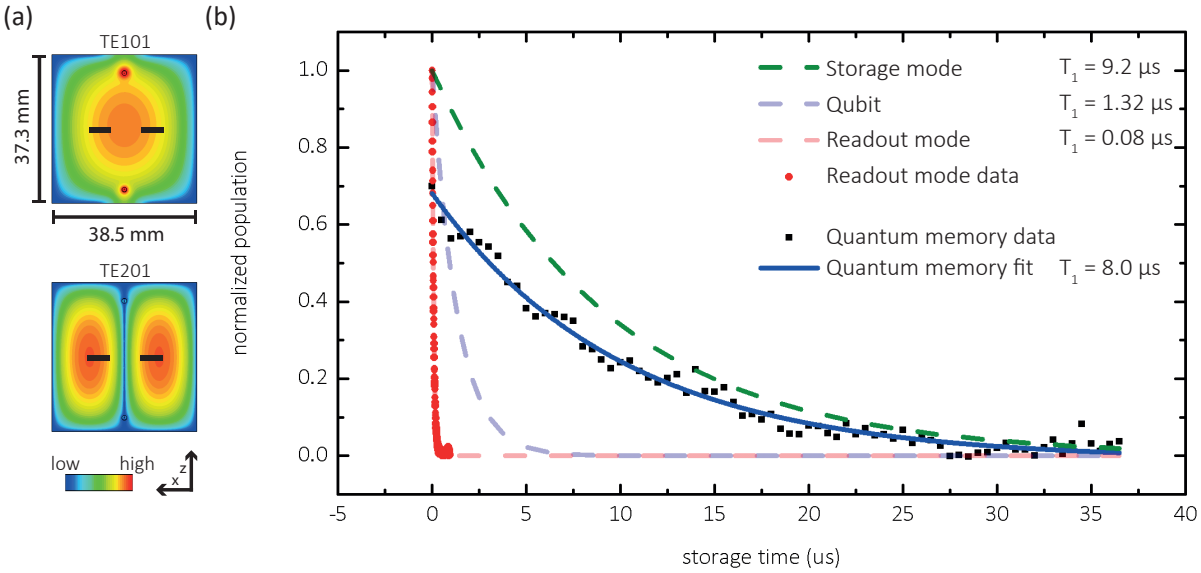

Figure 1: (a) Spatial distribution of the electric field amplitude inside the 3D cavity with dimensions (xyz) $38.5 \times 7.4 \times 37.3\,\mathrm{mm}^3$. Due to symmetric placements of two silicon chips (black rectangles), the field distribution remains symmetric with regard to the antenna positions (dots). (b) Exponential decay traces of the relevant system parameters. The memory lifetime is by a factor of 6 larger than the bare qubit lifetime.

not limited by any fundamental constraints, but can be further increased by well-known approaches increasing the external and internal quality factors of the storage mode.

For our quantum memory protocol, we are able to store and retrieve superposition states and find a Z-fidelity of $F_Z = 82\,\%$. For short drive pulses, the fidelity is limited by the limited qubit anharmonicity, which is a general weakness of transmon qubits. In detail, this means that the qubit is excited to higher levels beyond the computational space of $|g\rangle$ and $|e\rangle$. We expect that this problem can be overcome in future by optimal control pulses, which avoid state leakage [7]. For long drive pulses, the fidelity is limited by the qubit decay.

References

[1] M. H. Devoret, and R. J. Schoelkopf, Science **339**, 1169–1174 (2013).
[2] M. Reagor, H. Paik, G. Catelani, L. Sun, C. Axline, E. Holland, I. M. Pop, N. a. Masluk, T. Brecht, L. Frunzio, M. H. Devoret, L. Glazman, and R. J. Schoelkopf, Appl. Phys. Lett. **102**, 192604 (2013).
[3] E. Xie, F. Deppe, D. Repp, P. Eder, M. Fischer, J. Goetz, F. Wulschner, K. G. Fedorov, A. Marx, and R. Gross, WMI Ann. Rep. **2016**, 51–52 (2016).
[4] P. J. Leek, M. Baur, J. M. Fink, R. Bianchetti, L. Steffen, S. Filipp, and A. Wallraff, Phys. Rev. Lett. **104**, 100504 (2010).
[5] B. Vlastakis, G. Kirchmair, Z. Leghtas, S. E. Nigg, L. Frunzio, S. M. Girvin, M. Mirrahimi, M. H. Devoret, and R. J. Schoelkopf, Science **342**, 607–610 (2013).
[6] A. J. Sirois, M. A. Castellanos-Beltran, M. P. Defeo, L. Ranzani, F. Lecocq, R. W. Simmonds, J. D. Teufel, and J. Aumentado, Appl. Phys. Lett. **106**, 172603 (2015).
[7] F. Motzoi, J. M. Gambetta, P. Rebentrost, and F. K. Wilhelm, Phys. Rev. Lett. **103**, 110501 (2009).

Characterization of tunable resonators for quantum simulation

M. Fischer, C. Besson, P. Eder, S. Pogorzalek, E. Xie, K. Fedorov, F. Deppe, A. Marx, R. Gross[1]

Quantum simulation is believed to be a very promising tool to investigate the quantum mechanical behavior of many-body systems, which are too complex to be handled efficiently with current computing architectures. A particular system, where quantum simulation is beneficial, consists of interacting bosons on a lattice. It can be modelled on the platform based on superconducting quantum circuits using capacitively coupled waveguide resonators with DC-SQUIDs galvanically coupled to their current maxima [1, 2]. Due to the nonlinear inductance of the DC-SQUIDs an array of coupled nonlinear resonators with tuneable resonant frequency and nonlinearity is obtained. The latter results in an effective photon-photon interaction which is tuneable by an applied magnetic flux.

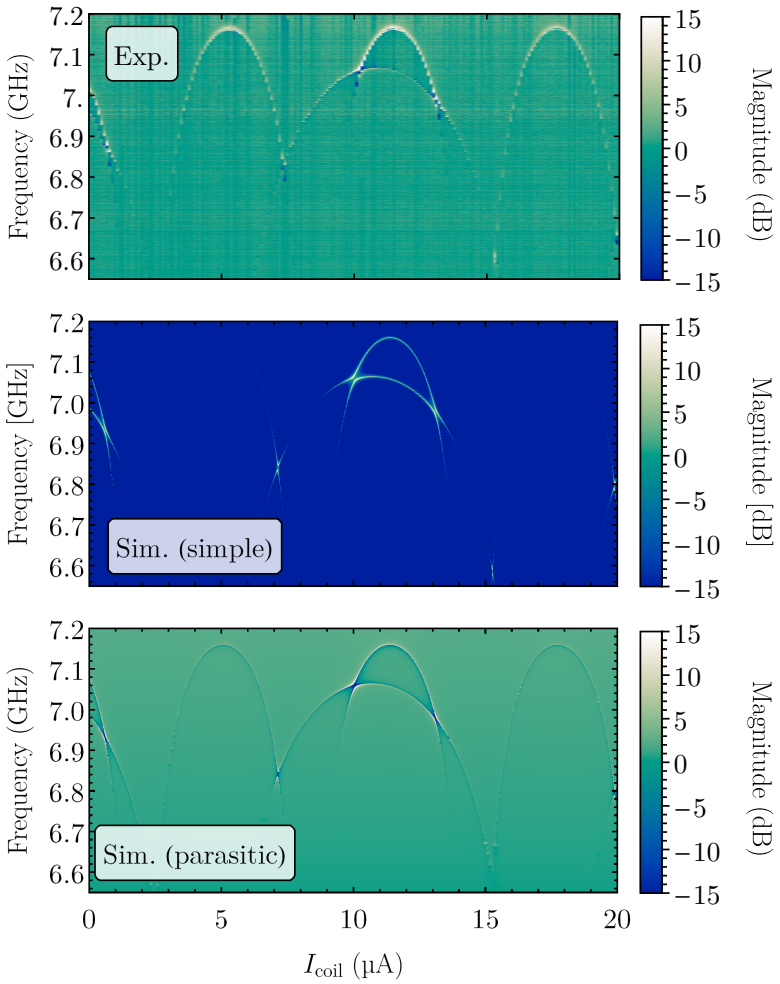

Figure 1: Top panel: Measured frequency response of the two-resonator chip as a function of the current through the coil, I_{coil}. Middle panel: Theoretical model without a parasitic path. Bottom panel: Theoretical model including a parallel parasitic path (see Fig. 2).

In our first experiments we use the simplest non-trivial case of a one-dimensional array, i.e., a chip with two nonlinear resonators coupled in series. In order to achieve good knowledge on our system, we investigate the microwave transmission while tuning the resonant frequency and nonlinearity of the resonators by an applied flux. The latter is generated either by a current fed through a superconducting coil placed near the sample or through one of the two on-chip antennas. As the coil creates a homogeneous magnetic field across the whole chip, the critical currents of both SQUIDs are modulated simultaneously. The antennas, on the other hand, are each placed directly next to one of the SQUIDs and are therefore expected to only affect the SQUID next to the antenna. By changing the critical current and hence the nonlinear inductance of the DC-SQUIDs, we change both the resonant frequency and the nonlinearity of the resonators. The latter is an important system parameter for the behavior of the simulated model, as it corresponds to an effective

[1]The authors acknowledge support from the German Research Foundation through FE 1564/1-1, the doctorate program ExQM of the Elite Network of Bavaria, the IMPRS 'Quantum Science and Technology', and the German Excellence Initiative via the 'Nanosystems Initiative Munich' (NIM).

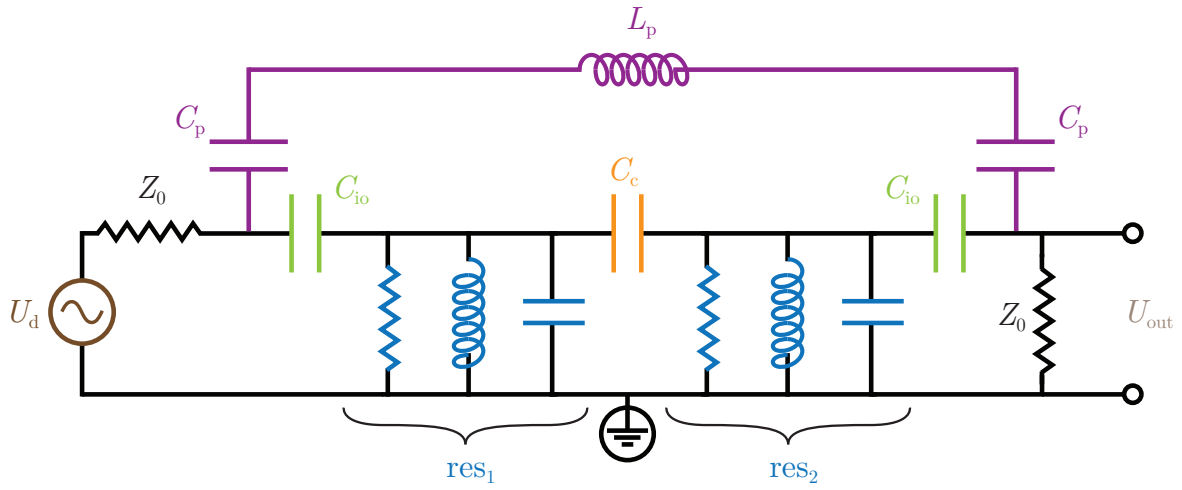

Figure 2: Circuit diagram of the extended model used for the simulations of the transmission magnitude shown in the bottom panel of Fig. 1. Z_0 is the impedance of the input and output lines, C_{io} the coupling capacitance of the resonators to these lines, and C_c the coupling capacitance between the resonators. C_p and L_p are the capacitance and inductance of the parasitic mode, respectively.

on-site interaction of the resonator photons. The change of the resonant frequency of the resonators can be easily observed in microwave transmission experiments as shown in Fig. 1. In the top panel, the transmission magnitude of the two-resonator chip is plotted versus frequency and applied coil current. Although the resonators are designed to be identical, they evidently show different maximum resonant frequencies and different tunability by the applied flux. This behavior is most likely due to fabrication spread resulting in different properties of the Josephson junctions of both SQUIDs. In addition, the measured frequency and flux dependence of the transmission magnitude shown in the top panel of Fig. 1 clearly differs from the behavior expected from a simple model calculation (cf. middle panel of Fig. 1) for certain coil currents.

We can explain this discrepancy by including an additional parallel parasitic mode which couples inductively and capacitively to the resonator modes (see Fig. 2) [3]. As shown in the bottom panel of Fig. 1), the transmission magnitude obtained by simulations based on this model agrees well with the measured transmission spectra. Moreover, the variation of the resonant frequency with control flux is reproduced more accurately. The microscopic nature of the parasitic mode is still under investigation. However, it is most likely related to a parasitic mode of the sample box and the printed circuit board used for sample mounting.

As mentioned above, in addition to the magnetic field created by an external coil, we can also tune the resonance frequencies individually via on-chip antennas. This additional tuning knob allows us to independently control the frequencies of both resonators, an ability which is needed for upcoming experiments. In these subsequent experiments, we plan to perform measurements of the correlations between the photon fields inside the resonators.

References

[1] M. Leib, F. Deppe, A. Marx, R. Gross, and M. J. Hartmann, New J. Phys. **14**, 75024 (2012).
[2] M. Fischer, WMI Ann. Rep. **2016**, 47–48 (2016).
[3] C. Besson. *Quantum Simulations of Many-Body Systems with Superconducting Devices*. Master's thesis, Technische Universitä München (2017).

Tunable magnon-photon coupling in a compensating ferrimagnet – from weak to strong coupling

H. Maier-Flaig, S. Klingler, M. Weiler, S. Geprägs, R. Gross, H. Huebl [1]
S.T.B. Goennenwein, [2,3] *M. Harder,* [4,5] *Z. Qiu, E. Saitoh* [6]

The coupling rate between an individual spin and an electromagnetic mode of a microwave resonator is typically very small. It can, however, be boosted by a factor of $\sqrt{n}$ in a spin ensemble consisting of n polarized spins [1–4]. Recently, the approach of strongly coupling a spin ensemble to a microwave resonator has been transferred to exchange coupled spin systems [5–9]. Interestingly, however, dedicated work on the nature of the coupling mechanism, the $\sqrt{n}$ scaling of the coupling rate, does not exist for exchange coupled spin ensembles. Here, we provide a direct experimental proof of the $\sqrt{n}$ scaling in an exchange coupled ensemble of spins in a gadolinium iron garnet (GdIG) sample.

GdIG is a compensating ferrimagnetic insulator with three magnetic sublattices. Two strongly coupled Fe sublattices form a net magnetization, which is only weakly temperature dependent. The magnetization of the Gd sublattice is antiferromagnetically coupled to the net Fe magnetization [10] and strongly increases with decreasing temperature T. At $T_{\mathrm{comp}} \approx 270\,\mathrm{K}$, the sublattice magnetizations compensate each other. The full temperature dependence of the total magnetization M of our thin-film GdIG sample is shown in Fig. 1.

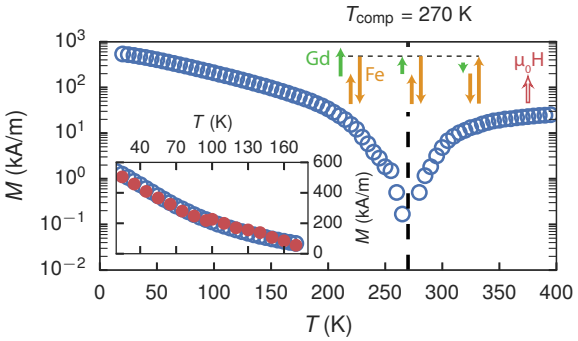

Figure 1: The total magnetization M as a function of temperature T (blue circles). The length of the arrows schematically represents the Fe and Gd sublattice magnetization configuration. Inset: The effective magnetization M_{eff} extracted from the FMR measurements (red data points) agrees very well with M.

For the magnon-photon coupling experiments, we place the sample in the magnetic field anti-node of the TE_{011} mode of a 3D microwave cavity with a center frequency of about 10 GHz. We use a vector network analyzer to measure the microwave reflection S_{11} from the cavity as a function of frequency and external magnetic field. Exemplary experimental results for two temperatures are shown in Fig. 2. The experimental data show an avoided crossing of GdIG and cavity resonances at low T, which becomes weaker with increasing T, indicating that the coupling deceases with increasing T. To quantify the effective coupling rate g_{eff} and the magnetization M, we fit the 2D S_{11} data-set obtained at each temperature to [11]

$$S_{11} = \frac{A\,(1-\kappa_{\mathrm{c}})}{i\,(\omega-\omega_{\mathrm{c}}) - \kappa_{\mathrm{c}} - i g_{\mathrm{eff}}^2\,(\omega-\omega_{\mathrm{FMR}}+i\gamma_{\mathrm{s}})^{-1}}. \tag{1}$$

Here, κ_{c} and γ_{s} describe the decay rates of the cavity and the magnon system, respectively. A is a complex scaling parameter, and the cavity resonance frequency is ω_{c}. The ferromagnetic

[1] We gratefully acknowledge funding by the German Research Foundation through project GR 1132/18, HU 1896/2-1 and the collaborative research center SFB 631
[2] Institut für Festköperphysik, TU Dresden, Dresden, Germany
[3] Funding from the German Research Foundation via projects GO 944/4 and GR 1132/18 is gratefully acknowledged.
[4] Department of Physics and Astronomy, University of Manitoba, Winnipeg, Canada
[5] Support from the NSERC MSFSS program is gratefully acknowledged
[6] WPI Advanced Institute for Materials Research, Tohoku University, Sendai, Japan

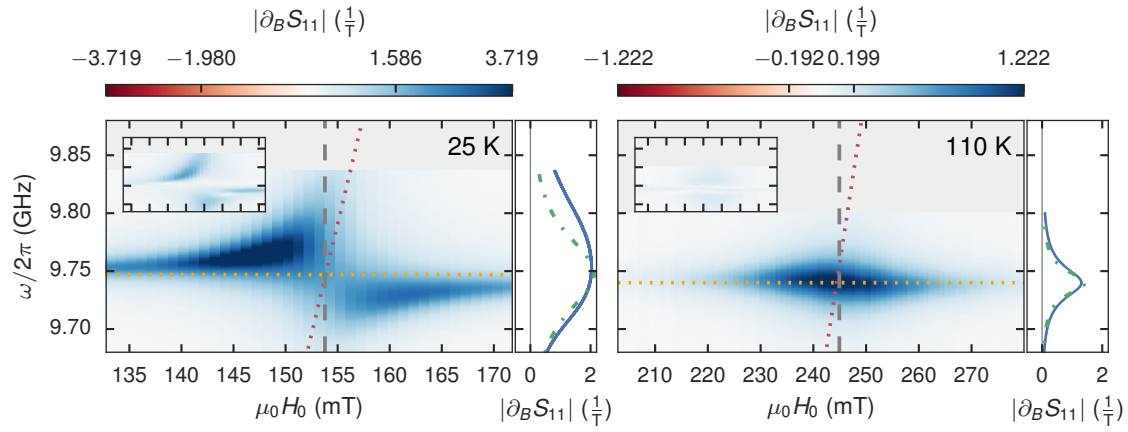

Figure 2: Magnitude of the magnetic field derivative of S_{11}. The horizontal line marks the resonance frequency $\omega_c/2\pi$ of the unperturbed cavity, the red dotted line marks the resonance frequency of the unperturbed spin system $\omega_{FMR}/2\pi$. Inset: Residuals of the fit to Eq. (1) on the same scale. Line cuts through the data at the vertical grey line are shown to the right of each colormap (solid line: data, dashed line: fit).

resonance frequency is $\omega_{FMR} = \gamma\mu_0\sqrt{H_0\,(H_0 + M_{eff})}$, where γ is the gyromagnetic ratio and M_{eff} is the effective magnetization. As shown in the inset of Fig. 1, $M_{eff} \approx M$.

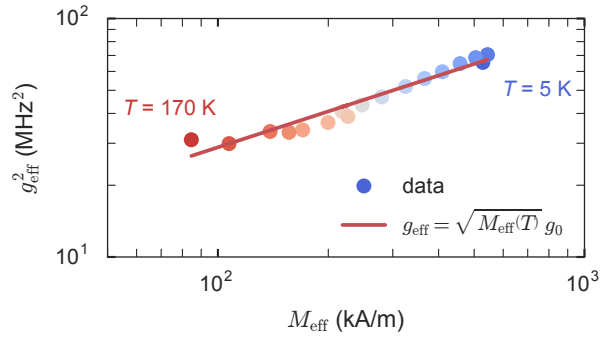

Figure 3: g_{eff}^2 as a function of M_{eff}. The data agrees very well with the expected scaling behavior $g_{eff} \propto \sqrt{M_{eff}}$ (red line).

As a key result, we confirm the expected scaling of the effective coupling rate g_{eff} with the magnetic moment. In Fig. 3 we have plotted g_{eff}^2 as a function of M_{eff}. The straight line indicates $g_{eff} \propto \sqrt{M_{eff}}$. This scaling behavior for the exchanged coupled spin ensemble is analog to the $g_{eff} \propto \sqrt{n}$ scaling observed for a non-interacting spin ensemble consisting of n polarized spins. By varying the temperature, we can tune M_{eff} and hence g_{eff} from the weak to the strong coupling regime (for details, see Ref. [12]). This makes GdIG a powerful model system to study magnon-photon coupling phenomena.

References

[1] M. Tavis, and F. W. Cummings, Phys. Rev. **170**, 379–384 (1968).
[2] J. M. Fink, R. Bianchetti, M. Baur, M. Göppl, L. Steffen, S. Filipp, P. J. Leek, A. Blais, and A. Wallraff, Phys. Rev. Lett. **103**, 083601 (2009).
[3] A. Imamoglu, Phys. Rev. Lett. **102**, 083602 (2009).
[4] I. Chiorescu, N. Groll, S. Bertaina, T. Mori, and S. Miyashita, Phys. Rev. B **82**, 024413 (2010).
[5] H. Huebl, C. W. Zollitsch, J. Lotze, F. Hocke, M. Greifenstein, A. Marx, R. Gross, and S. T. B. Goennenwein, Phys. Rev. Lett. **111**, 127003 (2013).
[6] X. Zhang, C.-l. Zou, L. Jiang, and H. X. Tang, Phys. Rev. Lett. **113**, 156401 (2014).
[7] Y. Tabuchi, S. Ishino, T. Ishikawa, R. Yamazaki, K. Usami, and Y. Nakamura, Phys. Rev. Lett. **113**, 083603 (2014).
[8] L. Bai, M. Harder, Y. P. Chen, X. Fan, J. Q. Xiao, and C.-M. Hu, Phys. Rev. Lett. **114**, 227201 (2015).
[9] N. Kostylev, M. Goryachev, and M. E. Tobar, Appl. Phys. Lett. **108**, 062402 (2016).
[10] G. F. Dionne, and P. F. Tumelty, J. Appl. Phys. **50**, 8257–8258 (1979).
[11] Y. Cao, P. Yan, H. Huebl, S. T. B. Goennenwein, and G. E. W. Bauer, Phys. Rev. B **91**, 094423 (2015).
[12] H. Maier-Flaig, M. Harder, S. Klingler, Z. Qiu, E. Saitoh, M. Weiler, S. Geprägs, R. Gross, S. T. B. Goennenwein, and H. Huebl, Appl. Phys. Lett. **110**, 132401 (2017).

Magnon transport in the compensated ferrimagnet GdIG

T. Wimmer, K. Ganzhorn, N. Vlietstra, S. Gepraegs, R. Gross, H. Huebl [1]
S.T.B. Goennenwein,[2] *J. Barker, G.E.W. Bauer, E. Saitoh,*[3] *A. Kamra,*[4] *Z. Qiu*[5]

The transport of spin angular momentum represents an interesting research topic in the field of spintronics. In insulating magnetic materials, the possibility to generate magnon-based pure spin currents without accompanying charge currents is of particular interest. A recently discovered effect associated with the propagation of incoherent magnons between a magnon generator (source) and a magnon detector (drain) is the so-called magnon mediated magnetoresistance (MMR) [1, 2] in ferromagnetic insulator/normal metal bilayers. After establishing a fundamental understanding of the incoherent magnon transport in the collinear ferromagnet Yttrium Iron Garnet (YIG) [1, 2], the next logical step is to study transport phenomena associated with the propagation of quantized excitations of the spin system in a more complex, compensated ferrimagnets such as Gadolinium Iron Garnet (GdIG). This particularly allows for the investigation of magnon generation and transport in a canted magnetic phase.

The investigated sample is a 2.6 µm thick GdIG film grown via liquid phase epitaxy (LPE). A 10 nm thick Pt film was deposited onto the GdIG via electron beam evaporation. Two Pt strips acting as source and drain with edge-to-edge separation d = 200 nm and strip width w = 500 nm were defined by electron beam lithography followed by Ar ion etching [see in Fig. 1(a)]. In our experiments we apply a constant charge current I_c to the Pt source strip. In this way we generate a magnon accumulation or depletion in the GdIG layer below the source strip which is diffusively propagation towards the detector strip. To detect the associated spin current we perform angle dependent magnetoresistance (ADMR) measurements on the Pt detector strip. More precisely, we measure the voltage drop (V_{nl}) along the detector strip as a function of an applied magnetic field of constant magnitude ranging between 1 and 15 T which is rotated within the thin film plane [see Fig. 1(b)]. The MMR signal is then defined as $\Delta V_{nl} = V_{nl}(0°) - V_{nl}(90°)$.

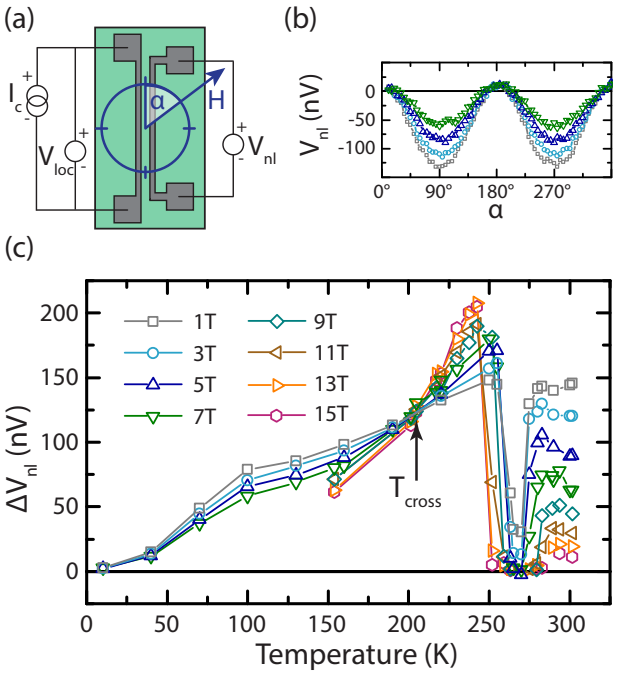

Figure 1: (a) Schematic representation of the GdIG(green)/Pt (grey) nanostructures consisting of two parallel Pt strips of width w and edge-to-edge separation d. (b) Voltage V_{nl} along the detector strip as a function of α at 300 K for $\mu_0 H = 1, 3, 5$ and 7 T. (c) Temperature dependence of the MMR amplitude $\Delta V_{nl} = V_{nl}(0°) - V_{nl}(90°)$ obtained from ADMR measurements for magnetic fields up to 15 T.

[1] This work is financially supported by the German Research Foundation through the Priority Program Spin Caloric Transport (GO 944/4, BA 2954/2 and GR 1132/18), the JSPS KAKENHI Grant Nos. 25247056, 25220910, 26103006, a Laura-Bassi stipend of the TU München (to NV), a AvH Postdoc Fellowship (to AK), and the Tohoku University Graduate Program in Spintronics.

[2] Institut für Festköperphysik, TU Dresden, Dresden, Germany
[3] Institute for Materials Research, Tohoku University, Sendai 980-8577, Japan
[4] Department of Physics, University of Konstanz, D-78457 Konstanz, Germany
[5] WPI Advanced Institute for Materials Research, Tohoku University, Sendai 980-8577, Japan

In Fig. 1(c), the MMR signal ΔV_{nl} is shown as a function of temperature for different magnetic fields. The vanishing signal at low temperatures $T < 10\,\mathrm{K}$ is consistent with previous measurements on YIG/Pt heterostructures [1]. Increasing the temperature, the MMR signal increases but then drops below the resolution limit of 5 nV at the compensation temperature $T_{\mathrm{comp}} = 268\,\mathrm{K}$ of GdIG for all magnetic field values. For $T > T_{\mathrm{comp}}$, finite MMR values are measured again. Regarding the magnetic field dependence of the MMR signal, we can distinguish three different temperature regimes: for $0 < T < T_{\mathrm{cross}} \approx 210\,\mathrm{K}$ and $T_{\mathrm{comp}} < T < 300\,\mathrm{K}$ the MMR signal decreases with increasing applied magnetic field, while in the intermediate regime, $T_{\mathrm{cross}} < T < T_{\mathrm{comp}}$, the MMR signal is found to increase with increasing field. This complex behaviour can be explained by taking into account the magnon spectrum of GdIG shown in Fig. 2 [3–5]. The spectra are shown for the above mentioned temperature regimes, as well as for two different magnetic fields $\mu_0 H_0 = 1\,\mathrm{T}$ and 7 T. For the following discussion, there are two relevant magnon modes, which we denote as the α-mode (red fundamental mode) and the β-mode (blue optical mode).

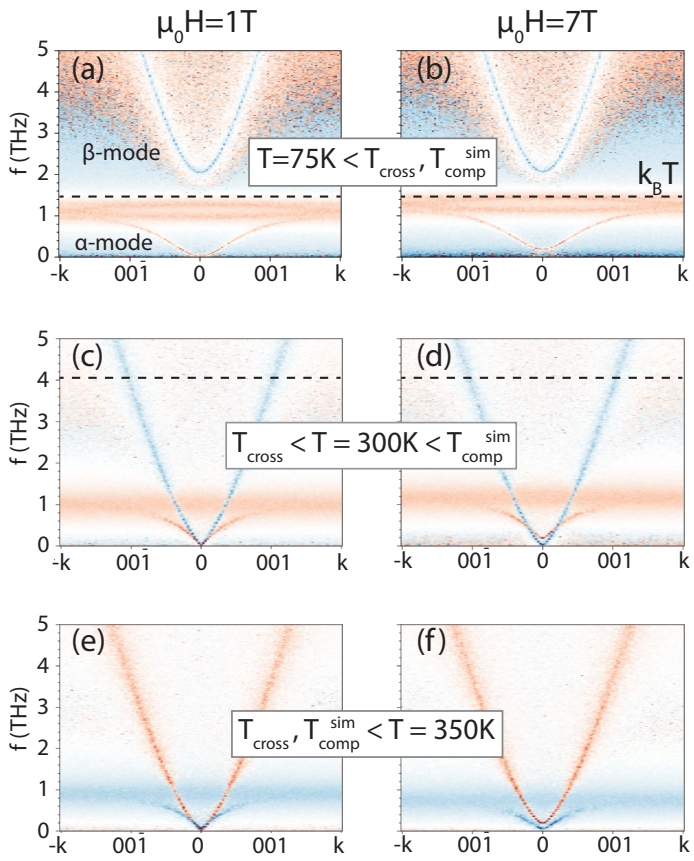

Figure 2: Magnon spectra of GdIG calculated by atomistic simulations for $\mu_0 H = 1\,\mathrm{T}$ and 7 T: (a)-(b) for $T = 75\,\mathrm{K}$, (c)-(d) just below $T_{\mathrm{comp}}^{\mathrm{sim}} = 310\,\mathrm{K}$, and (e)-(f) above the compensation point. The red and blue color indicates counter-clockwise and clockwise precession directions relative to the external magnetic field direction, respectively. The black dashed line corresponds to the thermal energy $k_{\mathrm{B}}T$.

For $0 < T < T_{\mathrm{cross}}$, the lower energy α-mode, which is mainly associated with the Gd sublattice, dominates spin transport. The mode occupancy increases with temperature, leading to an enhancement in the spin conductivity. With increasing temperatures, there is a positive contribution from an increasing mode occupancy and a negative contribution from critical fluctuations (CF) mediated damping, as the Gd becomes more and more disordered [3]. However, for $T < T_{\mathrm{comp}}$, the Gd magnetic moments are aligned with the magnetic field, such that the Gd sublattice is stabilized when the external magnetic field is increased. The CF mediated damping is therefore reduced, leading to an increase of the detected MMR signal. At a characteristic temperature T_{cross}, this enhancement of the MMR amplitude with magnetic field starts to dominate over the magnetic field suppression expected for all temperatures in the investigated range. This is consistent with the experimentally observed enhancement of the MMR amplitude between T_{cross} and T_{comp} [cf. Fig. 1(b)]. For $T > T_{\mathrm{comp}}$, the external field acts against the Gd sublattice and destabilizes it, leading to an enhancement in CF and a suppression of the magnon transport. This is consistent with the strong suppression of the MMR amplitude in this temperature regime.

Our results show that the MMR signal in the compensated ferrimagnet GdIG is suppressed in the canted phase. Furthermore, the MMR signal is suppressed by magnetic field at low

temperatures and above T_{comp}, but is enhanced just below T_{comp}. Atomistic simulations of the magnon spectra in GdIG and the corresponding transport properties of the modes can qualitatively explain the data by including Gilbert damping and critical fluctuations of the Gd sublattice moments at high temperatures.

References

[1] S. T. B. Goennenwein, R. Schlitz, M. Pernpeintner, K. Ganzhorn, M. Althammer, R. Gross, and H. Huebl, Appl. Phys. Lett. **107**, 172405 (2015).

[2] L. J. Cornelissen, J. Liu, R. A. Duine, J. B. Youssef, and B. J. van Wees, Nat. Phys. **11**, 1022 (2015).

[3] K. Ganzhorn, T. Wimmer, J. Barker, G. E. W. Bauer, Z. Qiu, E. Saitoh, N. Vlietstra, S. Geprägs, R. Gross, H. Huebl, and S. T. B. Goennenwein, arxiv:1705.02871 (2017).

[4] K. Ganzhorn, J. Barker, R. Schlitz, B. A. Piot, K. Ollefs, F. Guillou, F. Wilhelm, A. Rogalev, M. Opel, M. Althammer, S. Geprägs, H. Huebl, R. Gross, G. E. W. Bauer, and S. T. B. Goennenwein, Phys. Rev. B **94**, 094401 (2016).

[5] S. Geprags, A. Kehlberger, F. D. Coletta, Z. Qiu, E.-J. Guo, T. Schulz, C. Mix, S. Meyer, A. Kamra, M. Althammer, H. Huebl, G. Jakob, Y. Ohnuma, H. Adachi, J. Barker, S. Maekawa, G. E. W. Bauer, E. Saitoh, R. Gross, S. T. B. Goennenwein, and M. Klaui, Nat. Comm. **7**, 10452 (2016).

Materials, Thin Film and Nanotechnology, Experimental Techniques

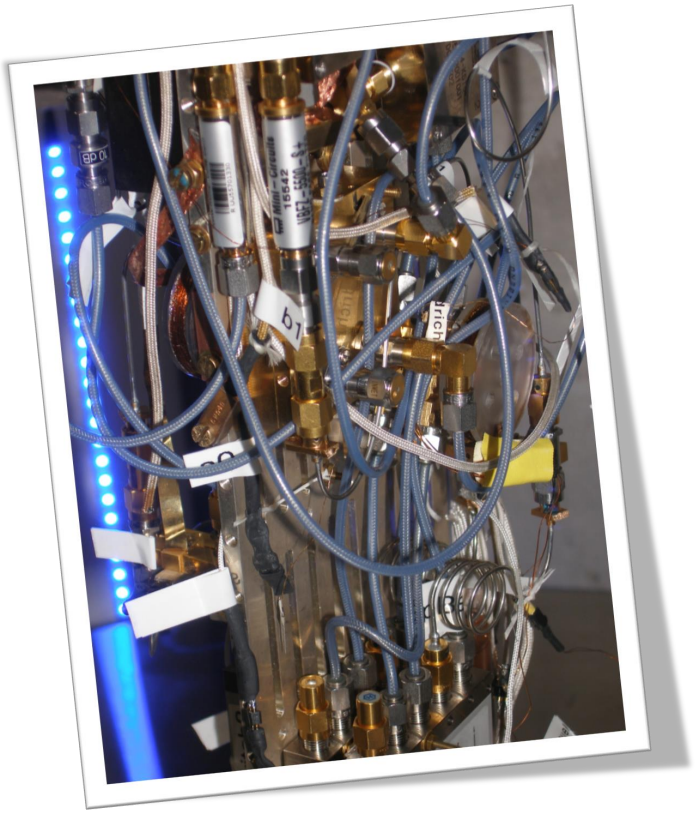

Installation of microwave cables and components on the mK part of a dilution refrigerator system used for experiments on solid state quantum systems.

New UHV Sputtering System «Superbowls» installed at Walther-Meißner-Institute

M. Althammer, R. Gross [1]

Most of the research projects carried out at the Walther-Meißner-Institute strongly depend on the availability of high quality thin film samples. To this end, WMI has established thin film laboratories equipped with state-of-the-art ultrahigh vacuum (UHV) deposition systems. In 2017, a new UHV sputter deposition system for the fabrication of complex heterostructures consisting of superconducting, ferromagnetic and non-ferromagnetic materials has been successfully installed and put into operation. The system was granted by the German Research Foundation through a proposal for major instrumentation and by support through the Nanosystems Initiative Munich. After the proposal was approed in March 2016 and the selection of the manufacturer in an European Union wide tender in July 2016, the system was delivered by the supplier Bestec GmbH in May 2017. At the WMI the system was installed in a new laboratory, which had to be equipped with an air filtering and airconditioning system, cooling water supply and gas feed lines), adjacent to the already available thin film labs. After passing the final acceptance tests, operation could finally be started in August 2017. The system has been given the name **S**putter **U**tensil **P**erforming **E**verything **R**equired for **B**est, **O**ptimized, **W**orld **L**eading **S**amples, or briefly «**SUPERBOWLS**».

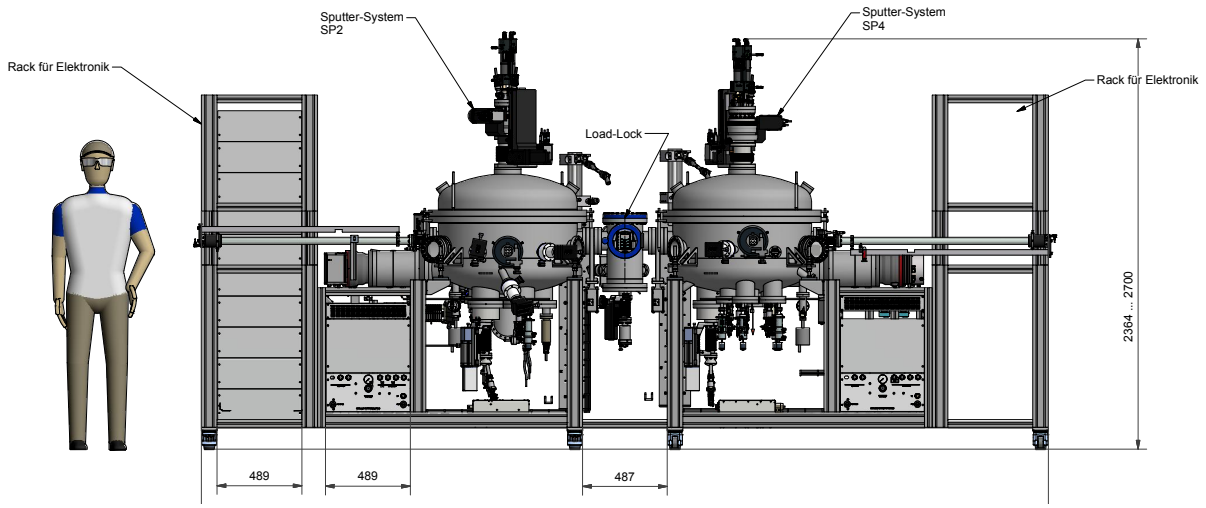

Figure 1: Technical drawing of the new UHV sputter deposition system.

The main purpose of the new UHV sputter system is the fully-automated fabrication of multilayers consisting of superconducting and magnetic materials. To avoid cross-contamination of the superconducting and magnetic materials the systems consists of two separate deposition chambers (see Fig.1 and 2). The one deposition chamber is dedicated for superconducting materials (Non-Ferromagnet Chamber: NFC) and the other for the growth of magnetic materials (All Ferromagnet Chamber: AFC). The loadlock chamber is positioned between the two deposition chambers. It serves for inserting substrates and masks into the deposition chambers and enables the in-situ transfer of samples between the two deposition chambers. Moreover, the system is designed in a modular, cluster tool-like fashion and allows for a further extension, for example, by a third deposition or analysis chamber. It also could be integrated into a larger cluster deposition system. Furthermore, the present deposition chambers can be extended by adding additional deposition sources and analysis tools. The system is designed

[1]Financial support from the German Research Foundation via INST 95/1333-1 FUGG and from the Nanosystems Initiative Munich (NIM) is gratefully acknowledged.

for a face-down substrate orientation with the sputter source residing at the bottom of the deposition chambers. During the final acceptance tests at the WMI both deposition chambers achieved a base pressure well below 8×10^{-10} mbar, paving the way for the deposition of high purity materials.

The loadlock chamber is equipped with a manually operated substrate and mask storage cassette with place for up to six substrates. Halogen lamp heaters are installed in the loadlock for thermal precleaning of the substrates. The pumpdown time from ambient pressure down to the transfer pressure $< 2 \times 10^{-7}$ mbar is below 30 min, which guarantees a fast sample exchange for the system.

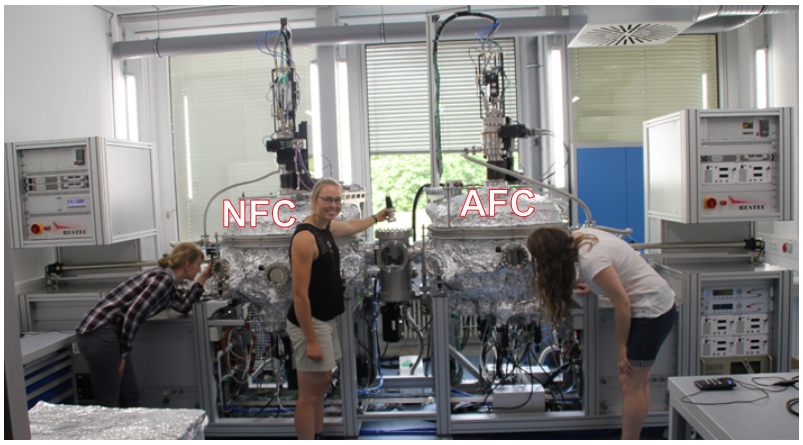

Figure 2: New UHV sputter deposition system **«SUPERBOWLS»** after the final acceptance test in the new thin film laboratory at WMI. Left chamber is the NFC dedicated to the deposition of superconducting materials, right chamber is the AFC equipped with magnetic materials. Between the two deposition chambers resides the loadlock (LL).

The NFC is currently equipped with two 3 inch magnetrons and one 2 inch magnetron. These magnetrons are suitable for both magnetic and non-magnetic target materials by changing the magnet configuration and for a deposition pressure down to 5×10^{-4} mbar. The deposition sources are equipped with pneumatic actuated shutters, tilts, and linear translations. This allows for both face-to-face and confocal deposition from all three sources.

The versatile substrate manipulator shown in Fig. 3 accommodates substrates with a diameter of up to 2 inch and features a resistive heater for substrate temperatures up to 800 °C, a motorized substrate shutter for wedge and step-profile deposition, a motorized linear translation for changing the source to substrate position, a main rotation to move the substrate in the chamber to the different deposition positions, a motorized substrate rotation at up to 40 rpm for homogenous deposition, and a quartz crystal microbalance (QCM) for growth rate monitoring. In addition, a Kaufmann source for reactive ion etching is installed in the system for in-situ surface cleaning procedures or even etching processes. Three 1 kW DC power supplies are used for the operation of the magnetrons, which make also high deposition rates feasible. The three separate massflow controllers for the sputter gas feed lines allow reactive gas sputtering processes. Optional ports on the chamber provide the opportunity to increase the number of magnetrons or install growth monitoring equipment like a residual gas analysis unit.

In the AFC we installed eight 2 inch tiltable magnetrons, again suitable for magnetic and non-magnetic materials and low deposition pressures (see Fig. 4). In this chamber the source can be either oriented into two confocal deposition clusters from 4 sources or 4 sources for face-to-face deposition, providing a large flexibility in the deposition conditions and enabling the fabrication of quaternary alloys from single element targets. The substrate manipulator is identical in specifications to the one in the NFC: automated wedge shutter, substrate translation, substrate heater, main rotation, substrate rotation, and a QCM are mounted on it. For the supply of the working gas atmosphere we have 4 mass flow controllers available for using oxygen and nitrogen as reactive sputter gases. As power supplies we have six 1 kW DC-supplies and two 600 W RF-supplies with automated matching circuits available at the system. In this

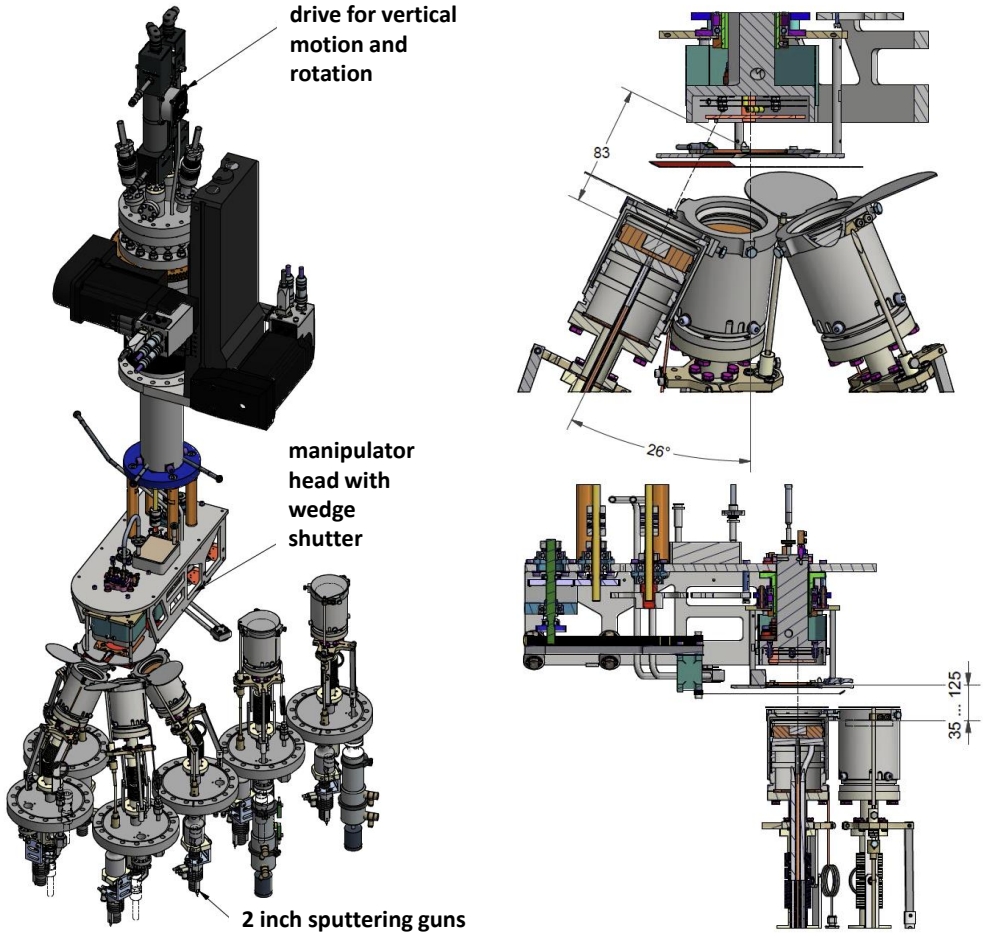

Figure 3: Technical drawing of the substrate holder (right). On the left, an enlarged view for the confocal (top) and the planar configuration (bottom) of the sputtering guns is shown.

way electrical conducting and isolating materials can be used for the deposition process. Due to the modular design, the two RF-units can be exchanged with two DC-units from the NFC, providing us with the full flexibility of the system.

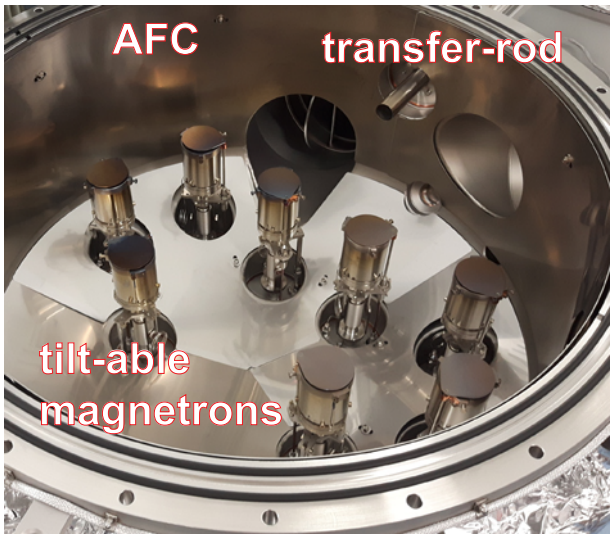

Figure 4: Inside view of the AFC after lifting the top flange. Eight tiltable 2 inch magnetrons are installed in this chamber, for face-to-face and confocal deposition configurations from up to 4 sources simultaneously.

Except for the manual process of sample loading and unloading into the deposition chambers all parts in the deposition chambers are fully automated and a client-server-based control software allows for a complete deposition process automatization. This ensures a highly reproducible deposition process from sample to sample and verifies a high repeatability of our deposition results. With two clients available, the two deposition chambers can be operated simultaneously, increasing the throughput of the system.

As evident from the system specifications, we expect this setup to extend our present research activities in the field of superconducting quantum circuits, superconducting quantum hybrid systems, magnetic materials, interfacial spin physics,

and proximity effects in magnetic/superconducting heterostructures and even to expand our research beyond those fields. In the next years this system will allow us to have direct access to state-of-the-art materials for conducting research on an international competitive level. Last but not least, the expansion in thin film deposition setups continues in the next year with the installation of a new UHV sputter system, which is dedicated to the homogenous large area deposition of superconducting thin films and alloys on substrates with a diameter of up to 100 mm.

Off-axis parabolic mirror optics for near-field Raman spectroscopy

D. Jost, J.-R. Scholz, N. Chelwani, D. Hoch, B. Botka, F. Kretzschmar, T. Böhm, R. Hackl [1]
K. Kamarás [2]

The *in situ* combination of different types of spectroscopies [1] at the identical position of a sample is crucial for reliable quantitative data analysis [2]. For instance, scanning tunneling spectroscopy (STS) and polarized Raman spectroscopy (pRS) would enable one to obtain simultaneous information from a single- and a two-particle probe. In addition, the tunneling tip may be used to locally enhance the electric field of the incoming laser and thus facilitate the exploitation of near-field effects for light scattering for improving the spatial resolution beyond the diffraction limit [3, 4].

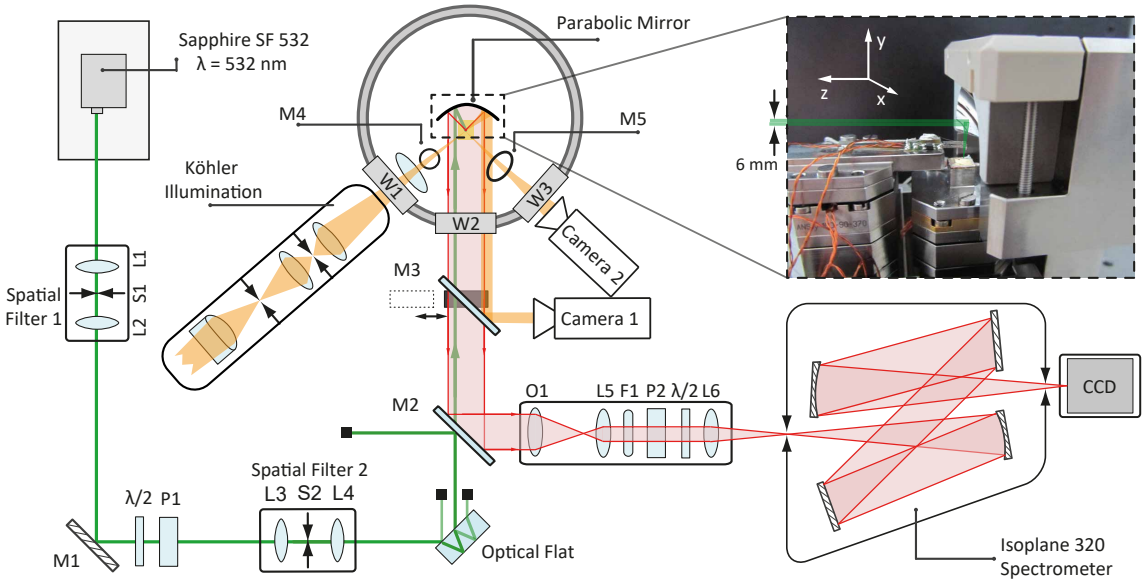

Figure 1: Schematic of the set-up. Sample and parabola are in the center of the cryostat. The polarized (P1) and spatially filtered (L3 S2 L4) incident light (green) passes through the semitransparent mirror M2 into the cryostat, hits the parabola and is focused on the sample (see inset). The scattered light (red) is reflected into a camera objective O1 via the parabola and the semitransparent mirror M2. Lens L5 makes the light parallel again. Using an edge filter (F1) the elastically scattered light can be filtered out. Different polarization states can be selected with a polarizer (P2). The wave-plate $\lambda/2$ rotates the polarization into a direction optimal for the Isoplane 320. Finally the light is focused (L6) on the entrance slit of the spectrograph. The sample is illuminated through viewport W1 using Köhler illumination. High-resolution images of the sample can be obtained via the parabola, the removable mirror M3, and camera 1. There is another direct observation system (camera 2) through viewport W3.

Near-field effects were used to study molecules with large Raman cross sections [4–6]. In solids the enhancement effects, specifically the contrast between far and near field are smaller, as shown for instance for Si or MoS_2 [7, 8]. Usually microscope objective lenses having ultra-large working distances are used, providing excellent optical images of the surface studied and enough space between the sample and the lens for the equipment required for the tip-enhanced Raman spectroscopy (TERS) [4]. Alternatively, a setup using an on-axis parabola was described recently, which due to the very large aperture facilitates optimal focusing and minimal spot size [7]. In both cases radially polarized light is required, which goes along with losses, and the aperture is always partially obscured, at least for nontransparent materials.

[1] The project was funded by the German Research Foundation via the TRR 80 and by the EU through the ITN Project FINELUMEN (PITN-GA-2008-215399). N. Chelwani, B. Botka and F. Kretzschmar are presently affiliated with Bruker AXS GmbH, Karlsruhe, the University of South Australia, Adelaide, Australia, and with Intel Mobile Communications, Neubiberg, Germany, respectively.

[2] Wigner Research Centre for Physics, Hungarian Academy of Sciences, 1525 Budapest, Hungary

Supported by the TRR 80 we developed a setup using an off-axis paraboloid as an objective lens. In this way the stray light contribution may be reduced substantially and all polarization combinations of incoming and scattered photons necessary for deriving the symmetry components of the Raman response become accessible. The setup is sketched schematically and described in Fig. 1. The sample surface is parallel to the axis of the paraboloid (inset of Fig. 1), thus simplifying the application of scanning techniques and minimizing the obscuration.

We use diode-pumped solid state (DPSS) lasers emitting either at 532 or 660 nm. The polarized parallel light is directed to one quadrant of the paraboloid and focused on the sample. The scattered light is collected by the paraboloid and refocused by the commercial camera objective lens O1. Lense L5 makes the light parallel again for filter F1 and polarizer P2 to work properly. Lense L6 focuses the light again. Until 2016 the Raman light was transferred to another lab via an optical fiber and analyzed by a triple spectrometer (not shown). Since 2017 L6 focuses the light on the entrance slit of a single stage spectrometer equipped with a CCD detector. The sensitivity could be increased by a factor of 20 facilitating all experiments on opaque samples intended for TRR 80.

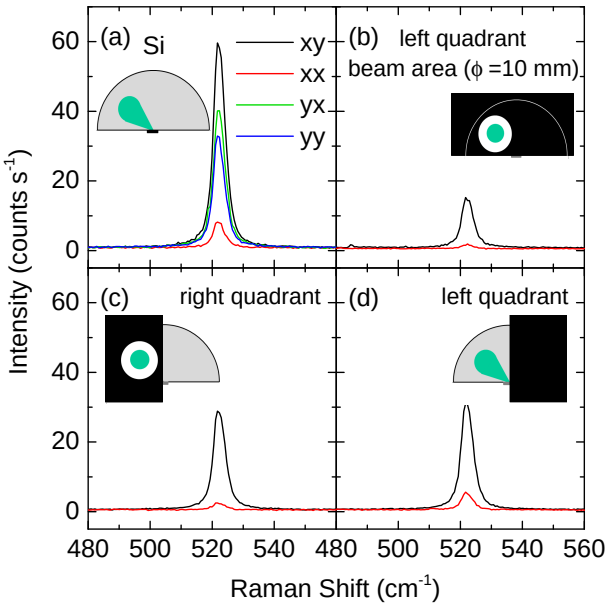

Figure 2: Spectra of Si for different photon polarizations. A {001} surface is used here. The polarizations refer to the coordinate system shown in Fig. 1. For x- and y-polarized photons the projections on the sample surface are close to [100] and [110], respectively, for illumination through the left quadrant as indicated [9]. (a) The scattered light is collected over the full aperture of the parabola. According to the selection rules of Si there is a contrast between the xy and xx polarized spectra, while the yy and yx spectra have similar intensities. (b)-(d) The contrast between the xy and xx polarized spectra is maintained if parts of the aperture are blocked as indicated.

For these experiments the selection rules are crucially important for improving the contrast. To this end we studied several polarization combinations on a silicon test sample having a {001} polished surface as shown in Fig. 2. Panel (a) shows that the ratio of the peak intensities between the xy and the xx spectra is approximately 14, whereas that between yx and yy is close to unity. This result looks counterintuitive at first glance but originates from the different apertures for incoming and scattered light and is by and large in accordance with the selection rules. In a second set of experiments [Fig. 2 (b)-(d)] the contributions from selected parts of the paraboloid were studied, confirming the conclusions. Further details can be found in Ref. [10].

References

[1] M. Lucas, and E. Riedo, Rev. Sci. Instrum. **83**, 061101 (2012).
[2] W. Prestel, F. Venturini, B. Muschler, I. Tüttő, R. Hackl, M. Lambacher, A. Erb, S. Komiya, S. Ono, Y. Ando, D. Inosov, V. B. Zabolotnyy, and S. V. Borisenko, Eur. Phys. J. Special Topics **188**, 163 (2010).
[3] R. M. Stöckle, Y. D. Suh, V. Deckert, and R. Zenobi, Chem. Phys. Lett. **318**, 131 – 136 (2000).
[4] A. Hartschuh, E. J. Sánchez, X. S. Xie, and L. Novotny, Phys. Rev. Lett. **90**, 095503 (2003).
[5] J. Steidtner, and B. Pettinger, Phys. Rev. Lett. **100**, 236101 (2008).
[6] Z. Zhang, S. Sheng, R. Wang, and M. Sun, Anal. Chem. **88**, 9328–9346 (2016).
[7] J. Steidtner, and B. Pettinger, Rev. Sci. Instrum. **78**, 103104 (2007).
[8] D. V. Voronine, G. Lu, D. Zhu, and A. Krayev, IEEE J. Sel. Topics Quantum Electron. **23**, 1–6 (2017).
[9] D. Hoch. *Tip-Enhanced Raman Spectroscopy*. Master's thesis, Technische Universität München (2015).
[10] N. Chelwani, D. Hoch, D. Jost, B. Botka, J.-R. Scholz, R. Richter, M. Theodoridou, F. Kretzschmar, T. Böhm, K. Kamarás, and R. Hackl, Appl. Phys. Lett. **110**, 193504 (2017).

Cryogen-free: Of course! Vibrations: Hell no!

K. Uhlig

Introduction: The outstanding advantage of pulse tube cryocoolers (PTC) compared to their cryocooler brethren (e.g. Gifford-McMahon, Sterling, Vuilleumier, Brayton) is the fact that there are no moving parts and therefore mechanical vibrations are minimized from the outset. Vibrational amplitudes are small enough so that PTCs can easily be used to precool millikelvin coolers such as dilution refrigerators (DR) or adiabatic demagnetization refrigerators.

However, for delicate applications, the very small vibrational disturbances caused by PTCs have to be compensated. For example, the pressure swings between 16 bar and 8 bar of the helium column in the PTC produce a periodic expansion and contraction of its tubes on the order of 5 µm. Usually the associated low-frequency vibrations around 1 Hz are compensated by copper braid between the PTC and the next cooling stage of the refrigerator. The pressure changes also cause a periodic length change of the pressure line connecting the rotary valve and the PTC. This results in a force acting on the cryostat. Usually, not enough attention is paid to this effect. The mass difference of the helium gas in the PTC between high and low pressure is on the order of 10 g. Therefore, the total weight of the cryostat varies by this amount with a frequency of 1 Hz. This effect is usually ignored. High frequency vibrations traveling through the pressure line towards the cold head are usually attenuated by a bellow dampers mounted between the cold head and the cryostat. Below, two very different approaches are described for achieving cryogen-free cryostats with a very low level of vibration.

Millikelvin cooler with remote precooling: Recently we have compiled several ideas on how to further reduce the vibration level in a cryogen-free cooler [1]. One way is to mechanically separate the PTC from the next cooling stage and its experimental platform and space. In this case, a cooling loop with supercritical helium makes the thermal connection between the PTC and a 1 K-stage or a DR unit as shown in Fig. 1. The refrigerator proposed here is subdivided in two parts. One part houses a 2-stage PTC where a small fraction of its helium flow is branched off from the 2nd stage via a check valve (v1 in Fig. 1) [2, 3]. This flow is fed through a thermally well isolated connecting tube (d) [4, 5] to a cryostat (e) where it cools a 1 K-refrigerator or a DR by means of two heat exchangers (hx1, hx2). The cooler in (e) is similarly constructed as a standard cryogen-free refrigerator where the colder heat exchanger (hx1) acts like the 2nd stage of a PTC and the warmer one (hx2) cools the trestle of the cooling unit and its outer radiation shield. From hx2 the helium flow is run back through the connector (d), a 2nd check valve (v2), and a cold valve v3 to the 1st stage of the PTC. With the check valves v1 and v2 the periodic pressure changes (16 bar to 8 bar) of the PTC are utilized to generate a constant flow in the cooling line, whereas v3 is used to adjust the flow rate. A thorough calculation of the temperature profile shows [1] that the temperature of hx1 at its hot end is about 4 K and that of hx2 near 80 K. Although the design of the remotely cooled refrigerator looks quite straightforward at first sight, a high amount of development work has to be done to put it into practice.

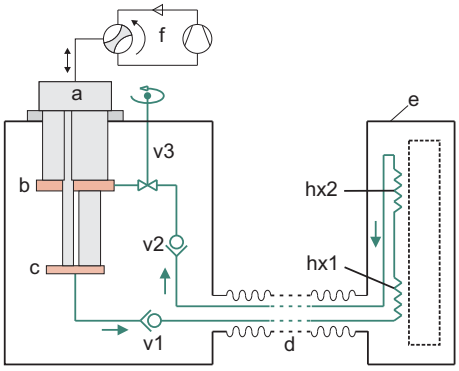

Figure 1: Cross-sectional drawing of a refrigerator with remote cooling. Left side: cryostat with a 2-stage PTC. Right side: cryostat with heat exchangers of the cooling loop. a - PTC; b - PTC 1st stage; c - PTC 2nd stage; d - connection tube; e - cryostat for DR or 1K-cooler; f - compressor with a rotary valve; v1 and v2 - cold check valves; v3 - cold valve.

Shutting off the PTC: An alternative that most certainly works to get rid of the vibrations of the PTC is to shut it off for as long as possible. In our present setup (Fig. 2) there is a 1 K-pot in the condensation line of the DR [6]. The original motivation to put it in was to obtain a higher cooling power of the fridge at a temperature near 1 K [7]. The idea in our new application is to fill up the 1 K-pot with $^4He_{liq}$, then stop the helium circulation and run the helium loop in a single cycle mode. Then the PTC is turned off and the DR is run as long as possible without the PTC in operation. Without taking any special measures, our DR could be run in this operating mode for 15 min. The 1st stage of the PTC cools a radiation shield and 2 charcoal traps (DR and 1K-stage). The shield is directly exposed to the 300 K radiation of the vacuum can and warms up when the PTC is off. When it reaches $T \approx 100$ K, we restart the PTC because the traps start to release air and contaminants above this temperature. Besides, the ^{4}He reservoir of the 1 K-stage is almost depleted. Importantly, the condensation pressure and the flow rate of the PTC were nearly constant during this span of time. The 2nd stage of the PTC warmed from 2.9 K to 6.8 K. Much to our surprise, the temperature of the mixing chamber did not remain constant but rose considerably from 5.6 mK to 9.2 mK (see Fig. 3).

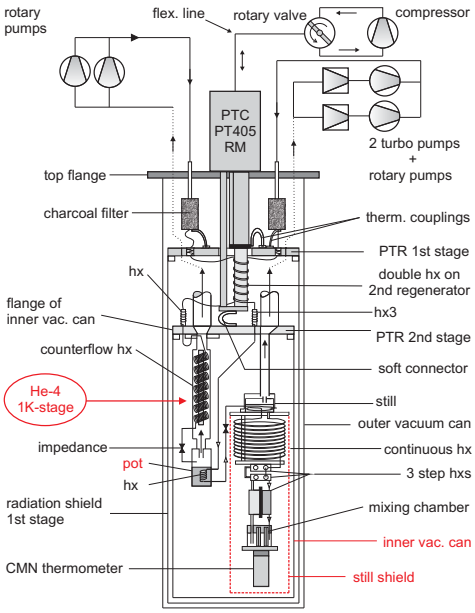

Figure 2: Cross-sectional view of our DR. It has 2 cooling circuits, a dilution circuit and a 1 K-He circuit. A radiation shield at the still flange (marked red) is not required for regular operation of the DR, but is necessary when the PTC is turned off temporarily (see text).

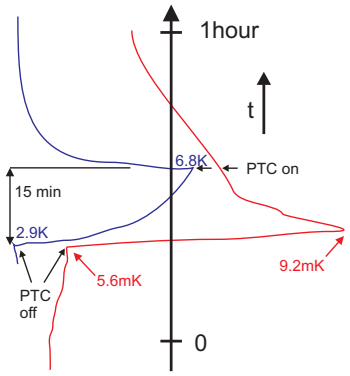

Figure 3: Temperature profile of the mixing chamber (red) and the inner vacuum can (blue) during and after a 15 min shut-off of the PTC.

The reason for this temperature rise is residual exchange gas which is trapped at the inner vacuum can. On warming up the can, the residual gas is slowly released into the vacuum space where it creates a small thermal short between the mixing chamber and the vacuum can. So far we haven't used a radiation shield at the still chamber (marked red in Fig. 2), but in the next experiments the still chamber will be replaced so that a radiation shield can be inserted to keep the residual gas from reaching the mixing chamber. Another measure will be to equip the radiation shield of the 1st stage of the PTC with superinsulation. The thermal load on this stage will then be reduced considerably and the turnoff time of the PTC prolonged, accordingly. And lastly, the size of the helium pot of the 1 K-stage will be increased, so the running time in single-shot operation will also be prolonged.

References

[1] K. Uhlig, Cryogenics **87**, 29–34 (2017).
[2] C. Wang, and E. Brown, AIP Conf. Proc. **1573**, 1149–56 (2014).
[3] J. Maddocks, P. Maddocks, M. Fay, B. Helvenstein, and A. Kashani. Performance test of pulse tube cooler with integrated circulator. CRYOCOOLERS 16, 591-9 (2011).
[4] M. Atrey, A. Healey, T. Janaway, and A. McMahon, AIP Conf. Proc. **823**, 41–8 (2006).
[5] T. Trollier, J. Tanchon, Y. Icart, and A. Ravex, AIP Conf. Proc. **1573**, 1461–1466 (2014).
[6] K. Uhlig, Cryogenics **66**, 6–12 (2015).
[7] K. Uhlig, AIP Conf Proc **1573**, 1393–1398 (2014).

Experimental Facilities

Overview of Key Experimental Facilities and Infrastructure

In the following basic information on the key experimental facilities and components of the technical infrastructure installed at the Walther-Meißner-Institute (WMI) is given.

UHV Laser-MBE

The WMI operates an UHV Laser-Molecular Beam Epitaxy (L-MBE) system for the growth of complex oxide heterostructures. The system has been designed to meet the special requirements of oxide epitaxy. The UHV cluster tool consists of the following main components:

- central transfer chamber;
- load-lock chamber with a heater system for substrate annealing;
- laser deposition chamber with a KrF excimer laser, *in-situ* reflection high energy electron diffraction (RHEED) system, laser substrate heating system, and atomic oxygen/nitrogen source; the RHEED system has been modified to allow for the operation at high oxygen partial pressure up to 0.5 mbar;
- surface characterization chamber with UHV scanning atomic force microscope (Omicron);
- metallization chamber with a four heart electron gun system and a liquid nitrogen cooled sample stage. The sample holder can be tilted for shadow evaporation.

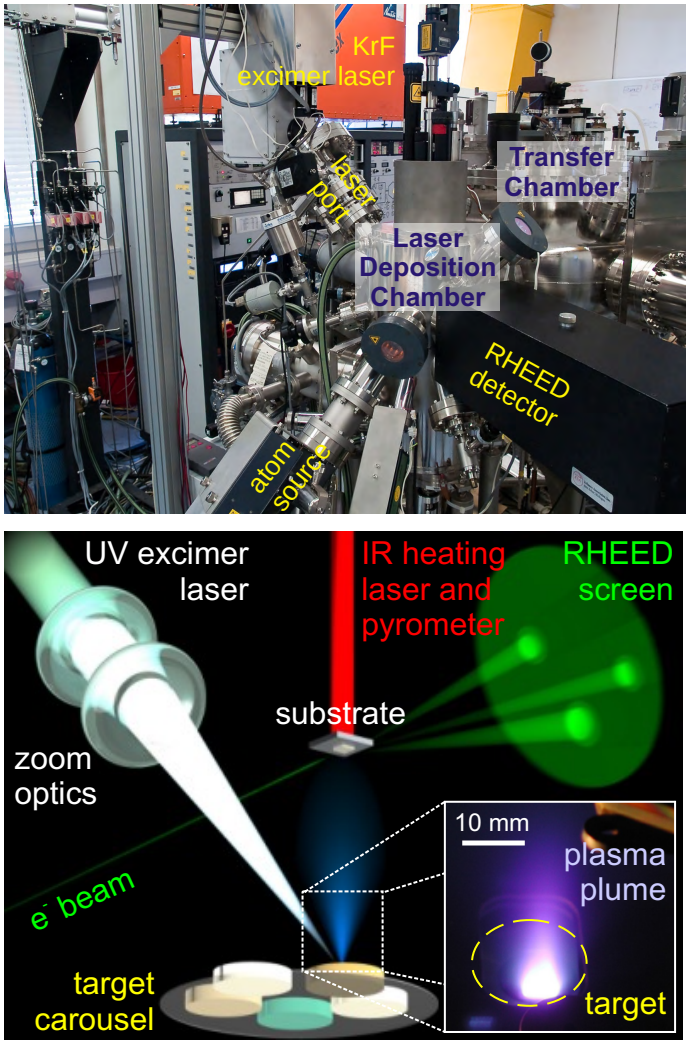

Figure 1: Top: UHV laser-molecular beam epitaxy system. Bottom: principle of the deposition process.

The system is used for the growth of complex oxide heterostructures consisting of superconducting, ferromagnetic, ferroelectric, and semiconducting materials such as high-temperature superconductors, doped manganites, (double) perovskites, magnetite, zinc oxide, rare earth iron garnets, pyrochlore iridates, etc.

The original laser molecular beam epitaxy system (laser-MBE) designed already in 1995/96 has been continuously upgraded and modified until now. In particular, the substrate heating system and the temperature control unit were changed from a resistive radiation heater to an infrared laser heating system (see Fig. 3, left) including a pyrometer for determining the sample temperature. In addition, a source for atomic oxygen and nitrogen has been installed. The main advantage of the new heating system is that only the substrate is heated while the surrounding parts are hardly affected (Fig. 3, right). In this way one can achieve a substantially better vacuum at temperatures well above 1000 °C. The achievable substrate temperature is limited by the melting point and the size of the substrate material (approx. 1410 °C for a 5 mm × 5 mm silicon substrate). The laser heating system has already been successfully used for removing the amorphous silicon oxide layer from the surface of silicon substrates at 1150 °C.

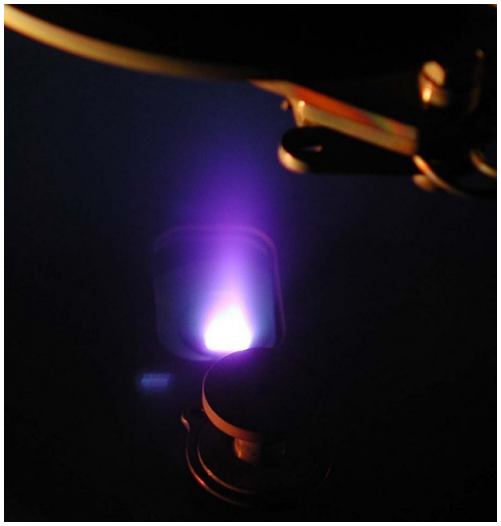

Figure 2: Pulsed Laser Deposition (PLD): When the pulse of the UV laser (KrF excimer laser, 248 nm) hits the target, the target material is ablated and the so-called laser "plume" containing highly excited atoms and molecules is formed.

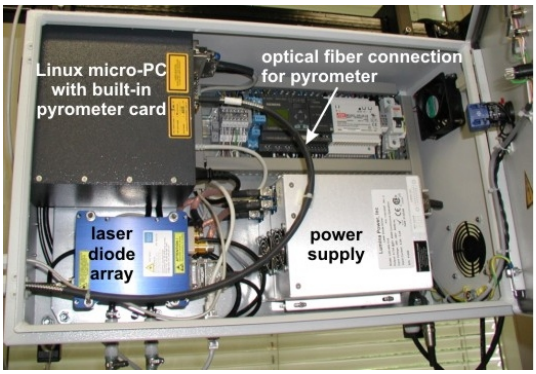

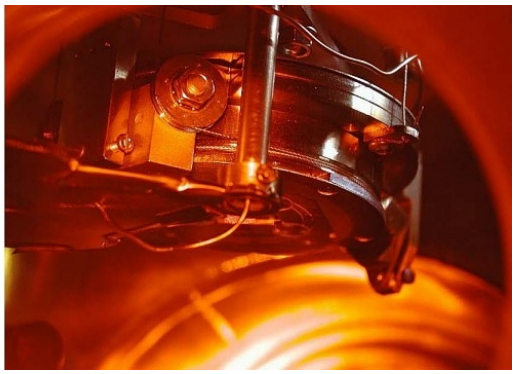

Figure 3: Components of the laser heating system: The substrate is heated using an IR diode laser head that is located in a separate box far away from the deposition chamber (left). The laser light is brought to the substrate (right) via an optical fiber.

We have further developed and installed a home-made telescope zoom optics for the pulsed UV laser light, consisting of in total five lenses on sliding lens holders allowing for a movement over a total distance of 1200 mm. The lens holders are attached to independent stepper motors, each connected to a controller providing an accurate positioning precision. The controllers are driven via a PC, thus allowing for a full automation of the lens system itself. With this telescope zoom optics we are able to change the area of the UV laser spot on the target, resulting in an accessible range of laser fluences from $\rho_L = 0.5\,J/cm^2$ to $5\,J/cm^2$. To maintain a stable laser fluence at the target, we have installed a so-called *intelligent* window (PVD Products) at the laser entrance port combining two unique features. First, it keeps the inner side of the entrance window free of coatings by blocking the ablated plasma plume via a rotatable disc consisting of UV grade fused silica. Second, an insertable mirror positioned in the light path after the disc allows to guide the incoming UV laser pulse through a side window, where its energy is determined by a pyroelectric detector. These measures help to improve the deposition processes by accurately monitoring ρ_L as one of the most critical process parameters.

UHV Electron Beam Evaporation System

The UHV metal MBE system allows for the growth of high quality metallic thin films by electron beam evaporation and molecular beam epitaxy. The system is optimized for the fabrication of superconducting persistent current qubits by aluminum shadow evaporation. It is equipped with an improved substrate holder allowing for multi-angle shadow evaporation. The main components of the system are:

- UHV system with a process chamber with a base pressure of $\sim 1 \times 10^{-8}$ mbar pumped by a 1000 l/s turbo molecular pump with magnetic suspension of the rotor adequate for corrosive gases.
- Load-lock chamber equipped with a magnetic transfer system (push-pull positioner) for sample transfer without breaking the vacuum in the process chamber.
- Downstream pressure control by an adaptive pressure controlled gate valve.
- Electron beam evaporator with six 8 cm^3 crucibles embedded in a linearly movable water cooled rail providing six different materials.
- Film thickness measurement and closed loop evaporation rate control by a quartz crystal microbalance in combination with the evaporation controller.
- Effusion cell for molecular beam epitaxy processes.
- Ion sputtering gun for in-situ sample cleaning
- Manipulator with UHV stepping motors for automated and precise sample tilt and options for rotating and cooling the sample.

A precise and reproducible tilt of the sample is realized by a sample manipulator with process specific degrees of freedom. The downstream pressure control allows for a fast adjustment and precise control of the oxygen partial pressure. This is crucial for a well-defined oxidation process of the Josephson junctions barriers. The entire process can be performed fully automated via a touch screen and is controlled by a LabView program. Up to six effusion cells can be optionally added to the system allowing for further materials. The manipulator allows for further degrees of freedom that can be used to align the sample to the effusion cells, the ion sputtering gun and to measuring equipment such as ellipsometry or RHEED.

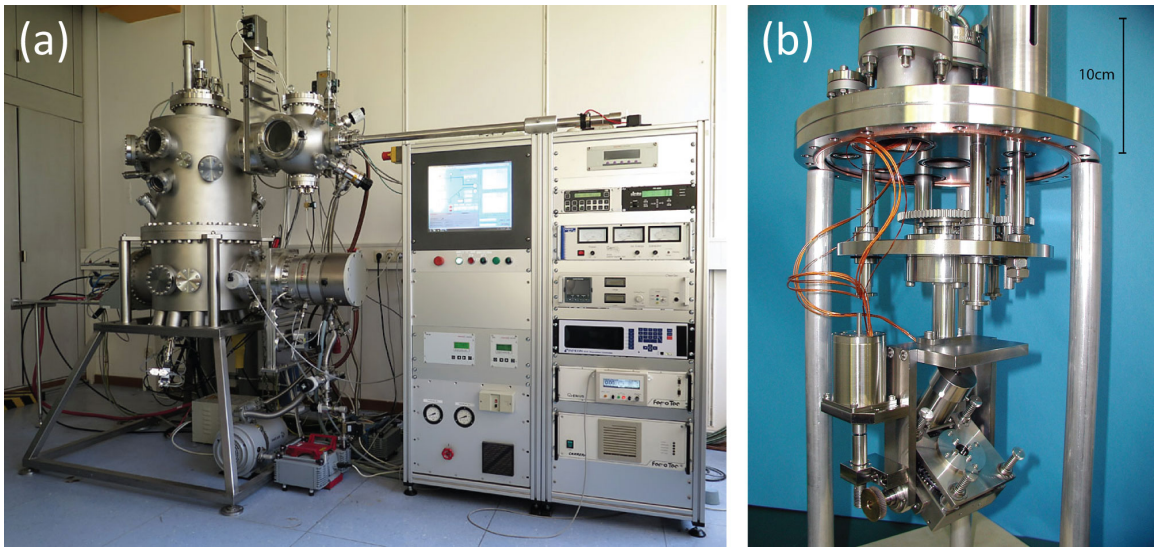

Figure 4: (a) Photograph of the UHV electron beam evaporation system. (b) Manipulator with UHV stepping motors for automated and precise sample tilt and options for rotation.

Single Crystal Growth and Synthesis of Bulk Materials

Transition metal oxides are of great interest due to their various interesting physical properties (e.g. high temperature superconductivity, colossal magnetoresistance, ferroelectricity, nonlinear optical properties etc.) and their high potential for applications. Therefore, the WMI operates a laboratory for the synthesis of bulk materials and single crystals of transition metal oxides. Besides various chamber- and tube furnaces a four-mirror image furnace is used for the crystal growth of various oxide systems. With this furnace crystals of many different compounds of the high temperature superconductors and various other transition metal oxides have been grown as single crystals using the traveling solvent floating zone technique. The furnace consists basically of 4 elliptical mirrors with a common focus on the sample rod and with halogen lamps in their other focus. By irradiation of the focused light the sample rod is locally heated and eventually molten. The molten zone can be moved up and down along the entire sample rod under simultaneous rotation. Due to the anisotropic growth velocity a preferential growth of those grains with the fastest growth velocity along the pulling direction is obtained and the formerly polycrystalline rod is transformed into a single crystal. Single crystal growth can be performed with this furnace at maximum temperatures up to 2200 °C in the pressure range from 10^{-5} mbar up to 10 bar and in oxidizing, reducing as well as inert atmosphere.

Figure 5: The four-mirror image furnace installed at the crystal laboratory of the WMI. Crystals can be grown by the floating zone and traveling solvent floating zone techniques at temperatures up to 2200 °C and pressures up to 10 bar.

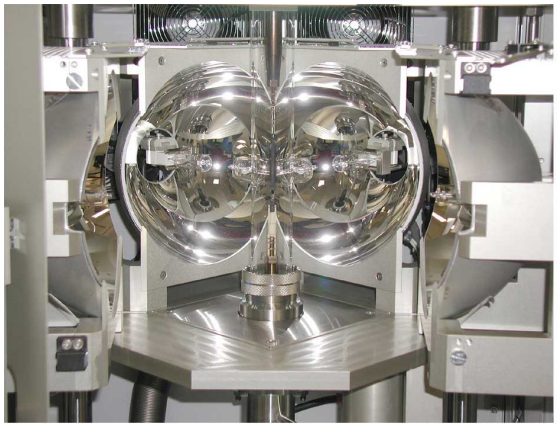

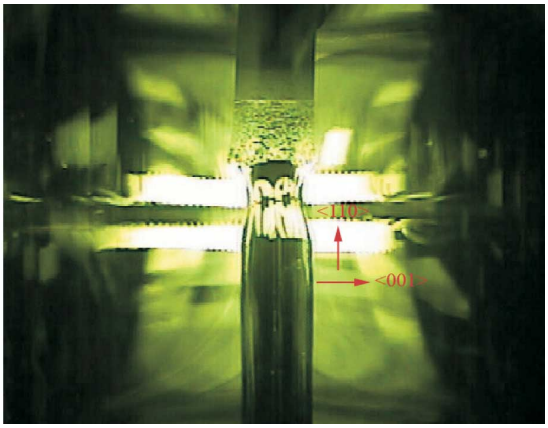

Figure 6: Left: Central part of the image furnace with four elliptical mirrors. In the center one can see the quartz tube with a polycrystalline rod. Right: View on the molten zone of $Pr_{2-x}Ce_xCuO_4$ (melting point: 1280 °C) obtained by a CCD camera.

The X-ray diffraction systems

For X-ray analysis the WMI operates two X-ray diffractometers (Bruker D8 Advance and D8 Discover). The two-circle system is used for powder diffraction. In this system the samples can be heated in oxygen atmosphere up to 1600 °C. It is equipped with a Göbel mirror and an area detector to save measuring time. The second system is a high resolution four-circle diffractometer that can be used for reciprocal space mappings. It is equipped with a Göbel mirror and an asymmetric two-fold Ge monochromator and allows for the texture analysis of thin film heterostructures, superlattices and single crystalline materials. In both systems measurements can be carried out fully computer controlled.

Beside these two Bruker X-ray systems a Laue camera for single crystal analysis and a Debye-Scherrer camera are available.

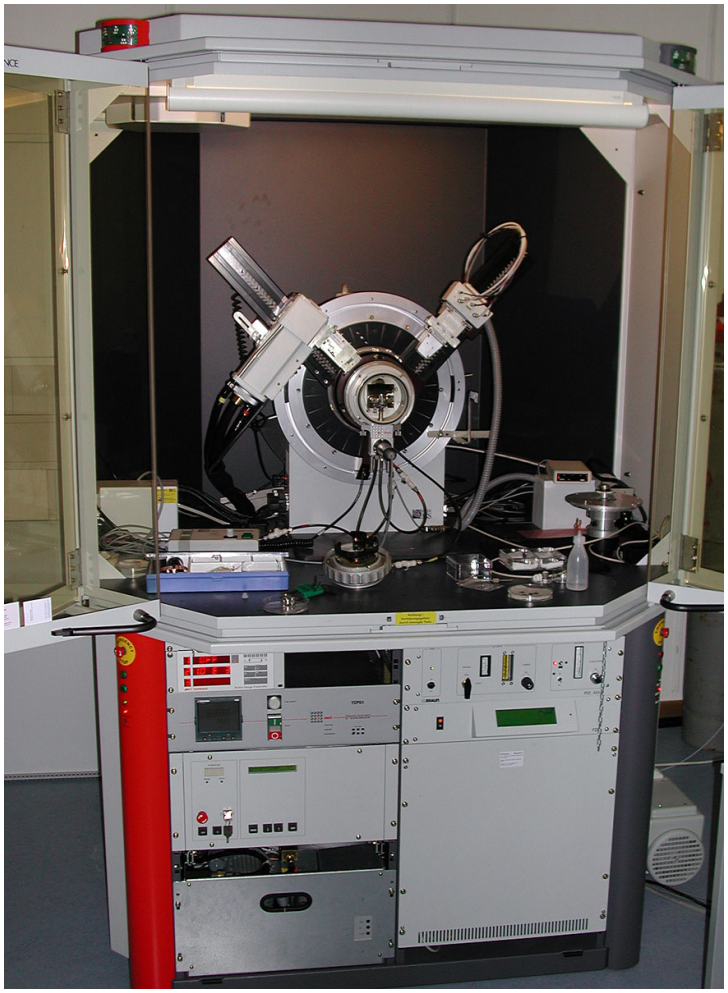

Figure 7: The two-circle X-ray diffractometer Bruker D8 Advance.

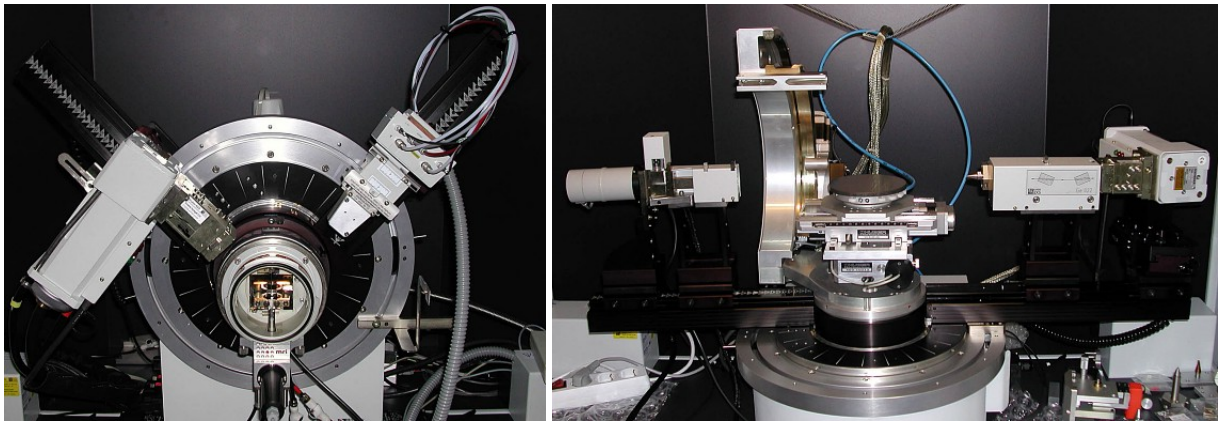

Figure 8: Left: High temperature sample holder of the D8 Advance system. Right: Four-circle high resolution X-ray diffractometer Bruker D8 Discover.

Figure 9: Quantum Design SQUID magnetometer.

The SQUID magnetometer

For the analysis of the magnetic properties of materials, a Quantum Design SQUID magnetometer system (Fig. 9) is operated at the WMI. The SQUID magnetometer allows for measurements in the temperature regime from 1.8 to 400 K and provides excellent sensitivity particularly in the low field regime. Due to the excellent sensitivity of the system, thin film samples with a very small sample volume can be analyzed. The SQUID magnetometer is equipped with a superconducting solenoid allowing for a maximum field of 7 T. At present, the magnetometer is used for the characterization of magnetic and superconducting materials (both in bulk and thin film form). Examples are the cuprate high temperature superconductors, the doped manganites, magnetite, the double perovskites, magnetic semiconductors, or multiferroics.

The High Field Laboratory

Transport and thermodynamic properties of samples are often studied as a function of the applied magnetic field. For such measurements several superconducting magnets are available at the WMI. Two of them (8/10 and 15/17 Tesla magnet system) are located in the high magnetic field laboratory in the basement of the WMI. The magnet systems are installed below the floor level to facilitate the access to the top flange and the change of the sample sticks. The magnet systems are decoupled from the building to avoid noise due to mechanical vibrations. A variety of sample holders can be mounted allowing for e.g. sample rotation during the measurement. For standard sample holders the accessible temperature regime is $1.5\,\mathrm{K} < T < 300\,\mathrm{K}$. However, also ^{3}He/^{4}He dilution refrigerator inserts ($T > 20\,\mathrm{mK}$) or high temperature units ($T < 700\,\mathrm{K}$) can be mounted. All measurements are fully computer controlled (by the use of the LabView software tool) allowing for remote control and almost continuous measurements.

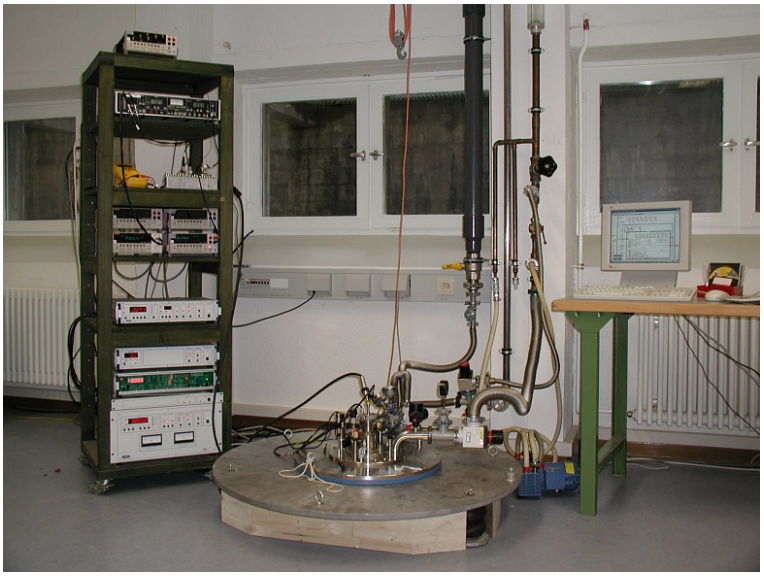

Figure 10: High field laboratory with Oxford 17 T magnet system.

Since 2012, a 3D vector magnet with variable temperature insert, allowing for 2.5 T in-plane and 6 T out-of-plane magnetic fields is available for thermal and electrical transport experiments. This system has been named "Chaos" cryostat (acronym for "Cold, Hot And Other Secret experiments"). It consists of a ^{4}He flow cryostat with a liquid nitrogen shield and in-

cludes a vertically oriented 6 T solenoid combined with two horizontally oriented split coil pairs. The magnet system can be operated in two ways:

- in a single axis mode: up to 6(2.5) T are provided in the vertical (horizontal) direction.
- in a arbitrary axis mode: the flux density vector can be oriented in arbitrary directions and the magnitude of the flux density is limited to 2.5 T.

The magnetic field is controlled by a Mercury IPS superconducting magnet power supply master/slave system. It provides output currents of up to 120 A in bipolar operation for each magnet axis. The control of the system is feasible either directly via touch-screen or remote using a LabView based software.

Figure 11: The 3D vector magnet with control electronics in the "CHAOS" Laboratory.

The Chaos cryostat has a IN100 variable temperature insert (VTI), enabling an operation for temperature setpoints between 1.5 K and 300 K. The temperature control of the sample space inside the VTI can be achieved via an automatic needle valve drive for helium flow control and/or an automatic heater system. The temperature of the VTI is read via a Cernox sensor fitted to the heat exchanger. A remote control of the system is realized by a LabView based software. It provides control of the VTI (heater, needle valve, temperature setpoint) and the IPS (control of the magnetic field setpoints and energizing rates for the three vector components of the field) as well as the display of the actual He and liquid nitrogen levels.

A further 3D vector magnet allowing for 1 T in-plane and 6 T out-of-plane magnetic fields is installed in the WMI Quantum Laboratories as part of a cryogen-free dilution system.

The Clean Room Facility

For the fabrication of solid state nanostructures and quantum circuits including superconducting, spintronic and nanomechanical devices the WMI operates a class 1000 clean room facility with an area of about 50 m^2. This clean room facility has been put into operation at the WMI within the year 2001. The clean room is subdivided into two parts for optical lithography and electron beam lithography, respectively. The clean room facility is equipped with the standard tools for optical lithography such as resist coaters, hot plates, wet benches, a Karl Süss MJB3 mask aligner and an optical projection lithography system. The technical infrastructure for the clean room is located in the basement of the WMI directly below the clean room area.

Figure 12: Top: Part of the clean room facility with optical lithography equipment and clean room benches. Bottom: Resist coater and hot plates.

The clean room also is equipped with a reactive ion etching system, Plasmalab 80 Plus with ICP plasma source (Oxford Instruments Plasma Technology).

Electron Beam Lithography

A 100 kV Electron Beam Lithography System nB5 fabricated by NanoBeam Ltd., UK, is installed in the second part of the clean room facility. The nB5 is a round-beam step-and-repeat system oriented towards high-end R&D applications at universities and research institutes. It is designed for nanopatterning and mix-and-match lithography. The innovative design of the electron optics and automation system enhances its throughput and reliability. It is an ideal tool for nano-device research and production. The electron beam lithography is used for the fabrication of nanostructures in metallic and oxide systems required for the study of quantum effects in mesoscopic samples.

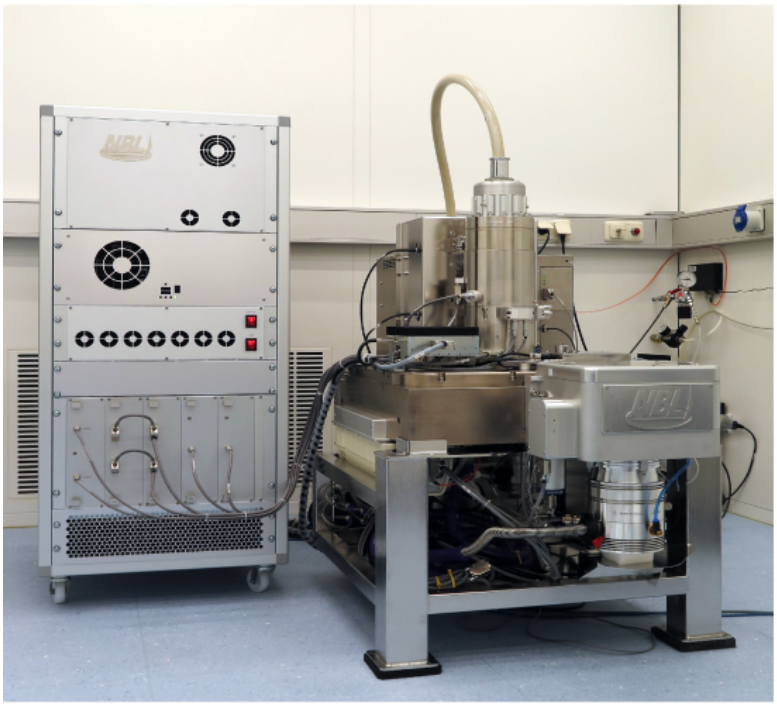

Figure 13: 100 kV Electron Beam Lithography System nB5 of NanoBeam Ltd., UK, inside the WMI cleanroom facility.

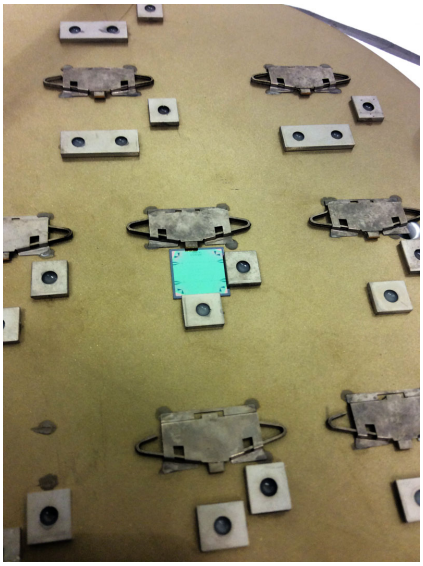

Figure 14: Chuck of the nB5 e-beam lithography system with a mounted $12 \times 12\,\mathrm{mm}^2$ silicon wafer.

The nB5 Electron Beam Lithography System employs low Coulomb-effect electron optics and sophisticated column designs to reduce beam size. The shorter optical column eliminates column bending and reduces system vibration. The modern electronics has low noise and low thermal effects. The perfectly integrated machine structure greatly improves system settling time and total stage move time. The advanced vibration tracking design enables the nB5 system to write on the fly. All these features combined with the fast deflection speed and high data processing rate make the nB5 the highest throughput system available today. Moreover, the nB5 requires undemanding cleanroom conditions, in particular regarding temperature stability, stray field magnitude, and floor vibration level.

The nB5 system is equipped with a thermal field emitter (TFE), an electrostatic lens and magnetic condenser lens, a conjugate beam blanking at $< 5\,\mathrm{ns}$ slew rate and a dual beam deflection. The latter is used to achieve ultra-high deflection speed for beam writing (clock rate: 55 MHz). The total deflection coverage is combined with the mainfield and the subfield and controlled by two independent deflection sub-systems (field size: $1000\,\mu\mathrm{m}$, address resolution: 1 nm). The characteristic performance parameters of the electron optics of the nB5 system are: (i) beam voltage range: 20 kV to 100 kV, (ii) minimum beam current: 0.1 nA, (iii) maximum beam current: 100 nA, (iv) theoretical beam size: 2.3 nm at 100 kV, (v) guaranteed writing beam size: $< 5\,\mathrm{nm}$ at 2 nA, (vi) beam current drift: $< 0.5\%$/hour at 5 nA, (vii) beam position drift: $< 50\,\mathrm{nm}$/hour for 3 nA beam current, including blanking, deflection and stage move.

The XY-stage allows for a traversal distance of 200 mm with a total stage move time of only 150 ms for 1 mm stage movement and a position measurement resolution of 0.3 nm using laser interferometry. The maximum substrate sizes are $2 - 8$ in for round substrates, $2 - 5$ for square glass masks up to 3 mm thickness. Finally, the nB5 system has airlock operation with automatic loading robotics with a loading cassette for 6 chucks with a maximum diameter of 8 inch.

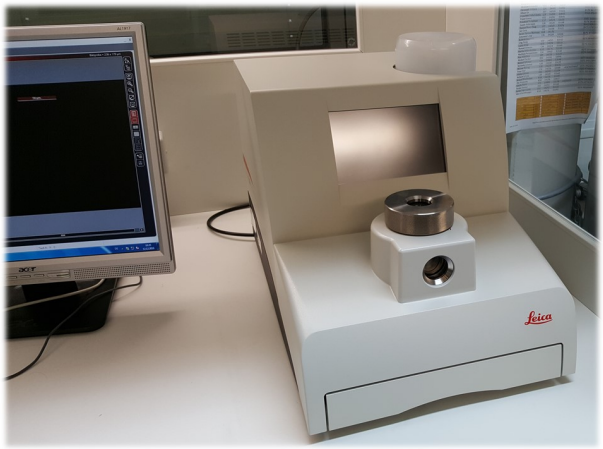

Figure 15: The fully automated Critical Point Dryer Leica EM CPD 300.

Automated Critical Point Dryer Leica EM CPD 300

The fabrication of nanomechanical systems requires the removal of solvent used for wet chemical processing by a critical point dryer. At WMI, we use the Critical Point Dryer Leica EM CPD 300, which allows the fully automated drying of biological specimens such as pollen, tissue, plants, insects etc., as well as NEMS (Nano Electro Mechanical Systems).

To ensure a low CO_2 consumption and a very short process time a new filler concept is used in the Leica EM CPD 300. Special attention has been put on safety issues by implementing software controlled cut-off functions and integrating a waste separator.

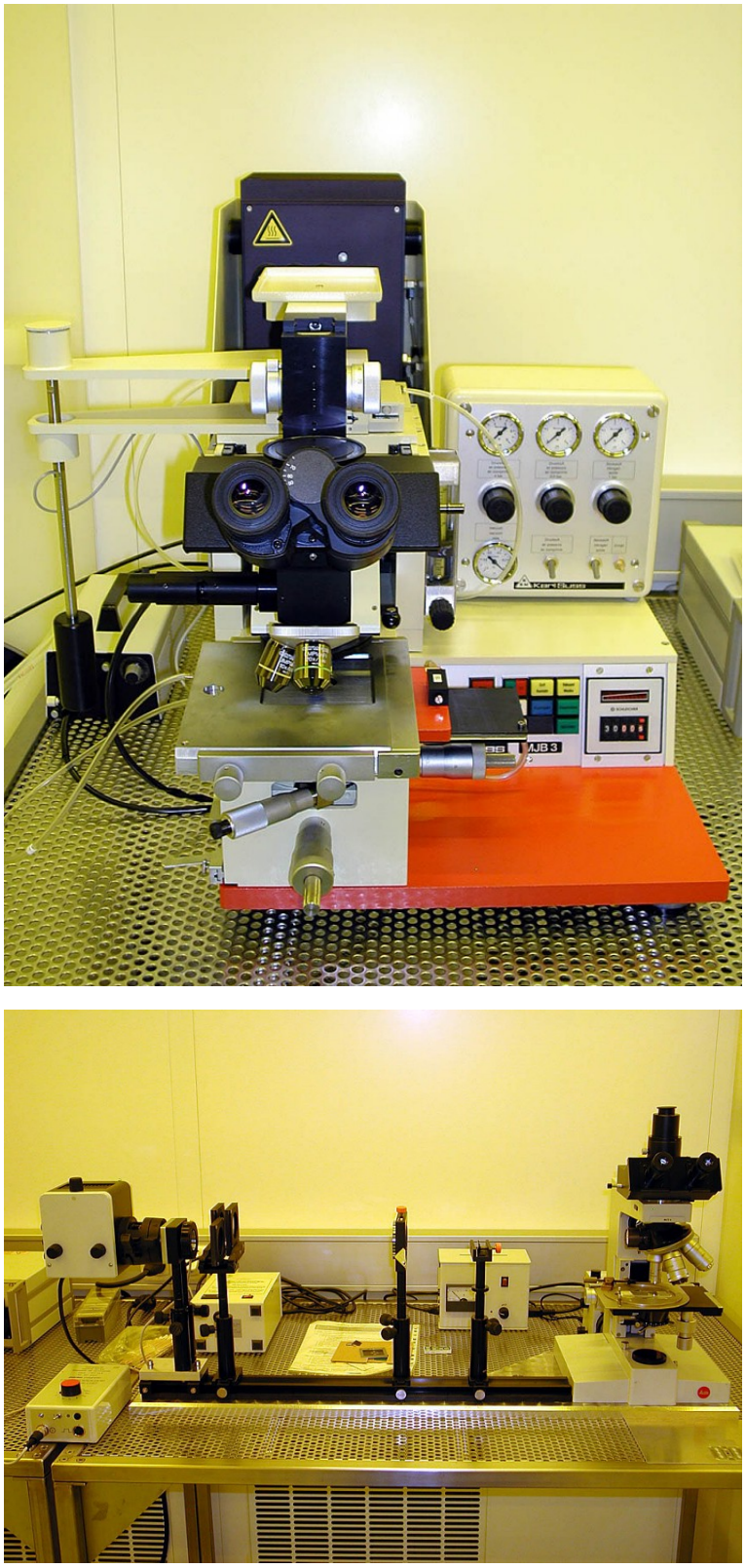

Figure 16: Top: Süss MJB 3 maskaligner for optical lithography. Bottom: Optical projection lithography based on an optical microscope.

Optical Lithography

For optical lithography, a Karl Süss MJB 3 maskaligner or an optical microscope based projection system are used. The maskaligner operates in the 1 : 1 soft or hard contact mode and uses chromium metal masks. In the projection system the mask pattern is demagnified by a factor of 5 to 100. Therefore, cheap foil masks can be used. With both systems microstructures with a lateral dimension down to 1 µm can be fabricated.

Low and Ultra-Low Temperature Facilities

At the WMI, we have constructed the first dilution refrigerator with pulse tube pre-cooling for ultra-low temperature experiments. This type of refrigerator works without cryo-liquids, and thus is a lot more practical, more economical and more reliable than cryostats with liquid helium pre-cooling. These days, all major cryo-engineering companies are offering commercial versions of this Millikelvin cooler, and these so-called "dry" refrigerators outsell conventional refrigerators by a wide margin. The general construction concept of most manufacturers is unchanged from our original prototype, where the refrigerator consists of three basic components. The first cooling stage is a commercial pulse tube cryocooler which reaches a base temperature of 2.5 K. The second stage is a Joule-Thomson stage, and the last stage is a dilution refrigeration stage, where the lowest temperature of the cryostat is about 0.01 K (Fig. 17).

Figure 17: The "dry" dilution refrigerator of the WMI.

Figure 18: Low-temperature unit of a WMI dilution refrigerator ready to go into a cryostat.

Figure 19: Two mixing chamber mounting plates with silver sponges. Those are needed to overcome the thermal resistance (Kapitza resistance) between the liquid ^{3,4}He and the mounting plate of the mixing chamber. To fabricate the mounting of the sponge (square pins embedded in the sponge) a spark erosion technique has been employed.

In many low temperature applications high refrigeration capacities are required. Our design allows for a high circulation rate of ^{3}He which in the end determines the cooling power of a dilution refrigerator. Presently our "dry" fridge reaches a refrigeration capacity of 700 µW at a temperature of the mixing chamber of 0.1 K, seven times the cooling power of the WMI nuclear demagnetization cryostat. Goals of our present work are a further increase of cooling power and a lower base temperature of the dry dilution refrigerator.

A smaller version of our cryogen-free fridge has become commercially available by *Oxford Instruments* (formerly *VeriCold Technologies, Ismaning*). It has a refrigeration capacity of 250 µW at a mixing chamber temperature of 0.1 K (Fig. 18).

The WMI also develops and fabricates dilution refrigerator inserts for temperatures down to

about 20 mK. The inserts fit into all cryogenic systems (e.g. superconducting magnets) having a two inch bore. They allow fast sample change and rapid cool down cycles of less than five hours. The dilution refrigerator inserts are engineered and fabricated in-house and are also provided to other low temperature laboratories for ultra-low temperature experiments.

Millikelvin Temperatures in Combination with 3D Vector Magnetic-Fields

Figure 20: The dilution refrigerator with the 3D vector magnet located in the Quantum Laboratories.

In one room of the WMI Quantum Laboratories a cryogen-free dilution refrigerator is installed. This system is equipped with a 3D vector magnet allowing for 1 T in-plane and 6 T out-of-plane magnetic fields. Additional microwave coaxial lines allow for the microwave spectroscopy up to 18 GHz under these experimental conditions.

Scientifically, several directions in the field of fundamental light-matter interaction are envisaged:

(i) Circuit quantum electrodynamics (circuit QED), where superconducting qubits form hybrids with microwave resonators. These experiments are time consuming, because quantum effects arise in the limit of low excitation numbers. Hereby, challenging requirements are imposed on the detection systems allowing to detect microwave signals in the attowatt regime.

(ii) Storage of quantum states. One possibility is the transfer of the quantum information contained in photons to long-lived spin states. Additionally, exchange coupled systems or ferromagetic systems come into focus, because the effective coupling strength scales with the square-root of the number of spins contributing. In general, we study the light-matter interaction with long-lived spin systems and integrate them into superconducting quantum circuits.

(iii) Spin systems. Here, our studies are not limited to paramagnetic spin systems, but also involve exchange coupled (ferro- or ferri-) magnetic systems. Hereby, magnetization damping can be investigated as a function of temperature, frequency and magnetic field direction.

(iv) Circuit electro-mechanical hybrid systems consisting of a nano-mechanical element coupled to a superconducting microwave resonator. In this context, sideband cooling of the mechanical system into its ground state and pulsed spectroscopy of hybrid system are performed and will be extended.

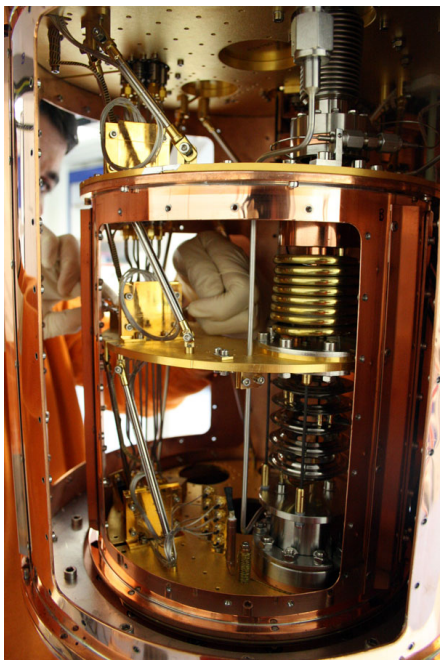

Figure 21: Inside of the dilution system. The windows of the 4 K and the still shield are removed providing access to the low temperature stages.

WMI Millikelvin Facilities for Experiments with Superconducting Quantum Circuits

The research on superconducting quantum circuits at WMI focuses mainly on systems sensitive to externally applied flux (flux qubits), circuit QED systems where flux qubits are coupled to transmission line resonators, squeezing physics in flux driven Josephson parametric amplifiers, and propagating quantum microwaves (e.g., quantum state reconstruction methods). In order to further develop our activities on quantum effects in the microwave regime, additional cryogenic capacities at millikelvin temperatures have been established. In addition to sufficient cooling power, the specifications for these cryostats are mainly dictated by the dimensions (typically a few centimeters in each direction) of bulky microwave components such as circulators or microwave switches.

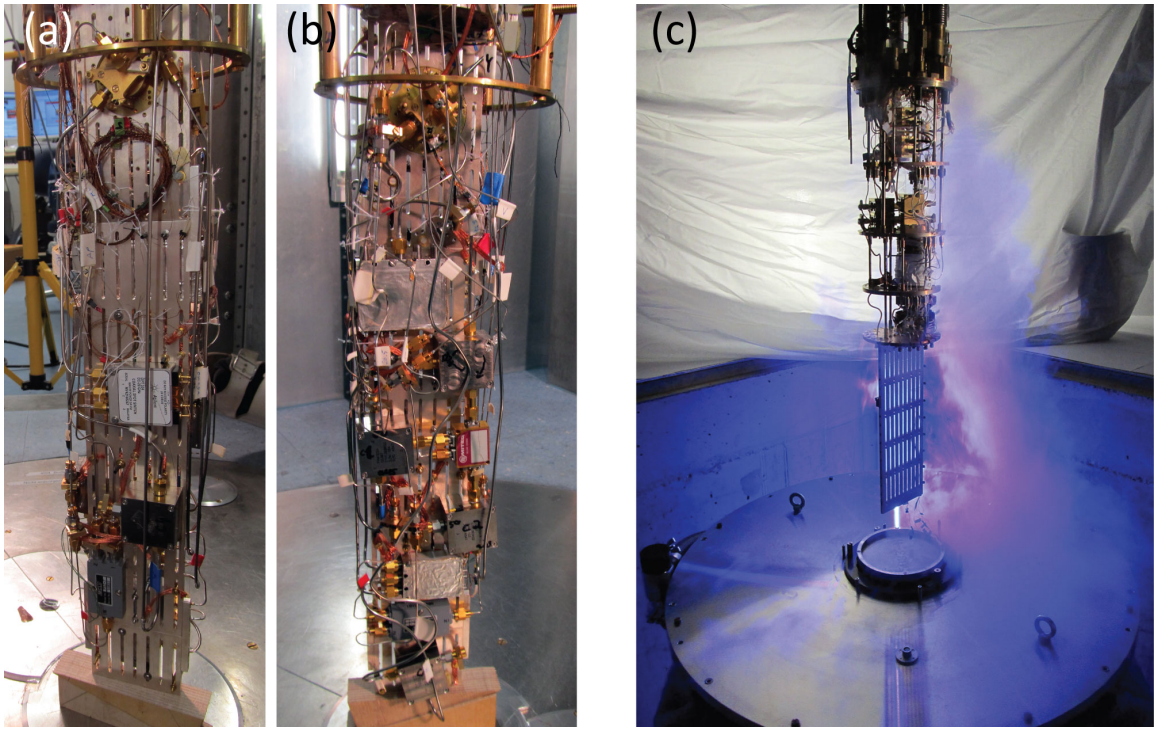

Figure 22: Liquid-helium precooled dilution refrigerators for experiments with superconducting quantum circuits. (a), (b) Back and front sides of the sample stage of the K12-refrigerator equipped with four circuit QED experiments. The height of the silver rod is 50 cm. (c) Sample stage and dewar of the dilution refrigerator in the quantum laboratory K04.

Two liquid-helium precooled dilution refrigerators are available for experiments with superconducting quantum circuits. The dilution refrigerator in laboratory K12 provides a sample space with a cylindrical volume with 11 cm diameter 55 cm height. The refrigerator is equipped with four microwave amplifiers at the 4 K-stage, seven broadband input lines and 80 twisted pair DC lines. This allows for mounting four experiments simultaneously to avoid idle times by interleaved measurements (see Fig. 22(a) and (b)). The base temperature of this refrigerator is 20 mK.

A new liquid-helium precooled dilution refrigerator for experiments with superconducting quantum circuits has been set up in the quantum laboratory K04. To provide enough space at the sample stage we have installed a Cryogenic Ltd. stainless steel dewar with a ^{4}He volume of 89 l. The time between two refills exceeds nine days. The cryostat is equipped with 16 coaxial measurement lines suitable for microwave frequencies down to the mixing chamber stage and low-noise cryogenic high electron mobility transistor (HEMT) amplifiers. Presently up to four samples can be mounted simultaneously to the sample stage. By expanding the number of input lines in the near future a more complex experiment can be set up. The cooling power of

the mixing chamber at 100 mK was determined to about 140 µW.

A new cryogen-free dilution refrigerator with a pulse tube refrigerator (PTR) for precooling and with a large sample stage has been set up in room K21 of the WMI Quantum Laboratories using the longstanding experience in dry dilution refrigerators at WMI. This refrigerator features large diameters (tens of centimeters) of all temperature stages providing sufficient space for advanced quantum experiments. The main components of the refrigerator are the PTR, a 1 K-stage and a dilution unit. The two stages of the PTR cool the incoming ^{4}He and the ^{3}He/^{4}He mixture as well as one radiation shield at each stage. To provide sufficiently high cooling power near 1 K to cool microwave components and cables, this refrigerator has been equipped with a 1 K-stage operating in a closed cycle. A refrigeration capacity of the 1 K-stage of up to 100 mW could be reached. The dilution refrigerator is precooled by a dedicated ^{4}He circuit. The minimum base temperature of the refrigerator is below 11 mK. The cooling power at 100 mK was determined to about 300 µW at the maximum ^{3}He flow rate.

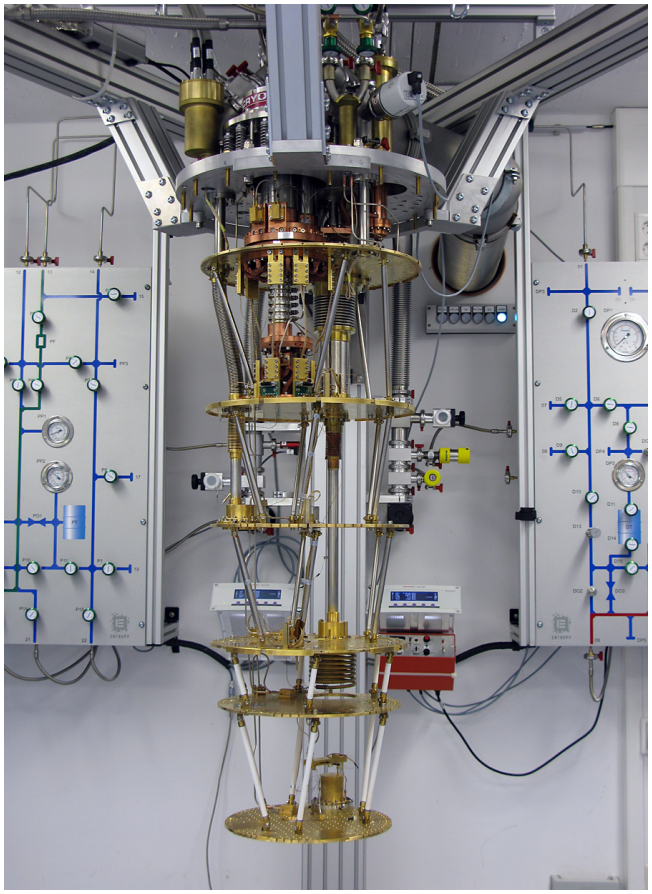

Figure 23: Dry dilution refrigerator with a large sample space.

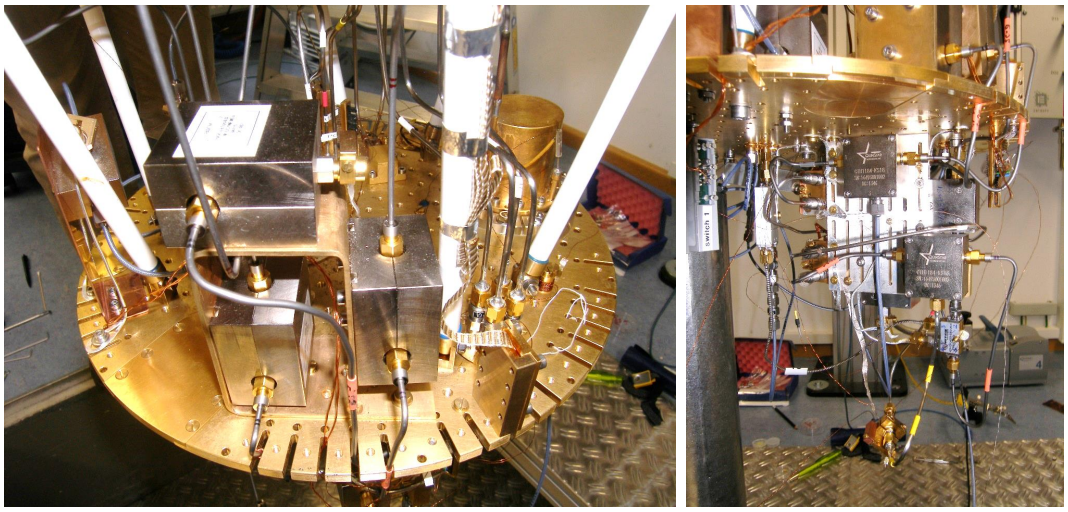

Figure 24: Low temperature platform of K21 dilution refrigerator with experimental setup for circuit QED experiments.

Statistics

Publications

1. **Helimagnon Resonances in an Intrinsic Chiral Magnonic Crystal**
Mathias Weiler, Aisha Aqeel, Maxim Mostovoy, Andrey Leonov, Stephan Geprägs, Rudolf Gross, Hans Huebl, Thomas T. M. Palstra, Sebastian T. B. Goennenwein
Phys. Rev. Lett. **119**, 237204 (2017).

2. **Observation of Caroli-de Gennes-Matricon Vortex States in $YBa_2Cu_3O_{7-\delta}$**
Christophe Berthod, Ivan Maggio-Aprile, Jens Bruér, Andreas Erb, and Christoph Renner
Phys. Rev. Lett. 119, 237001 (2017).

3. **Comprehensive phase diagram of two-dimensional space charge doped $Bi_2Sr_2CaCu_2O_{8+x}$**
Edoardo Sterpetti, Johan Biscaras, Andreas Erb, Abhay Shukla
Nature Commun. **8**, 2060 (2017).

4. **Interplay between the d- and π-electron systems in magnetic torque of the layered organic conductor κ-$(BETS)_2Mn[N(CN)_2]_3$**
O. M. Vyaselev, W. Biberacher, N. D. Kushch, and M. V. Kartsovnik
Phys. Rev. B **96**, 205154 (2017).

5. **A Microwave Interferometer of the Michelson-Type to Improve the Dynamic Range of Broadband Ferromagnetic Resonance Measurements**
E. R. J. Edwards, A. B. Kos, M. Weiler, and T. J. Silva
IEEE Magnetics Letters **8**, 1 (2017).

6. **Concepts for a low-vibration and cryogen-free tabletop dilution refrigerator**
Kurt Uhlig
Cryogenics **87**, 29 - 34 (2017).

7. **Production and characterization of long-term stable superparamagnetic iron oxide-shell silica-core nanocomposites**
Angelika Nistler, Carolin Hartmann, Christine Rümenapp, Matthias Opel, Bernhard Gleich, Natalia P. Ivleva, Reinhard Niessner, Michael Seidel
J. Magn. Magn. Mater. 442 , 497 (2017).

8. **$Co_{11}Li[(OH)_5O][(PO_3OH)(PO_4)_5]$, a Lithium-Stabilized, Mixed-Valent Cobalt(II,III) Hydroxide Phosphate Framework**
Jennifer Ludwig, Stephan Geprägs, Dennis Nordlund, Marca M. Doeff, Tom Nilges
Inorg. Chem. **56**, 10950 (2017).

9. **Direct synthesis and characterization of mixed-valent $Li_{0.5-\delta}CoPO_4$, a Li-deficient derivative of the Cmcm polymorph of $LiCoPO_4$**
Jennifer Ludwig, Carlos Alarcón-Suesca, Stephan Geprägs, Dennis Nordlund, Marca M. Doeff, Inés Puente Orench, Tom Nilges
RSC Adv. **7**, 28069-28081 (2017).

10. **Temperature dependent magnetic damping of yttrium iron garnet spheres**
Hannes Maier-Flaig, Stefan Klingler, Carsten Dubs, Oleksii Surzhenko, Rudolf Gross, Mathias Weiler, Hans Huebl, Sebastian T. B. Goennenwein
Phys. Rev. B **95**, 214423 (2017).

11. **Off-axis parabolic mirror optics for polarized Raman spectroscopy at low temperature**
N. Chelwani, D. Hoch, D. Jost, B. Botka, J.-R. Scholz, R. Richter, M. Theodoridou, F. Kretzschmar, T. Böhm, K. Kamarás, and R. Hackl
Appl. Phys. Lett. **110**, 193504 (2017).

12. **Temperature dependence of the non-local spin Seebeck effect in YIG/Pt nanostructures**
Kathrin Ganzhorn, Tobias Wimmer, Joel Cramer, Richard Schlitz, Stephan Geprägs, Gerhard Jakob, Rudolf Gross, Hans Huebl, Mathias Kläui, Sebastian T. B. Goennenwein
AIP Advances **7**, 085102 (2017).

13. **Magnon mode selective spin transport in compensated ferrimagnets**
Joel Cramer, Er-Jia Guo, Stephan Geprägs Andreas Kehlberger, Yurii P. Ivanov, Kathrin Ganzhorn, Francesco Della Coletta, Matthias Althammer, Hans Huebl, Rudolf Gross, Jürgen Kosel, Mathias Kläui, and Sebastian T. B. Goennenwein
Nano Letters **17**(6), 3334–340 (2017).

14. **Pure spin current transport in gallium doped zinc oxide**
Matthias Althammer, Joynarayan Mukherjee, Stephan Geprägs, Sebastian T. B. Goennenwein, Matthias Opel, M.S. Ramachandra Rao, and Rudolf Gross
Appl. Phys. Lett. **110**, 052403 (2017).

15. **Strong evidence for d-electron spin transport at room temperature at a $LaAlO_3/SrTiO_3$ interface**
Ryo Ohshima, Yuichiro Ando, Kosuke Matsuzaki, Tomofumi Susaki, Mathias Weiler, Stefan Klingler, Hans Huebl, Eiji Shikoh, Teruya Shinjo, Sebastian T. B. Goennenwein, Masashi Shiraishi
Nature Materials **16**, 609-614 (2017).

16. **Gilbert damping of magnetostatic modes in a yttrium iron garnet sphere**
Stefan Klingler, Hannes Maier-Flaig, Carsten Dubs, Oleskii Surzhenko, Rudolf Gross, Hans Huebl, Sebastian T.B. Goennenwein, Mathias Weiler
Appl. Phys. Lett. **110**, 092409 (2017).

17. **Dark-Photon Search using Data from CRESST-II Phase 2**
G. Angloher, P. Bauer, A. Bento, C. Bucci, L. Canonica, X. Defay, A. Erb, F. v. Feilitzsch, N. Ferreiro Iachellini, P. Gorla, A. Gütlein, D. Hauff, J. Jochum, M. Kiefer, H. Kluck, H. Kraus, J.C. Lanfranchi, J. Loebell, M. Mancuso, A. Münster, C. Pagliarone, F. Petricca, W. Potzel, F. Pröbst, R. Puig, F. Reindl, K. Schäffner, J. Schieck, S. Schönert, W. Seidel, L. Stodolsky, C. Strandhagen, R. Strauss, A. Tanzke, H.H. Trinh Thi, C. Türkoğlu, M. Uffinger, A. Ulrich, I. Usherov, S. Wawoczny, M. Willers, M. Wüstrich, A. Zöller
Eur. Phys. J. C **77**, 299 (2017).

18. **Quantum illumination reveals phase-shift inducing cloaking**
U. Las Heras, R. Di Candia, K. G. Fedorov, F. Deppe, M. Sanz, E. Solano
Scientific Reports **7**, 9333 (2017).

19. **Hysteretic Flux Response and Nondegenerate Gain of Flux-Driven Josephson Parametric Amplifiers**
Stefan Pogorzalek, Kirill G. Fedorov, Ling Zhong, Jan Goetz, Friedrich Wulschner, Michael Fischer, Peter Eder, Edwar Xie, Kunihiro Inomata, Tsuyoshi Yamamoto, Yasunobu Nakamura, Achim Marx, Frank Deppe, Rudolf Gross
Phys. Rev. Applied **8**, 024012 (2017).

20. **New radical cation salt κ-$(BETS)_2Co_{0.13}Mn_{0.87}[N(CN)_2]_3$ with two magnetic metals: Synthesis, structure, conductivity and magnetic peculiarities**
N.D. Kushch, O.M. Vyaselev, V.N. Zverev, W. Biberacher, L.I. Buravov, E.B. Yagubskii, E. Herdtweck, E. Canadell, M.V. Kartsovnik
Synth. Metals **227**, 52-60 (2017).

21. **Photon Statistics of Propagating Thermal Microwaves**
J. Goetz, S. Pogorzalek, F. Deppe, K. G. Fedorov, P. Eder, M. Fischer, F. Wulschner, E. Xie, A. Marx, R. Gross
Phys. Rev. Lett. **118**, 103602 (2017).

22. **Tunable magnon-photon coupling in a compensating ferrimagnet - from weak to strong coupling**
H. Maier-Flaig, M. Harder, S. Klingler, Z. Qiu, E. Saitoh, M. Weiler, S. Geprägs, R.Gross, S. T. B. Goennenwein, H. Huebl
Appl. Phys. Lett. **110**, 132401 (2017).

23. **Second-order decoherence mechanisms of a transmon qubit probed with thermal microwave states**

J. Goetz, F. Deppe, P. Eder, M. Fischer, M. Müting, J. P. Martínez, S. Pogorzalek, F. Wulschner, E. Xie, K. G. Fedorov, A. Marx, R. Gross
Quantum Sci. Technol. **2**, 025002 (2017).

24. **Spin injection into silicon detected by broadband ferromagnetic resonance spectroscopy**
Ryo Ohshima, Stefan Klingler, Sergey Dushenko, Yuichiro Ando, Mathias Weiler, Hans Huebl, Teruya Shinjo, Sebastian T.B. Goennenwein, Masashi Shiraishi
Appl. Phys. Lett. **110**, 182402 (2017).

25. **Shubnikov-de Haas oscillations and electronic correlations in the layered organic metal κ-(BETS)$_2$Mn[N(CN)$_2$]$_3$**
M. V. Kartsovnik, V. N. Zverev, W. Biberacher, S. V. Simonov, I. Sheikin, N. D. Kushch, E. B. Yagubskii
Low Temperature Physics **43**, 239-243 (2017).

26. **Observation of the spin Nernst effect**
Sibylle Meyer, Yan-Ting Chen, Sebastian Wimmer, Matthias Althammer, Stephan Geprägs, Hans Huebl, D. Ködderitzsch, Hubert Ebert, Gerrit E.W. Bauer, Rudolf Gross, Sebastian T.B. Goennenwein
Nature Materials **16**, 977–981 (2017).

27. **Quantum Memristors with Superconducting Circuits**
J. Salmilehto, F. Deppe, M. Di Ventra, M. Sanz, E. Solano
Scientific Reports **7**, 42044 (2017).

28. **Impact of the interface quality of Pt/YIG(111) hybrids on their spin Hall magnetoresistance**
Sabine Pütter, Stephan Geprägs, Richard Schlitz, Matthias Althammer, Andreas Erb, Rudolf Gross, and Sebastian T.B. Goennenwein
Appl. Phys. Lett. **110**, 011101 (2017).

29. **Spin Hall magnetoresistance in the non-collinear ferrimagnet GdIG close to the compensation temperature**
Bo-Wen Dong, Joel Cramer, Kathrin Ganzhorn, H. Y. Yuan, Er-Jia Guo, Sebastian T. B. Goennenwein, and Mathias Kläui
Journal of Physics - Condensed Matter **30**, 035802 (2018).

30. **Magnetically Ordered Insulators for Advanced Spintronics**
Matthias Althammer, Sebastian T.B. Goennenwein, Rudolf Gross
arXiv:1712.08517, submitted for publication (2017).

31. **Spin waves in coupled YIG/Co heterostructures**
Stefan Klingler, Vivek Amin, Stephan Geprägs, Kathrin Ganzhorn, Hannes Maier-Flaig, Matthias Althammer, Hans Huebl, Rudolf Gross, Robert D. McMichael, Mark D. Stiles, Sebastian T.B. Goennenwein, Mathias Weiler
arXiv:1712.02561, submitted for publication (2017).

32. **Phonon anomalies in FeS**
A. Baum, A. Milosavljevic, N. Lazarevic, M. M. Radonjic, B. Nikolic, M. Mitschek, Z. Inanloo Maranloo, M. Šcepanovic, M. Grujuic-Brojcin, N. Stojilovic, M. Opel, Aifeng Wang, C. Petrovic, Z.V. Popovic, R. Hackl
arXiv 1712.02724, submitted for publication (2017).

33. **Determination of spin Hall effect and spin diffusion length of Pt from self-consistent fitting of damping enhancement and inverse spin-orbit torque measurements**
A. J. Berger, E. R. J. Edwards, H. T. Nembach, O. Karis, M. Weiler, and T. J. Silva
arXiv 1711.07654, submitted for publication (2017).

34. **Proof of bulk charge ordering in the CuO$_2$ plane of the cuprate superconductor YBa$_2$Cu$_3$O$_{6.9}$ by high pressure NMR**
Steven Reichardt, Michael Jurkutat, Robin Gühne, Jonas Kohlrautz, Andreas Erb, Jürgen Haase
arXiv 1710.01520, submitted for publication (2017).

35. **Spin Hall magnetoresistance in antiferromagnet/normal metal heterostructures**
Johanna Fischer, Olena Gomonay, Richard Schlitz, Kathrin Ganzhorn, Nynke Vlietstra, Matthias Althammer, Hans Huebl, Matthias Opel, Rudolf Gross, Sebastian T.B. Goennenwein, S. Geprägs
arXiv:1709.04158, accepted for publication in Phys. Rev. B (2018).

36. **Parity-engineered light-matter interaction**
Jan Goetz, Frank Deppe, Kirill G. Fedorov, Peter Eder, Michael Fischer, Stefan Pogorzalek, Edwar Xie, Achim Marx, Rudolf Gross
arXiv:1708.06405, submitted for publication (2017).

37. **Frustrated spin order and stripe fluctuations in FeSe**
A. Baum, H. N. Ruiz, N. Lazarevic, Yao Wang, T. Böhm, R. Hosseinian Ahangharnejhad, P. Adelmann, T. Wolf, Z. V. Popovic, B. Moritz, T. P. Devereaux, and R. Hackl
arXiv 1709.08998, submitted for publication (2017).

38. **Characterizing spin transport: detection of spin accumulation via magnetic stray field**
Matthias Pernpeintner, Akashdeep Kamra, Sebastian T.B. Goennenwein, Hans Huebl
arXiv 1709.01820, submitted for publication (2017).

39. **Perpendicular magnetic anisotropy in insulating ferrimagnetic gadolinium iron garnet thin films**
H. Maier-Flaig, S. Geprägs, Z. Qiu, E. Saitoh, R. Gross, M. Weiler, H. Huebl, S. T. B. Goennenwein
arXiv:1706.08488, submitted for publication (2017).

40. **Analysis of broadband ferromagnetic resonance in the frequency domain** Hannes Maier-Flaig, Sebastian T. B. Goennenwein, Ryo Ohshima, Masashi Shiraishi, Rudolf Gross, Hans Huebl, Mathias Weiler
arXiv:1705.05694, submitted for publication (2017).

41. **Non-local magnon transport in the compensated ferrimagnet GdIG**
Kathrin Ganzhorn, Tobias Wimmer, Joseph Barker, Gerrit E. W. Bauer, Zhiyong Qiu, Eiji Saitoh, Nynke Vlietstra, Stephan Geprägs, Rudolf Gross, Hans Huebl, Sebastian T.B. Goennenwein
arXiv:1705.02871, submitted for publication (2017).

42. **Magnetic excitations and amplitude fluctuations in insulating cuprates**
N. Chelwani, A. Baum, T. Böhm, M. Opel, F. Venturini, A. Erb, H. Berger, L. Forró, and R. Hackl
arXiv 1705.01496, submitted for publication (2017).

43. **The case for spin-fluctuation induced superconductivity in $Ba_{1-x}K_xFe_2As_2$**
T. Böhm, F. Kretzschmar, A. Baum, M. Rehm, D. Jost, R. Hosseinian Ahangharnejhad, R. Thomale, C. Platt, T. A. Maier, W. Hanke, B. Moritz, T. P. Devereaux, D. J. Scalapino, S. Maiti, P. J. Hirschfeld, P. Adelmann, T. Wolf, Hai-Hu Wen, and R. Hackl
arXiv 1703.07749, submitted for publication (2017).

44. **Finite-time quantum correlations of propagating squeezed microwaves**
Kirill G. Fedorov, S. Pogorzalek, U. Las Heras, M. Sanz, P. Yard, P. Eder, M. Fischer, J. Goetz, E. Xie, K. Inomata, Y. Nakamura, R. Di Candia, E. Solano, A. Marx, F. Deppe, R. Gross
arXiv:1703.05138, submitted for publication (2017).

45. **Frequency control and coherent excitation transfer in a nanostring resonator network**
Matthias Pernpeintner, Philip Schmidt, Daniel Schwienbacher, Rudolf Gross, Hans Huebl
arXiv:1612.07511, submitted for publication (2016).

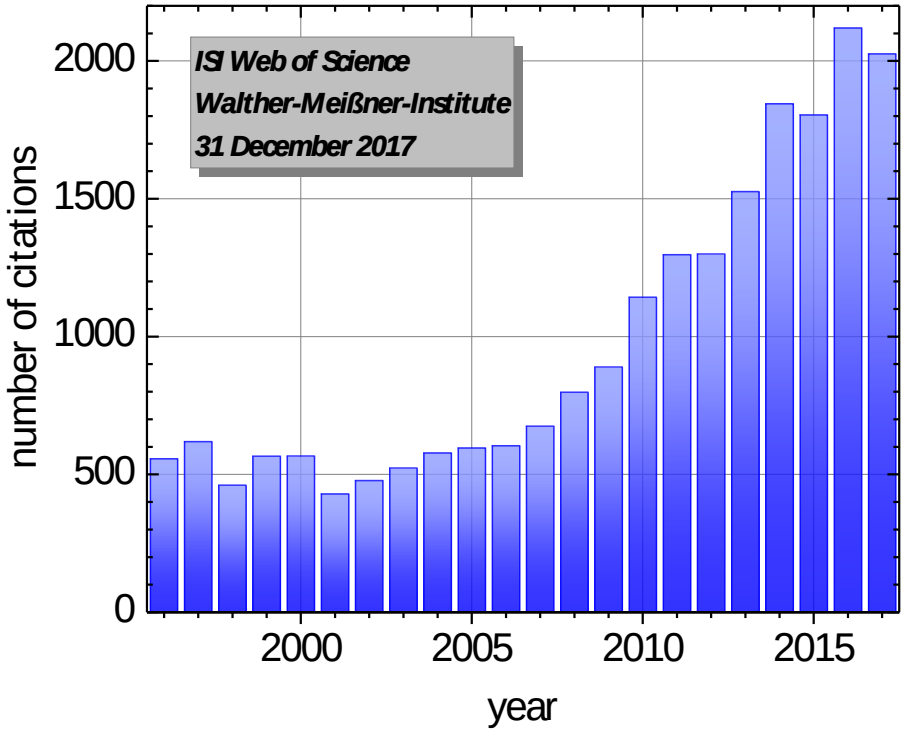

The total number of citations per year of papers published by members of WMI since 1996. This number is continuously increasing and has more than tripled within the last fifteen years. Presently it is exceeding 2 000.

Books

Festkörperphysik (3. überarbeitete und erweiterte Auflage)

The first and second edition of the solid state physics textbook ***Festkörperphysik*** by Rudolf Gross and Achim Marx appeared in 2012 and 2014. The textbook as well as the related book with exercises and solutions are well received by university teachers and highly esteemed by the students (see e.g. review by Prof. Daniel Hägele in Physik Journal **12** (2013) Nr. 10, p. 60). Since the second edition is going to be out of print, a third expanded edition has been prepared during 2017. The printing process of the third edition has been started in December 2017 and the new book will be available from De Gruyter Oldenbourg in January 2018 (ISBN 978-3-11-055822-7). It will be also available as an ebook (ISBN 978-3-11-055918-7).

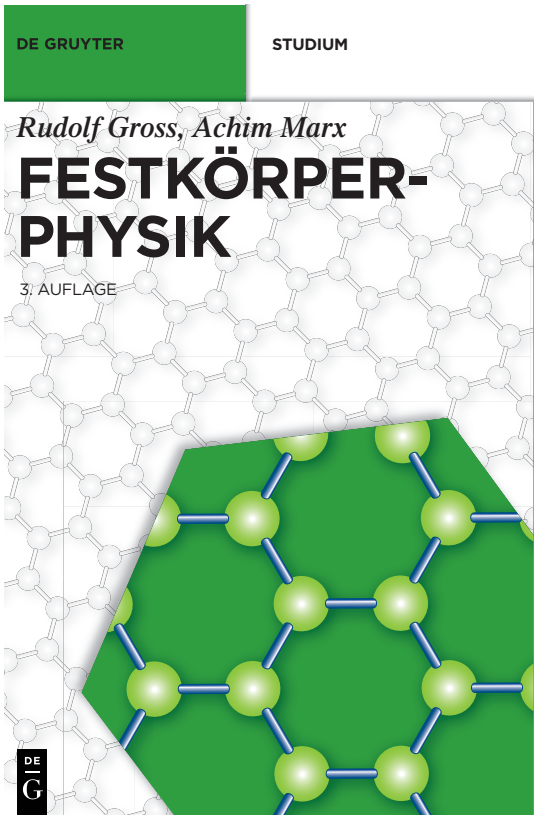

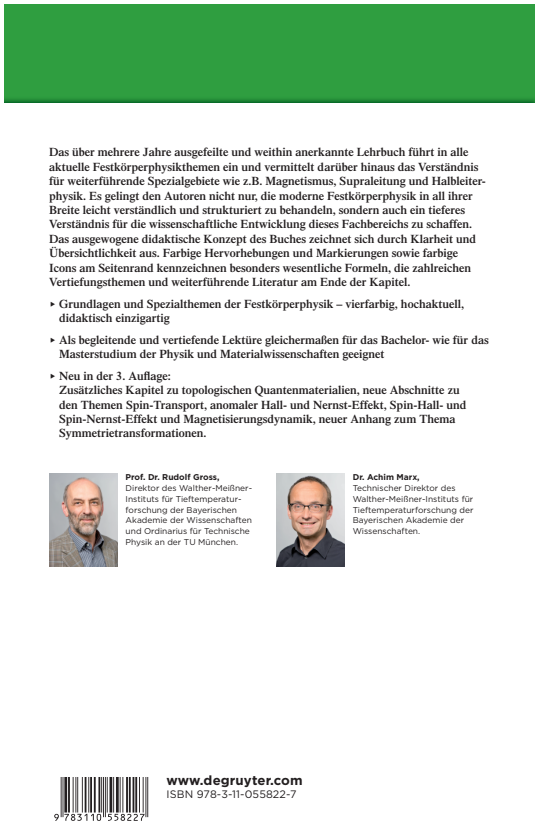

Since quantum matter and the concept of topology became important topics in solid state physics over the past years, the third edition of the textbook has been expanded by a new chapter on topological quantum matter. Furthermore, the chapter on transport phenomena has been revised and now includes the key aspects of the novel transport phenomena resulting from spin orbit coupling such as the Spin Hall effect, as well as a discussion of the anomalous transport effects (e.g. anomalous Hall and Nernst effect) in materials with finite magnetization. It also gives an introduction to the plethora of the novel spin-thermo-electric transport phenomena such as the spin Hall, spin Seebeck, spin Nernst and spin Ettingshausen effect. These effects naturally arise when one is expanding the well-known thermo-electric coupling by the spin degree of freedom to arrive at the spin-thermo-electric coupling. Since these transport phenomena have been studied intensively over the past years – e.g. within the DFG Priority Program 1538 on Spin Caloritronics – it was now time to provide an introductory overview to students. Very recently, one of the fundamental spin-thermo-electric transport effects – the spin Nernst effect – has been measured for the first time at WMI within the PhD

thesis of Sibylle Meyer (see *Observation of the spin Nernst effect*, Sibylle Meyer , *et al.*, Nature Materials **16**, 977–981 (2017)).

Festkörperphysik. Aufgaben und Lösungen (2. überarbeitete und erweiterte Auflage)

In December 2013, the supplementary book entitled ***"Festkörperphysik. Aufgaben und Lösungen"*** by Rudolf Gross, Achim Marx and Dietrich Einzel has been published by the Oldenbourg Wissenschaftsverlag München. The book contains model solutions to all exercises listed at the end of the chapters of the related solid state physics textbook ***Festköperphysik***. The exercises & solutions book is ideal for preparing for examinations and for learning on one's own. It is used and recommended by many colleagues teaching solid state physics.

Since also this book is going to be out of print, a second revised edition has been prepared recently by Rudolf Gross, Achim Marx, Dietrich Einzel and Stephan Geprägs with several new exercises and solutions. Unfortunately, the LaTex documents and figures could not be completed until Christmas and therefore the second edition of the exercises & solutions book could not be processed in parallel with the third edition of the solid state physics textbook. However, De Gruyter Oldenbourg will make it hopefully available in March 2018 (ISBN: 978-3-11-056613-0), just in time for the Spring Meeting of the German Physical Society.

Bachelor, Master, Doctoral, and Habilitation Theses

A. Completed and Ongoing Habilitation Theses

The promotion of highly qualified young scholars is a key concern of WMI. The fostering of young scholars goes hand in hand with equipping them to stand on their own in fields that are very competitive on both the national and international scales. At present, three postdoctoral researcher – Mathias Weiler, Matthias Althammer and Kirill Fedorov – are passing through the habilitation procedure of the Technical University of Munich. The habilitation serves as the formal assessment tool ascertaining whether or not a candidate is suitable, from an academic and a pedagogical point of view, to be a professor in a particular field at the university level. Frank Deppe already finished this assessment and received the teaching qualification in experimental physics.

1. Dr. Frank Deppe

In the past few years, Frank Deppe developed into an internationally renowned junior scientist in the field of quantum science and technology. He was project leader within the Cooperative Research Center 631 on "Solid State Quantum Information Processing". Presently, he is Associate Member within the Excellence Cluster "Nanosystems Initiative Munich" and Member of the "Munich Quantum Center". He also was principal investigator in several European Projects such as the EU Collaborative Project (call identifier FP7-ICT-2011-C) on *Quantum Propagating Microwaves in Strongly Coupled Environments – PROMISCE* and the Marie Curie Network for Initial Training (call identifier FP7-PEOPLE-2010-ITN) on *Circuit and Cavity Quantum Electrodynamics (CCQED)*.

Technische Universität München

HABILITATIONSURKUNDE

Die Technische Universität München

stellt für

Herrn Dr. rer. nat.

FRANK DEPPE

geboren am 16. Februar 1975 in Gräfelfing

die Lehrbefähigung für das Fachgebiet

„EXPERIMENTALPHYSIK"

fest, nachdem die Fakultät für Physik das ordnungsgemäße Verfahren nach der Habilitationsordnung durchgeführt hat. Die Habilitationsschrift trägt den Titel „Microwave quantum science with superconducting circuits".

München, 19. Oktober 2016

Prof. Dr. Dr. h.c. mult. Wolfgang A. Herrmann
Präsident

Prof. Dr. rer. nat. Johannes Barth
Dekan

Technische Universität München

URKUNDE

Die Technische Universität München erteilt

Herrn Dr. rer. nat.

Frank Deppe

die Lehrbefugnis für das Fachgebiet

Experimentalphysik

mit dem Recht zur Führung der Bezeichnung

Privatdozent.

München, 11. Mai 2017

Wolfgang A. Herrmann
Präsident

In 2010, Frank Deppe started the habilitation process at TU Munich under the scholarly guidance of a *Fachmentorat* committee consisting of Rudolf Gross (TU Munich, chairman), Jonathan Finley (TU Munich) and Enrique Solano (Universidad del País Vasco and Ikerbasque Foundation, Bilbao, Spain). His habilitation thesis was accepted by the Faculty of Physics of TU Munich and the habilitation process was finally completed in October 2016. In May 2017, Frank Deppe received the teaching qualification (Venia Legendi) in Experimental Physics from the Technical University of Munich. WMI congratulates Frank Deppe on the successful completion of the habilitation process and receiving the teaching licence which entitles him to bear the title "Privatdozent".

2. Dr. Mathias Weiler

Mathias Weiler started the habilitation process at TUM in June 2015. The research topic of his habilitation project is *Spin-Orbit Interactions in Magnetic Thin Film Systems*. On November 2, 2017 he successfully passed the intermediate evaluation of his habilitation process. He was presenting a talk entitled *"Spin-Orbit Dynamics"* within the Solid State Physics Colloquium of TUM, summarizing his recent scientific achievements. The *Fachmentorat* consisting of Rudolf Gross (TU Munich), Christian Pfleiderer (TU Munich) and Christian Back (University of Regensburg) was pleased to see that many of the goals fixed in 2015 were overfulfilled. Therefore, the *Fachmentorat* recommended to finish the habilitation process within the coming two years.

Mathias Weiler joined WMI in December 2014 after a two-year postdoctoral stay at the National Institute of Standards and Technology, Boulder, Colorado, USA, where he worked on spin current transport. His stay abroad was supported by a DAAD fellowship. Besides his successful research work, he took over the lectures on *Magnetism* (winter semester 2015/2016 and 2017/2018) and *Spin Electronics* (summer semester 2016), and contributed to several WMI seminars.

3. Dr. Matthias Althammer

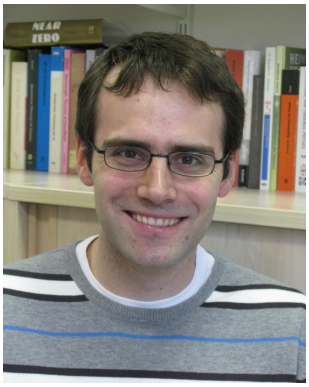

Matthias Althammer joined WMI in December 2013 after a postdoctoral stay (10/2012 – 11/2013) at the Center for Materials for Information Technology, University of Alabama, Tuscaloosa, USA, where he worked on oxide based spintronics. From 05/2014 to 02/2015 he was on leave from WMI to acquire experience in industry as an Engineering Consultant at Esprit Engineering GmbH, Munich.

Matthias Althammer was accepted as a *"Habilitand"* by the Faculty of Physics of TU Munich in January 2016. In his case, Rudolf Gross (TU Munich), Martin Brandt (TU Munich) and Arunava Gupta (MINT Center, University of Alabama) form the *Fachmentorat*. The research topic of his habilitation project is the *"Experimental Study of Spin-dependent Transport Phenomena"*.

4. Dr. Kirill Fedorov

Kirill Fedorov studied physics in Russia (Institute for Physics of Microstructures, Russian Academy of Sciences, Nizhny Novgorod) where he received his master degree in 2008. He then joined the group of Prof. Ustinov at the Karlsruhe Institute of Technology as a PhD student. He finished his PhD thesis entitled *Fluxon readout for superconducting flux qubits* in 2013 and then joined Walther-Meißner-Institut as a postdoctoral researcher in December 2013. His key research topic is the realization of seminal quantum experiments based on propagating quantum microwaves.

Kirill Fedorov was accepted as a *"Habilitand"* by the Faculty of Physics of TU Munich in September 2016. In his case, Rudolf Gross (TU Munich), Jonathan Finley (TU Munich/Walther Schottky Institute) and Enrique Solano (Universidad del País Vasco and Ikerbasque Foundation, Bilbao, Spain) form the *Fachmentorat*.

B. Completed and Ongoing Ph.D. Theses

Completed Ph.D. Theses:

1. **The case for spin-fluctuation induced pairing in $Ba_{1-x}K_xFe_2As_2$**
   Thomas Böhm, Technical University of Munich, April 2017.
2. **Spin Transfer Torque Mediated Magnetization Dynamics**
   Michael Sebastian Schreier, Technical University of Munich, Juni 2017.
3. **The Interplay of Superconducting Quantum Circuits and Propagating Microwave States**
   Jan Goetz, Technical University of Munich, Juni 2017.

Two of the Ph.D. students of the Walther-Meißner-Institute finishing their Ph.D. theses in 2017.

Ongoing Ph.D. Theses:

4. **Vibrational Investigations of Luminescence Molecules**
   Nitin Chelwani, Technical University of Munich, since September 2010.
5. **Untersuchung der verschiedenen Phasen eisenbasierter Supraleiter mittels Raman-Streuung**
   Andreas Baum, Technical University of Munich, since April 2012.
6. **Quantum Information Processing with Propagating Quantum Microwaves**
   Peter Eder, Technical University of Munich, since November 2012.
7. **Spin dynamics and spin transport in solid state systems**
   Hannes Maier-Flaig, Technical University of Munich, since November 2013.
8. **Circuit Quantum Electrodynamics with Three-dimensional Cavities**
   Edwar Xie, Technical University of Munich, since December 2013.

9. **Spin Currents in Ferrimagnetic Materials**
   Kathrin Ganzhorn, Technical University of Munich, since December 2014.
10. **Chains of Nonlinear and Tunable Superconducting Resonators**
    Michael Fischer, since Januar 2015.
11. **Magnetization Dynamics in Coupled Photon/Phonon-Magnon Systems**
    Stefan Klingler, Technical University of Munich, since February 2015.
12. **Nanomechanical Quantum Systems**
    Philip Schmidt, Technical University of Munich, since October 2015.
13. **Magnetic Resonance at Millikelvin Temperatures**
    Stefan Weichselbaumer, Technical University of Munich, since December 2015.
14. **Untersuchung des Wärmetransports in porösen Pulvermedien zur Entwicklung einer ökonomischen Hochtemperatur-Vakuumsuperisolation auf Perlitbasis für Anwendungen in Wärmespeichern bis zu 700°C**
    Matthias Johannes Demharter, Technical University of Munich, since February 2016.
15. **Quantum gates with continuous variable microwaves**
    Stefan Pogorzalek, Technical University of Munich, since März 2016.
16. **Momentum and Spatially Resolved Raman Experiments in Correlated Systems**
    Daniel Jost, Technical University of Munich, since October 2016.
17. **Spin Currents in Magnetic Heterostructures**
    Tobias Wimmer, Technical University of Munich, since Januar 2017.
18. **ReBCO-Schichten auf ISD biaxial texturierten Substraten für supraleitende Bandleiterder 2. Generation**
    Oleksiy Troshyn, Technical University of Munich, since August 2016.
19. **Direct and inverse spin-orbit torques**
    Lukas Liensberger, Technical University of Munich, since January 2018.

C. Completed and Ongoing Bachelor and Master Theses

Completed Master Theses:

1. **Shubnikov-de Haas-Effekt und magnetischer Durchbruch im geschichteten organischen Supraleiter κ-(BEDT-TTF)$_2$Cu(NCS)$_2$/Shubnikov-de Haas Effect and Magnetic Breakdown in the Layered Organic Superconductor κ-(BEDT-TTF)$_2$Cu(NCS)$_2$**
   Sergej Fust, Masterarbeit, Technical University of Munich, November 2016.
2. **Spin Transport in Magnetic Nanostructures**
   Tobias Wimmer, Masterarbeit, Technical University of Munich, November 2016.
3. **Frequency- and Time-Domain Characterization of a Transmon Qubit in a Transmission Line**
   Tuan Le anh, Masterarbeit, Technical University of Munich, Februar 2017.
4. **Process and Design of ISFET-based Electrochemical Sensors**
   Sebastian Meier, Masterarbeit, Technical University of Munich, April 2017.
5. **Magnetismus und Supraleitung in Eisenchalkogeniden**
   Merlin Mitschek, Masterarbeit, Technical University of Munich, April 2017.
6. **Spin-Hall-Magnetwiderstand in antiferromagnetischem NiO und α-Fe$_2$O$_3$ / Spin Hall magnetoresistance in antiferromagnetic NiO and α-Fe$_2$O$_3$**
   Johanna Fischer, Masterarbeit, Technical University of Munich, September 2017.
7. **Investigation of Magnetoresistance Tuned by Interface States of YIG/Pt Heterostructures**
   Saki Matsuura, Masterarbeit, Technical University of Munich, September 2017.
8. **Spin-Hall-Magnetwiderstand in oxidischen Heterostrukturen**
   Sarah Gelder, Masterarbeit, Technical University of Munich, Oktober 2017.
9. **Spin-Orbit Torques and Magnetization Dynamics in Non-collinear Magnets**
   Lukas Liensberger, Masterarbeit, Technical University of Munich, Oktober 2017.
10. **Effective Cyclotron Mass and Electronic Properties of κ-Phase Organic Superconductors in the Vicinity of the Mott-Insulator Transition**
    Sebastian Oberbauer, Masterarbeit, Technical University of Munich, Oktober 2017.
11. **Tunneling Spectroscopy in Conductive Ferromagnets**
    Michaela Schleuder, Masterarbeit, Technical University of Munich, November 2017.
12. **Microwave Frequency Magnetoacoustic Interactions in Ferromagnetic Thin Films**
    Clemens Mühlenhoff, Masterarbeit, Technical University of Munich, November 2017.
13. **Quantum Simulations of Many-Body Systems with Superconducting Devices**
    Christian Alexander Besson, Masterarbeit, Technical University of Munich, November 2017.
14. **Raman Scattering Study of the Superconducting Pairing in CaKFe$_4$As$_4$**
    Jan-Robin Scholz, Masterarbeit, Technical University of Munich, November 2017.
15. **Superconducting Microwave Resonator Designs for Electron Spin Resonance Applications**
    Petio Natzkin, Masterarbeit, Technical University of Munich, Dezember 2017.

Completed Bachelor Theses:

16. **Numerical Simulation of a Driven-dissipative Bose-Hubbard Dimer**
    Stefan Binder, Bachelorarbeit, Technical University of Munich (2017)
17. **Finite Size Effects of the Anisotropic Magnetoresistance**

Manuel Müller, Bachelorarbeit, Technical University of Munich (2017)

18. **Untersuchung von Magnetismus und Supraleitung in unterdotiertem $YBa_2Cu_6O_{6+x}$**
Mirko Riedel, Bachelorarbeit, Technical University of Munich (2017)
19. **Tip-Enhanced Raman Spectroscopy (TERS)**
Pablo Cova Fariña, Bachelorarbeit, Technical University of Munich (2017)
20. **Sensitive Breitbandmagnetresonanzspektroskopie**
Jonathan Zerhoch, Bachelorarbeit, Technical University of Munich (2017)
21. **Quantum correlations beyond entanglement**
Stephan Trattnig, Bachelorarbeit, Technical University of Munich (2017)
22. **Shubnikov-de Haas Oscillations and Effective Cyclotron Mass in the Organic Superconductors κ-$(ET)_2Cu[N(CN)_2]Cl$ and κ-$(ET)_2Cu(NCS)_2$ near the Mott-Insulator Transition**
Paul Weinbrenner, Bachelorarbeit, Technical University of Munich (2017)
23. **Umbau eines Freistrahlinterferometers zur Charakterisierung nanomechanischer Saiten**
Andreas Faltermeier, Bachelorarbeit, Technical University of Munich (2017)
24. **Topological Hall effect in $SrRuO_3$-$SrIrO_3$ heterostructures**
Moritz Feil, Bachelorarbeit, Technical University of Munich (2017)
25. **Spin-Hall-Magnetwiderstand und Spin-Seebeck-Effekt in $Gd_3Fe_5O_{12}$ | Pt-Heterostrukturen**
Maxim Dietlein, Bachelorarbeit, Technical University of Munich (2017)

Ongoing Master Theses:

26. **Aufbau eines Systems für Raman-Experimente unter UHV-Bedingungen / Construction of a system for Raman-experiments under UHV conditions**
Florian Löffler, Masterarbeit, Technical University of Munich, since January 2017.
27. **Untersuchung der magnetoelastischen Eigenschaften von magnetoresistiven Sensorstrukturen / Investigation of magnetoelastic properties of magnetoresistive sensor structures**
Moritz Keller, Masterarbeit, Technical University of Munich, since February 2017.
28. **Remote state preparation with quantum microwaves**
Seyedbehdad Ghaffari, Masterarbeit, Technical University of Munich, since March 2017.
29. **Vorhersage einer zeitlichen Leistungsverfügbarkeit eines Fahrzeugspeichers in der Elektromobilität**
Markus Full, Masterarbeit, Technical University of Munich, since April 2017.
30. **Magnetische und elektronische Anregungen in unterdotiertem YBCO / Magnetic and electronic excitations in underdoped YBCO**
Ulricke Zweck, Masterarbeit, Technical University of Munich, since April 2017.
31. **Elektromechanische Quantenschaltkreise / Circuit Quantum Electromechanics**
Christoph Utschick, Masterarbeit, Technical University of Munich, since May 2017.
32. **Engineering Interfacial Spin-Orbit Torques**
Luis Flacke, Masterarbeit, Technical University of Munich, since June 2017.
33. **Nanomechanik gekoppelt an supraleitende Quantenschaltkreise / Nanomechanics coupled to superconducting quantum circuits**
Lisa Rosenzweig, Masterarbeit, Technical University of Munich, since June 2017.
34. **Laserablationsladen und kohärente Kontrolle von Strontiumionen in einer linearen**

Paul Falle / Ablation Loading and Coherent Control of Strontium Ions in a Linear Paul Trap
Andreas Pöschl, Masterarbeit, Technical University of Munich, since June 2017.

35. **Verifizierung der Normalkraftmessung sowie Bestimmung der Streubreiten an elektrischen Kontakten zur Ermittlung der Kraftgrenzen für den Einsatz in der Sereinfertigung**
Stefanie Blob, Masterarbeit, Technical University of Munich, since July 2017.
36. **Ein optisches Transportsystem für ultrakalte Strontiumatome / An optical transport system for ultracold strontium atoms**
Fabian Finger, Masterarbeit, Technical University of Munich, since October 2017.
37. **Growth and optimization of ferromagnetic thin films for spintronics**
Birte Cöster, Masterarbeit, Technical University of Munich, since August 2017.
38. **Quantenprozess-Tomographie für einen Quanten-Speicher / Quantum Process Tomography of a Quantum Memory**
Michael Uwe Renger, Masterarbeit, Technical University of Munich, since October 2017.
39. **Quantenteleportation im Mikrowellenbereich / Quantum Microwave Teleportation**
Minxing Xu, Masterarbeit, Technical University of Munich, since November 2017.
40. **Magnon-Phonon-Kopplung in Nanostrukturen / Magnon-Phonon Coupling in Nanostructures**
Thomas Luschmann, Masterarbeit, Technical University of Munich, since November 2017.
41. **Fabrication and Measurement of an enhanced Josephson Parametric Amplifier**
Daniel Arweiler, Masterarbeit, Technical University of Munich, since December 2017.

Research Projects

A large number of our research projects are benefiting from the collaboration with external groups in coordinated research projects, as well as from individual collaborations, exchange programs and visitors. Most collaborations are based on joint projects, which are funded by different research organizations (see list below). A considerable number of collaborations also exists with universities, other research institutions and industry without direct financial support.

A. German Research Foundation: Excellence Initiative

Cluster of Excellence "Nanosystems Initiative Munich"

1. Research Area I: *Quantum Nanophysics*
   F. Deppe, R. Gross, H. Huebl, A. Marx
2. Research Area II: *Hybrid Nanosystems*
   R. Gross, H. Huebl

B. German Research Foundation: Collaborative Research Centers

Transregional Collaborative Research Center TRR 80: "From Electronic Correlations to Functionality"

1. Project A2: *Spatially and Momentum Resolved Raman Studies of Correlated Systems*
   R. Hackl

C. German Research Foundation: Priority Programs

1. Pulsed Electron Paramagnetic Resonance at Millikelvin Temperatures
   within the DFG Priority Program 1601 *New frontiers in sensitivity for EPR spectroscopy: from biological cells to nano materials*
   H. Huebl (Az. HU 1896/2-1)
2. Spin-dependent thermo-galvanic effects: experiment
   within the DFG Priority Program 1538 *Spin-Caloric Transport – SpinCAT*
   R. Gross (Az. GR 1132/18-2)
3. Spin-dependent thermo-galvanic effects: experiment
   within the DFG Priority Program 1538 *Spin-Caloric Transport – SpinCAT*
   S.T.B. Gönnenwein, R. Gross (Az. GO 944/4-1, GO 944/4-2)
4. Project: *Raman study of electron dynamics and phase transitions in iron-pnictide compounds*
   within the DFG Priority Program 1458 *"High-Temperature Superconductivity in Iron-Pnictides"*
   R. Hackl, R. Gross, B. Büchner, D. Johrendt, C. Honerkamp (Az. HA 2071/7-1, HA 2071/7-2)

D. German Research Foundation: Research Projects

1. Project: *Direct and Inverse Spin-Orbit Torques*
   M. Weiler (Az. WE 5386/14-1)
2. Project: *Correlated Quantum Microwaves: Continuous-Variables for Remote State Preparation and Quantum Illumination*
   K.G. Fedorov (Az. FE 1564/1-1)

3. Project: *Interaction Between Spin, Lattice, and Charge in Correlated Metals without Inversion Center*
   R. Hackl, R. Gross (Az. HA 2071/8-1)

E. European Union

1. EU Collaborative Project (call identifier H2020-FETOPEN-1-2016-2017), project title *Magnetomechanical Platforms for Quantum Experiments and Quantum Enabled Sensing Technologies – MaQSens*
   H. Huebl, R. Gross, Grant Agreement No. 736943
   partners: several European Universities and research facilities.
2. EU Collaborative Project (call identifier FP7-ICT-2011-C), project title *Quantum Propagating Microwaves in Strongly Coupled Environments – PROMISCE*
   F. Deppe, A. Marx, R. Gross, Grant Agreement no. 284566
   partners: several European Universities and research institutions.

F. Free State of Bavaria

1. International PhD Programme of Excellence *Exploring Quantum Matter (ExQM)* within the Elite Network of Bavaria, Project No. K-NW-2013-231
   R. Gross, A. Marx, F. Deppe, K. Fedorov
   Partners: jointly with 12 quantum physics research groups at the TU Munich, the LMU Munich, and the Max Planck Institute of Quantum Optics.

G. Max Planck Society

1. International Max Plank Research School for *Quantum Science and Technology (IMPRS-QST)*, Spokesperson: Prof. Dr. J. Ignacio Cirac
   R. Gross, A. Marx, F. Deppe, K. Fedorov
   with several partners from the Max Planck Institute of Quantum Optics, the Ludwig-Maximilians-Universität Munich and the Technical University of Munich.

H. Bavaria California Technology Center (BaCaTeC)

1. Project: *Nematic Order and New Phases in Quantum Materials*
   R. Hackl,
   partners: Profs. Thomas Devereaux, Steve Kivelson, and Sri Raghu (Stanford University)

I. German Academic Exchange Service

1. Project-based Personnel Exchange Programme (PPP) with Serbia (project 57335339: Spin and Charge Instabilities in Sulfur-substituted FeSe), collaboration with the Institute of Physics, University of Belgrade (Dr. Z.V. Popovic).
   R. Hackl
2. Project-based Personnel Exchange Programme (PPP) with India (project 57085749: Spin Current Generation and Detection Using FMI/NM Hybrids), collaboration with the IIT Madras, Chennai (Prof. Dr. M. S. Ramachandra Rao).
   R. Gross

J. Scientific Instrumentation

1. UHV Sputtering System for Superconducting and Magnetic Materials
   R. Gross, DFG-GZ: INST 95-1333-1 FUGG
2. Critical Point Dryer Leica EM CPD 300
   BMBF project Q.com, FKZ: 16KIS0110 4515.1545.4556
3. Maskless lithography UV Direct Laser Writer, SPS PicoMaster 200 UV
   BMBF project Q.com, FKZ: 16KIS0110 4515.1545.4556
4. UHV Sputtering System for Superconducting Materials
   BMBF project Q.com, FKZ: 16KIS0110 4515.1545.4556

Conferences, Workshops, Public Outreach

The Walther-Meißner-Institute has organized/co-organized several conferences, workshops and symposia in 2017. It also was participating in several public outreach events aiming at making science accessible to the public.

A. 633. WE-Heraeus-Seminar: «Spin Orbit Dynamics – Connecting Timescales from Nano- to Femtoseconds» (04 – 06 January 2017, Physikzentrum Bad Honnef, Germany)

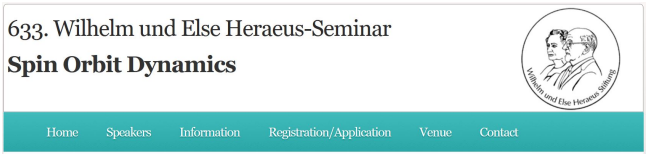

The *633. WE-Heraeus-Seminar* was organized by Mathias Weiler (WMI) together with Tobias Kampfrath (Fritz-Haber Institut, Berlin) and Stefan Mathias (I. Physics Institute, University of Göttingen). It was addressing spin-orbit coupling which plays a central role in spin dynamics and acts as a link connecting the nano- and femtosecond time scales. For instance, in conducting multilayers of paramagnetic and magnetically ordered thin films, spin-orbit coupling enables control of the magnetization through electrical currents. These so-called spin-orbit torques are fundamentally interesting and exhibit substantial potential for future applications.

Unfortunately, the investigation of spin-orbit torques has so far concentrated on time scales much slower than the intrinsic time scale of spin-orbit coupling. In complementary studies, the femtosecond laser community investigates magnetization dynamics on the time scales of spin-orbit coupling. Central research topics in this field are, for instance, spin-polarized ultrafast superdiffusive currents and spin-flip processes via Elliot-Yafet scattering. Although the fields of spin-orbit torques and femtosecond magnetization dynamics are so far quite disconnected, they both deal with the coupling of spins to light, electron currents and lattice vibrations that altogether determine the dynamical response of the magnetic material.

The goal of the 633. WE-Heraeus-Seminar was to bridge the time-scale gap between the two worlds of nanosecond magneto-electronics and femtosecond magnetization dynamics by bringing together researchers from the fields of spin-orbit torques and femtosecond magnetization dynamics. The seminar aimed at encouraging research that enables an understanding of the interaction of magnetic moments with electrical currents on the time scale of spin-orbit coupling.

B. 28. Edgar Lüscher-Seminar 2017 (04 – 10 February 2017, Klosters, Switzerland)

Rudolf Gross (WMI) organized a symposium on *Superconducting Quantum Electronics* at the 28. Edgar Lüscher-Seminar together with Christian Enss (University of Heidelberg). The symposium was addressing modern aspects of superconducting quantum electronics with particular focus on applications of superconducting devices and circuits in quantum information science and ultra-sensitive low temperature detectors. The list of speakers included Alexey Ustinov (Karlsruhe Institute of Technology, Superconducting Quantum Circuits), Frank Deppe (WMI, Engineering Selection Rules in Superconducting Flux Qubits), Sebastian Kempf (University of Heidelberg, Readout and Applications of Metallic Magnetic Microcalorimeters), and Lisa Gamer (University of Heidelberg, MOCCA – A 4k-Pixel Molecule Camera for Detection of Neutral Molecular Fragments).

C. 3. Int. Conference on Resonator Quantum Electrodynamics (R-QED 2017) (29 August – 01 September 2017, Kardinal-Wendel-Haus Munich, Germany)

The *R-QED 2017 Conference* was organized by Rudolf Gross (WMI) together with Gerhard Rempe (Max Planck Institute of Quantum Optics) and Jonathan Finley (Walter Schottky Institute) at the beautiful Kardinal-Wendel-Haus in the heart of Schwabing. It was a continuation of the highly successful EU-supported R-QED 2013 and the NIM supported R-QED 2015 conferences, all taking place at Munich. The R-QED 2017 conference consisted of tutorials and invited talks, as well as a small number of contributed talks and poster presentations. The Joint Quantum Institute (JQI) of the University of Maryland provided substantial financial support to R-QED 2017.

Like in the previous meetings, for the 2017 conference researchers from several areas of quantum physics were invited. Unifying theme was the study of individual and artificial atoms coupled to optical or microwave resonators. Pioneers of the fields gave introductory tutorial lectures, followed by state-of-the-art research talks. This blend was ideal in sharing the rapidly growing knowledge and establishing connections between solid-state and atomic physics. The conference was a great success and another stepping stone for the promotion of Munich quantum physics.

D. MagQSens Workshop: «Science Meets Industry: Ultra-Low Vibration Cryogenic Platforms» (10 – 11 July 2017, Munich Residence, Germany)

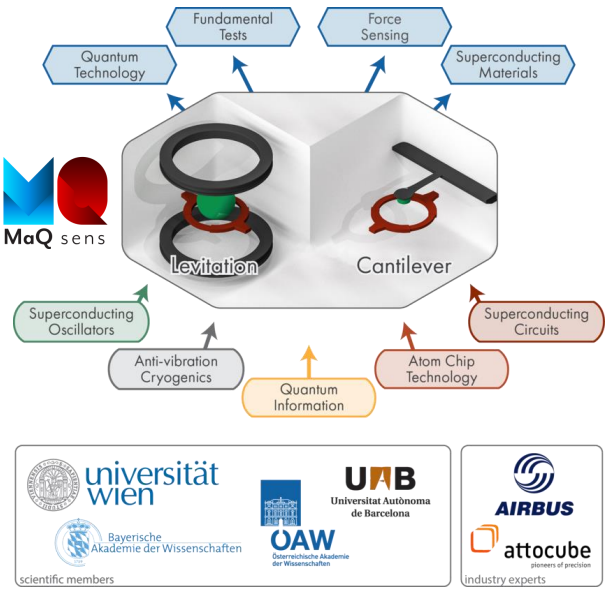

The workshop was organized by Hans Hübl and Rudolf Gross (WMI) together with Khaled Karrai (attocube systems) within the European project *Magnetomechanical Platforms for Quantum Experiments and Quantum Enabled Sensing Technologies – MaQSens*. The workshop was bringing together theorists, experimentalists and industry actors to work out the requirements for future ultra-low vibration cryogenic platforms that can be used in experiments on macroscopic quantum phenomena and on quantum enabled sensing. The fundamental motivation to develop designs and technical solutions for such platforms originates from the plan to perform experiments exploiting magnetic

coupling between superconducting quantum circuits and superconducting mechanical resonators – both levitated and suspended – to enter a hitherto inaccessible parameter regime of both unprecedented force sensitivity and full quantum control of massive, macroscopic objects. To this end, the ultimate goal is to enable quantum experiments of otherwise unachievable coherence times and masses, which has immediate implications for testing fundamental physical questions, for performing hybrid quantum information processing and, on the applied side, for ultra-sensitive force detectors. During the workshop the key requirements for low-vibration cryogenics have been mapped out.

E. Course 3 of the Ferienakademie: «Physics and Electronics in Everyday Life» (17 – 29 September 2017, Sarntal, Italy)

As in the previous years, WMI co-organized the course on «Physics and Electronics in Everyday Life»of the *Ferienakademie*. The Ferienakademie is jointly organized by the Technical University of Munich, the University of Erlangen/Nuremberg, and the University of Stuttgart to motivate and foster highly talented students. It takes place annually at Sarntal in the Italian Alps. The course was hold by Rudolf Gross (WMI) together with Prof. Dr. Gert Denninger (University of Stuttgart), and Prof. Dr. Vojislav Krstic (University of Erlangen-Nuremberg) as visiting lecturer.

Within the course 3 on «Physics and Electronics in Everyday Life»of the Ferienakademie the students prepare presentations on physical phenomena and problems which play an important role in our everyday-life, but usually are poorly understood. Besides the seminar talks there are intensive discussions with the professors and members of other courses. A particular emphasis of course 3 of Ferienakademie is put on hands-on experiments. They aim at providing students an in-depth insight into physical phenomena by performing experiments by themselves. WMI contributes with a variety of experiments on superconductivity, magnetism and low temperature properties of solids. A relaxing and inspiring atmosphere is provided by a varied supporting program (mountain hiking, excursions to Bozen, table tennis and chess tournament, Törgelen, etc.). Moreover, within the Ferienakademie the students have the opportunity to meet leaders from industry, politics and science.

F. Conference: «Kryoelektronische Bauelemente 2017» (08 – 10 October 2018, Bad Aibling, Germany)

The Walther-Meißner-Institute (Rudolf Gross, Achim Marx) organized the conference ***«Kryoelektronische Bauelemente 2017»***. Since more than 30 years, this conference series provides an important forum for physicists and electrical engineers from universities, national research institutes and industry to discuss future developments in the field of superconducting electronics and low temperature technology as well as to present their latest results.

The key topics of «Kryoelektronische Bauelemente 2017»have been

- superconducting quantum bits and circuits,
- superconducting devices and precision measurement systems,
- novel Josephson junctions and hybrid structures,
- SQUIDs, SQIFs, and Josephson arrays,
- Josephson voltage standard, superconducting SETs, and RSFQ,
- superconducting microwave devices,
- integrated superconducting circuits,
- ultrasensitive low temperature detectors,
- cooling techniques and cryoengineering.

To increase the attractiveness of the conference for students and young scientists, the opening day of the conference was reserved for three tutorials on the following topics:

- Superconducting quantum technology (Martin Weides, KIT)
- Continuous-variable propagating quantum microwaves (Frank Deppe, WMI)
- Atomic tunneling systems – two-level fluctuators (Christian Enss, University of Heidelberg)

The organization of conferences, workshops and public outreach events not only requires the preparation of an interesting and well-balanced scientific program, but also a perfect organization and taking care of a large number of international guests. The Executive Committee of WMI would like to particularly thank the administrative and technical staff of WMI for their professional support and considerable extra hours of work. It significantly contributes to the outside visibility of WMI.

Cooperations

Other collaborations without direct project funding involve:

- Stanford University, Stanford, USA (T.P. Devereaux, M. Greven, Z.-X. Shen, I. Fisher, B. Moritz, H.N. Ruiz, C. Platt)
- Universidad del País Vasco and Ikerbasque Foundation, Bilbao, Spain (E. Solano, M. Sanz, L. Lamata)
- Instituto de Física Fundamental, CSIC, Madrid, Spain (J.J. Garcia-Ripoll)
- Instituto de Ciencia de Materials de Barcelona, CSIC, Spain (E. Canadell, J. Fontcuberta)
- Osaka Prefecture University, Osaka, Japan (H. Fujiwara)
- Green Innovation Research Laboratories, NEC Corporation, Japan (J.S. Tsai, K. Inomata, T. Yamamoto)
- University of Tohoku, Sendai, Japan (G.E.W. Bauer, E. Saitoh, J. Barker, H. Naganuma)
- Japan Science and Technology Agency, Sendai, Japan (H. Adachi, S. Maekawa)
- University of Tokyo, Tokyo, Japan (Y. Nakamura)
- University of Vienna, Austria (M. Aspelmeyer)
- Heriot Watt University, Edinburgh, Scotland (M. Hartmann)
- Technische Universität Dresden, Germany (S.T.B. Gönnenwein)
- Fritz Haber Institut Berlin, Germany (T. Seifert, T. Kampfrath)
- Technische Universität Dortmund, Germany (M. Müller)
- Johannes-Gutenberg- Universität Mainz, Germany (O. Gomomay)
- Universität des Saarlandes, Saarbrücken (F.K. Wilhelm-Mauch)
- University of Groningen, The Netherlands (T. Palstra, M. Mostovoy)
- European Synchrotron Radiation Facility (ESRF), Grenoble (H. Müller, F. Wilhelm, K. Ollefs, A. Rogalev)
- Lund University, Lund, Sweden (D. Mannix)
- Materials Science Research Centre, IIT Madras, India (M.S. Ramachandra Rao, J. Mukherjee)
- ETH-Zurich, Switzerland (A. Wallraff, L. Degiorgi, R. Monnier, M. Lavagnini)
- University of Geneva, Geneva, Switzerland (I. Maggio-Aprile)
- Chalmers University of Technology Gothenburg, Sweden (P. Delsing, G. Wendin)
- University of Alabama, MINT Center, Tuscaloosa, USA (A. Gupta)
- Helsinki University of Technology, Materials Physics Laboratory, Finland (T. Heikkilä)
- Delft University of Technology, Kavli Institute of NanoScience, Delft, The Netherlands (T.M. Klapwijk, G.E.W. Bauer)
- B. Verkin Institute for Low Temperature Research and Engineering, Kharkov, Ukraine (V.G. Peschansky)
- Landau Institute for Theoretical Physics, Chernogolovka, Russia (P. Grigoriev)
- University of Oxford, Clarendon Laboratory, England (A. Karenowska)
- Russian Academy of Sciences, Chernogolovka, Russia (N. Kushch, A. Palnichenko)
- High Magnetic Field Laboratory, Dresden (E. Kampert, J. Wosnitza)
- High-Magnetic-Field Laboratory, Grenoble, France (I. Sheikin)
- High Magnetic Field Laboratory, Toulouse (C. Proust, D. Vignolles)
- National High Magnetic Field Laboratory, Tallahassee, USA (J. Brooks)

- IFW Dresden, Germany (B. Büchner, J. Fink, S.V. Borisenko, M. Knupfer, A. Thomas)
- Max-Planck-Institut für Festkörperforschung, Stuttgart (B. Keimer, L. Boeri)
- University of Tübingen, Germany (R. Kleiner, D. Kölle)
- University of Würzburg, Germany (W. Hanke, F. Assaad, C. Honerkamp, M. Potthoff)
- University of Augsburg, Germany (P. Hänggi, A. Wixforth, A. Kampf, A. Loidl, J. Deisenhofer, V. Tsurkan)
- University of Hamburg, Germany (G. Meier, W. Wurth)
- University of Leipzig, Germany (J. Haase)
- University of Ulm, Abt. Halbleiterphysik, Germany (W. Limmer, M. Abdi)
- Ernst-Moritz-Arndt Universität Greifswald, Germany (M. Münzenberg)
- Martin-Luther-Universität Halle, Germany (G. Woltersdorf)
- Universität Regensburg, Institut für Experimentelle und Angewandte Physik, Germany (Ch. Back, A. Aqeel)
- Universität Bielefeld, Germany (G. Reiss, T. Kuschel M. Meinert)
- Freie Universität Berlin, Berlin, Germany (R. Di Candia)
- University of British Columbia, Vancouver, Canada (D. Bonn, A. Damascelli)
- TU München, Physics Department, Germany (P. Böni, Ch. Pfleiderer, F.C. Simmel, P. Müller-Buschbaum, W. Zwerger)
- TU München, Walter Schottky Institut, Germany (M. Stutzmann, J. Finley, M. Brandt, A. Holleitner, U. Wurstbauer)
- TU München, Lehrstuhl für Technische Elektronik (M. Becherer)
- LMU München, Physics Department, Germany (J. von Delft)
- LMU München, Chemistry Department, Germany (H. Ebert, D. Ködderitzsch)
- Universidad de Zaragoza, Departamento de Fisica de la Materia Condensada, Spain (L. Morellon, J.M. de Teresa, D. Zueco)
- EPFL Lausanne, Switzerland (T. Kippenberg, H. Ronnov)
- University of New South Wales, Sydney, Australia (M. Simmons, A. Morello)
- McMaster University, Hamilton, Canada (J.P. Carbotte)
- Technische Universität Graz, Austria (E. Schachinger)
- Universität Konstanz (A. Leitenstorfer, E. Weig, J. Demsar, A. Pashkin)
- BMW Group, Munich, Germany (J. Schnagl, W. Stadlbauer, G. Steinhoff)
- Attocube Systems, Munich, Germany (K. Karrai, D. Andres, E. Hoffmann)
- THEVA Dünnschichttechnik, Ismaning, Germany (W. Prusseit)
- Johannes-Kepler-Universität Linz, Institut für Halbleiter- und Festkörperphysik, Austria (A. Ney)
- Jülich Centre for Neutron Science JCNS, Garching, Germany (S. Pütter)
- Université de Toulouse, Laboratoire de Physique Théorique, Toulouse, France (R. Ramazashvili)
- Lawrence Berkeley National Laboratory, Berkeley, USA (A. F. Kemper)
- University of Belgrade, Belgrade, Serbia (Z. Popovic, N. Lazarevic, D. U. Ralevic, R. Gajic)
- University of Aveiro, Portugal (N. A. Sobolev)
- Macquarie University, MQ Research Centre for Quantum Science and Technology, Australia (J. Twamley)

- Hungarian Academy of Sciences, Research Institute for Solid State Physics and Optics, Budapest, Hungary (K. Kamaras, I. Tüttö, J. Balogh)
- University of Rome "La Sapienza", Rome, Italy (S. Caprara, C. Di Castro, M. Grilli)
- Hungarian Academy of Sciences, Budapest University of Technology and Economics, Budapest, Hungary (A. Virosztek, G. Mihály)
- Goethe University, Frankfurt, Germany (S. Winter)
- National Institute of Standards and Technology, Boulder, USA (H. Nembach, J. Shaw, T.J. Silva)
- University of Manitoba, Winnipeg, Canada (C.-M. Hu)
- Kyoto University, Japan (M. Shiraishi)
- Technische Universität Braunschweig, Germany (D. Menzel, S. Süllow)
- Universidad Nacional de Colombia, Colombia (O. Moran)
- University of Birmingham, UK (E.M. Forgan)
- Innovent Technologieentwicklung Jena, Germany (C. Dubs, O. Surzhenko)

Stays abroad

Extended visits of members of the Walther-Meißner-Institute at foreign research laboratories:

1. **Matthias Althammer**
   Center for Materials for Information Technology, University of Alabama, USA
   08. 03. - 13. 03. 2017
2. **Stephan Geprägs**
   European Synchrotron Radiation Facility (ESRF), Grenoble, France
   31. 10. - 05. 11. 2017
3. **Rudolf Gross**
   Indian Institute of Technology, Chennai, India
   19. 11. - 24. 11. 2017
4. **Rudolf Hackl**
   Institute of Physics, University of Belgrade, Serbia
   24. 11. - 29. 11. 2017
5. **Rudolf Hackl**
   Stanford Institute of Materials and Energy Sciences (SIMES), Stanford Linear Accelerator Center (SLAC), Stanford, USA
   08. 03. - 01. 04. 2017
6. **Hans Hübl, Stefan Weichselbaumer**
   Centre for Quantum Computing and Communication Technology, Sydney, Australia
   31. 03. - 21. 04. 2017
7. **Mark Kartsovnik**
   Institute of Solid State Physics, Russian Academy of Sciences, Chernogolovka, Russia
   16. 08. - 26. 08. 2017
8. **Mark Kartsovnik, Sebastian Oberbauer**
   High Magnetic Field Laboratory, Grenoble, France
   21. 05. - 29. 05. 2017
9. **Matthias Opel**
   Unité Mixte de Physique, CNRS, Université Paris-Sud, Université Paris-Saclay, Palaiseau, France
   01. 03. - 06. 03. 2017
10. **Matthias Opel**
    Stanford Institute of Materials and Energy Sciences (SIMES), Stanford Linear Accelerator Center (SLAC), Stanford, USA
    26. 06. - 30. 06. 2017
11. **Matthias Opel**
    European Synchrotron Radiation Facility (ESRF), Grenoble, France
    31. 10. - 08. 11. 2017
12. **Nynke Vlietstra**
    European Synchrotron Radiation Facility (ESRF), Grenoble, France
    03. 12. - 07. 12. 2017
13. **Nynke Vlietstra**
    ALBA Synchrotron, Barcelona, Spain
    30. 11. - 03. 12. 2017

Conference Talks and Seminar Lectures

Matthias Althammer

1. **Spin Hall Magnetoresistance**
   Invited Talk, Center for Materials for Information Technology, University of Alabama, USA
   10. 03. 2017
2. **Investigation of the Tunnel Magnetoresistance in Junctions with a Strontium Stannate Barrier**
   APS March Meeting 2017, New Orleans, USA
   16. 03. 2017
3. **Anomalous Hall Effect, Spin Hall Effect and Magnetoresistance**
   Invited lecture, 48^{th} IFF Spring School: Topological Matter-Topological Insulators, Skyrmions and Majoranas, Jülich, Germany
   04. 04. 2017
4. **Pure Spin Currents in Compensated Rare Earth Iron Garnets**
   Invited Zernike Talk, Zernike Institute, University of Groningen, The Netherlands
   12. 04. 2017

Thomas Böhm

1. **Doping Dependence and Competing pairing channels in BKFA**
   Spring Meeting of the American Physical Society (APS), New Orleans, USA
   12. - 17. 03. 2017

Frank Deppe

1. **Continuous-Variable Propagating Quantum Microwaves**
   Invited Talk, Technical University of Vienna, Vienna, Austria
   07. 04. 2017
2. **Continuous-Variable Propagating Quantum Microwaves**
   Invited Talk, Kryoelektronische Bauelemente 2017, Bad Aibling, Germany
   08. 10. 2017
3. **Superconducting Circuit for Quantum Science and Technology**
   Invited Talk, Advanced Seminar on Condensed Matter Physics, Kirchhoff-Institute, University of Heidelberg, Heidelberg, Germany
   24. 11. 2017

Kirill Fedorov

1. **Finite-time Correlations of Balanced Two-Mode Squeezed Microwave Status**
   Spring Meeting of the DPG, Dresden, Germany
   19. - 24. 03. 2017
2. **Finite-time Correlations and Noise Tolerance of Two-Mode Squeezed Microwave States**
   Conference on Mesoscopic Transport and Quantum Coherence, Espoo, Finland
   04. - 09. 08. 2017
3. **Quantum Communication with Squeezed Microwaves**
   Invited Talk, NIM Conference on Resonator QED, Munich, Germany
   29. 08. - 01. 09. 2017

Rudolf Gross

1. **Low Temperature Physics: An Ongoing Success Story**
   Invited Talk, Humboldt Colloquium "Global Research in the 21^{st} Century", Washington D.C., USA.
   02 – 04 March 2017
2. **Superconducting Quantum Circuits for Science and Technology**
   Colloquium of SFB 668, University of Hamburg, Germany.
   05 July 2017
3. **Superconducting Quantum Circuits: Present Status and Future Prospects**
   Invited Talk, Colloquium on "Quantum Technologies in Electrical and Computer Engineering",

Department of Electrical and Computer Engineering, TU München, Germany.
18 July 2017

4. **Superconducting Quantum Circuits**
Tutorial Lecture Part I, Nanotechnology meets Quantum Information – NanoQI 2017, Palacio de Miramar, San Sebastian, Spain.
24 July 2017
5. **Superconducting Quantum Circuits**
Tutorial Lecture Part II, Nanotechnology meets Quantum Information – NanoQI 2017, Palacio de Miramar, San Sebastian, Spain.
25 July 2017
6. **PLD Grown Oxide Heterostructures for Spin Current Experiments**
Keynote Plenary Lecture, International Conference on Laser Deposition – iCOLD 2017, Chennai, India.
19 – 22 November 2017
7. **Superconducting Quantum Circuits: Science Meets Technology**
Colloquium, Indian Institute of Technology Madras, Chennai, India.
23 November 2017
8. **Superconducting Quantum Electronics: Science Pushes Technology**
Invited Talk, Workshop of the Collaborative Research Center on "Foundations and Applications of Quantum Science", Austrian Academy of Sciences, Vienna, Austria.
14 – 15 December 2017

Rudolf Hackl

1. **The Magnetic Phases of FeSe**
Invited Talk, 32. Workshop on Novel Materials and Superconductors, BSFZ Obertraun, Austria
08. 02. 2017
2. **Raman Study of Low-Energy Excitations in the Metallic Glass Ni67Zr33**
Spring Meeting of the American Physical Society (APS), New Orleans, USA
12. - 17. 03. 2017
3. **Light Scattering on Electronic and Magnetic Excitations in Unconventional Superconductors**
Invited Talk, International Symposium on Frontiers of Superconductivity Research (VII), Optical Spectroscopy on Unconventional Superconductors, Beijing, China
26. - 28. 10. 2017
4. **Magnetism and Fluctuations in FeSe**
Seminar Talk, Karlsruher Institut für Technologie, Karlsruhe, Germany
20. 11. 2017

Hans Hübl

1. **Hybrid Systems-Coupling Spins, Strings, and Transmon Qubits to superconducting resonators**
Seminar Talk, University of Melbourne, Melbourne, Australia
11. 04. 2017
2. **Circuit Nano-Electromechanics**
Seminar Talk, Centre for Quantum Computing and Communication Technology, University of New South Wales, Sydney, Australia
19. 04. 2017
3. **Circuit Nano-Electromechanics**
Seminar Talk, Karlsruher Institut für Technologie, Karlsruhe, Germany
08. 05. 2017
4. **Frequency Tuning and Coherent Dynamics of Nanostring Resonators**
Spring Meeting of the American Physical Society (APS), New Orleans, USA
14. 03. 2017
5. **Frequency Tuning and Coherent Dynamics of Nanostring Resonators**
Invited Talk, Spin Mechanics 4, Lake Louise, Canada
01. 03. 2017
6. **Frequency Tuning and Coherent Dynamics of Nanostring Resonators**

Invited Talk, Frontiers in Nanomechanics, La Thuile, Italy
06. 02. 2017

7. **Strings, Transmons, and Microwave Resonators**
Invited Talk, MagQSens Workshop, Barcelona, Spain
27. 03. 2017
8. **Controlling the Collective Coupling in Spin-Photon Hybrids**
Invited Talk, Optomagnonics, MPI des Lichts, Erlangen, Germany
28. 06. 2017
9. **Controlling the Collective Coupling in Spin-Photon Hybrids**
Invited Talk, SPICE Young Research Leaders Group Workshop, Insulator Spintronics, Mainz, Germany
01. 08. 2017
10. **Using Superconducting Circuits for Pulsed Electron Spin Resonance**
Invited Talk, SHARED-EPR Workshop, New Paltz, NY, USA
10. 10. 2017

Mark Kartsovnik

1. **Vladimir Laukhin's Milestones in the Physics of Organic Superconductors**
Plenary lecture, Workshop in honor of retiring Prof. Dr. V.N. Laukhin, Institute of Materials Science of Barcelona, Bellaterra, Spain
06. 10. 2017

Matthias Opel

1. **Static Magnetic Proximity Effects and Spin Hall Magnetoresistance in Collinear and Canted Ferrimagnetic Insulators**
Invited Talk, Séminaire Unité Mixte de Physique, Université Paris-Sud, Université Paris-Saclay, Palaiseau, France
03. 03. 2017
2. **Spin Hall Magnetoresistance (SMR) in Magnetic Insulators**
Invited Talk, Seminar at the Stanford Linear Accelerator Center, Stanford, USA
22. 06. 2017

Mathias Weiler

1. **Magneto-Acoustics**
Invited Talk, SAWtrain Summer School: Physics and Applications of GHz Vibrations, Cargése, France
12. 07. 2017
2. **Magnetization Dynamics in Magnetic Insulators in the Presence of Dipolar, Exchange and Dzyaloshinskii-Moriya Interactions**
Invited Talk, SPICE Young Research Group Leader Workshop, Mainz, Germany
31. 07. 2017
3. **Phase-Sensitive Detection of Inverse Spin Orbit Torques at Microwaves Frequencies**
Invited Talk, Magnonics 2017, Oxford, UK
09. 08. 2017
4. **Spin Dynamics in the Presence of Strong Spin-Orbit Interactions**
Invited Talk, MAINZ Seminar, University Mainz, Germany
24. 05. 2017
5. **Spin Dynamics in the Presence of Strong Spin-Orbit Interactions**
Invited Talk, University Innsbruck, Innsbruck, Austria
14. 06. 2017

Honors and Awards

Several members of Walther-Meißner-Institute were receiving honors and awards in 2017.

William E. Gifford Award

Kurt Uhlig of the Walther-Meißner-Institute received the prestigious ***William E. Gifford Award*** of the Cryogenic Society of America Inc. This award is named in honor of Mr. Gifford, co-inventor of the Gifford-McMahon cycle and founder of Cryomech, Inc. It is given to a recipient in academia or a government laboratory using a pulse tube or Gifford-McMahon cycle cryocooler as a key research component. The Gifford Award is given every odd-numbered year during the international Cryogenic Engineering Conference (CEC).

Kurt Uhlig received the William E. Gifford Award 2017 for his ground-breaking work in developing the world's first dry (cryogen free) dilution refrigerator using a 4 K pulse tube cryocooler. His subsequent R&D led to many innovations and improvements to dry dilution refrigerators and fostered the creation and growth of several manufacturers. As a brilliant experimentalist, his work has inspired the international cryogenics community. The prize has been presented to Kurt Uhlig during the 2017 Cryogenic Engineering Conference taking place at the Monona Terrace Community and Convention Center in Madison, Wisconsin, from 9-13 July 2017.

Kurt Uhlig with the William E. Gifford Award plaque.

WMI congratulates Kurt Uhlig on the award, recognizing his pioneering work which he performed at WMI in the development of dry dilution refrigerators. His ideas and technological developments completely changed the way of using dilution refrigerators. It finally resulted in push-button instruments easily usable for everybody. Needless to say that dry dilution refrigerator meanwhile have a world market share of above 90%.

Wilhelm und Else Heraeus Foundation Awards

Two PhD students of the Walther-Meißner-Institute were awarded for their excellent presentations given during the 633. WEH Workshop on *Spin Orbit Dynamics – Connecting Timescales from Nanoseconds to Femtoseconds* at Bad Honnef. **Hannes Maier-Flaig** received the ***Best Impulse Talk Prize*** while **Katrin Ganzhorn** received a ***Best Poster Prize***. We congratulate them on their awards, demonstrating the high quality of their research work as well as the high standard and creativeness of their presentations.

D ELSE HERAEUS-STIFTUNG

Certificate

Best Poster Prize for

Katrin Ganzhorn

Participant at the 633. WE-Heraeus-Seminar on

Spin Orbit Dynamics

Connecting timescales from nanoseconds to femtoseconds

January 4 - 6, 2017
at the Physikzentrum Bad Honnef (Germany)

Scientific Organization:
Dr. Mathias Weiler (Walther-Meißner-Institut, Garching, Germany)
Prof. Dr. Stefan Mathias (Universität Göttingen, Germany)
Dr. Tobias Kampfrath (Fritz-Haber Institut der MPG, Berlin, Germany)

Bad Honnef, January 2017

Prof. Dr. J. Treusch | Ursula Heraeus | Prof. Dr. J. Mlynek

The Wilhelm und Else Heraeus-Stiftung is a private foundation that supports research and education in science, especially in physics. German physicists recognize it as the most important private funding institution in their fields. Some activities of the foundation are carried out in cooperation with The German Physical Society (Deutsche Physikalische Gesellschaft).

D ELSE HERAEUS-STIFTUNG

Certificate

Best Impulse Talk Prize for

Hannes Maier-Flaig

Participant at the 633. WE-Heraeus-Seminar on

Spin Orbit Dynamics

Connecting timescales from nanoseconds to femtoseconds

January 4 - 6, 2017
at the Physikzentrum Bad Honnef (Germany)

Scientific Organization:
Dr. Mathias Weiler (Walther-Meißner-Institut, Garching, Germany)
Prof. Dr. Stefan Mathias (Universität Göttingen, Germany)
Dr. Tobias Kampfrath (Fritz-Haber Institut der MPG, Berlin, Germany)

Bad Honnef, January 2017

Prof. Dr. J. Treusch | Ursula Heraeus | Prof. Dr. J. Mlynek

The Wilhelm und Else Heraeus-Stiftung is a private foundation that supports research and education in science, especially in physics. German physicists recognize it as the most important private funding institution in their fields. Some activities of the foundation are carried out in cooperation with The German Physical Society (Deutsche Physikalische Gesellschaft).

Membership in Advisory Boards, Committees, etc.

1. **Frank Deppe** is associate member of the Cluster of Excellence *Nanosystems Initiative Munich (NIM)*.
2. **Andreas Erb** is spokesmen of the "Arbeitskreis Intermetallische und oxydische Systeme mit Spin- und Ladungskorrelationen" of the *Deutsche Gesellschaft für Kristallzüchtung und Kristallwachstum (DGKK)*.
3. **Rudolf Gross** is member of the Scientific Advisory Board of the Bayerisches Geoinstitut, Bayreuth, Germany.
4. **Rudolf Gross** is member of the Scientific Advisory Board of the Institut de Ciència de Materials de Barcelona, Spain.
5. **Rudolf Gross** is member of the committee for the allocation of Alexander von Humboldt Foundation Research Awards.
6. **Rudolf Gross** is spokesman of the selection committee of the Stern-Gerlach-Medal of the German Physical Society.
7. **Rudolf Gross** is member of the Appointment and Tenure Board of the Technical University of Munich.
8. **Rudolf Gross** is member of the Executive Board of the Cluster of Excellence *Nanosystems Initiative Munich (NIM)* and coordinator of the Research Area 1 on *Quantum Nanosystems*.
9. **Rudolf Gross** is member of the *Munich Quantum Center (MQC)*.
10. **Rudolf Gross** is course leader at the Ferienakademie of the Universities Munich (TU), Stuttgart and Erlangen-Nürnberg since 2005.
11. **Rudolf Hackl** is deputy coordinator of the DFG Priority Program SPP 1458 on *High Temperature Superconductivity in the Iron Pnictides*.
12. **Rudolf Hackl** is member of the evaluation board of the neutron source Heinz Maier-Leibnitz (FRM II).
13. **Hans Hübl** is member and principal investigator of the Cluster of Excellence *Nanosystems Initiative Munich (NIM)*.
14. **Hans Hübl** is member of the *Munich Quantum Center (MQC)*.
15. **Mark Kartsovnik** is member of the Selection Committee of EMFL (European Magnetic Field Laboratories).
16. **Mark Kartsovnik** is member of the International Advisory Committee of the 11^{th} International Symposium on Crystalline Organic Metals Superconductors and Ferromagnets (ISCOM 2017).
17. **Matthias Opel** is one of the four elected members of the Speaker Council for the scientists of the Bavarian Academy of Sciences and Humanities.
18. **Matthias Opel** was member of the International Advisory Committee of the EMN (Energy, Materials, Nanotechnology) Meetings, Las Vegas, USA.
19. **Mathias Weiler** is member of the Editorial Review Board of IEEE Magnetics Letters.

TUM Appointment and Tenure Board

Rudolf Gross is member of the Appointment and Tenure Board (ATB) of the Technical University of Munich (TUM) since meanwhile 5 years and thereby contributes to the success of the «***TUM Faculty Tenure Track***» program.

To maintain a leading position in the competition for the best brains, the TUM – uniquely in Germany – offers promising young scientists from around the world attractive career perspectives with its new career model ***"TUM Faculty Tenure Track"***. Highly qualified candidates are appointed as assistant professors (W2) with prospects for performance-based advancement to a permanent professorship (associate professor, W3). With further research achievements at the highest international level, this path can lead to promotion to a chair position (full professor, W3). Since 2012, TUM has hired 85 tenure track professors. In total, 100 of such positions will be filled until 2020 within the TUM program ***«TUM 100»*** as part of the German Excellence Initiative.

The new TUM hiring system builds on a professional appointment and evaluation process. After a careful evaluation of candidates by committees on the faculty level and external expert, the TUM-ATB takes over as a university-wide board, providing additional quality assurance and guaranteeing university-wide evaluation and quality standards. It formulates written recommendations for new hirings or tenure track decisions to the TUM Board of Management.

The TUM Appointment and Tenure Board (from left): Eckehard Steinbach, Wolfgang Wall, Roland Fischer, Thomas Hofmann, Andreas S. Schulz, Susanne Albers, Arne Skerra, Arthur Konnerth, Gero Friesecke, Rudolf Gross (©Astrid Eckert).

The TUM-ATB has 12 members, including the TUM Vive President for Research and Innovation as its chairman. Ten TUM-ATB members are experienced TUM professors with outstanding scientific profile covering the fields of Natural Sciences & Mathematics, Humanities & Business Studies, Engineering & Computer Sciences, as well as Medicine & Life Sciences. They are supported by a scientific member of the Max Planck Society. The present members of the TUM-ATB are:

- Chairman:
  - Thomas Hofmann (WZW)
- Members/*Deputy Members*:
  - Natural Sciences & Mathematics: Rudolf Gross (PH)/*Axel Haase (PH)*, Roland Fischer (CH)/*Horst Kessler (CH, EoE)*, Gero Friesecke (MA)/*Barbara Wohlmuth (MA)*
  - Humanities & Business Studies: Andreas S. Schulz (WI)/*Kristina Reiss (EDU)*
  - Engineering & Computer Sciences: Nikolaus A. Adams (MW)/*Wolfgang Wall (MW)*, Gerhard Kramer (EI)/*Eckehard Steinbach (EI)*, Susanne Albers (IN)/*Isabell M. Welpe (WI)*, Jörg Drewes (BGU)/*Arne Skerra (WZW)*
  - Medicine & Life Sciences: Markus Schwaiger (ME)/*Arthur Konnerth (ME)*, Chris-Carolin Schön (WZW)/*Claus Schwechheimer (WZW)*
- External member:
  - Petra Schwille (MPI of Biochemistry)/*Reinhard Genzel (MPI of Extraterrestrial Physics)*

Teaching

Lectures, Courses and other Teaching Activities

Several members of the Walther-Meißner-Institute give lectures and seminars at the Technical University of Munich.

Matthias Althammer

WS 2016/2017
- Magnetismus (Magnetism)
- Übungen zu Magnetismus (Magnetism, Problem Sessions)
- Seminar: Spin Caloritronics and Spin Pumping (with H. Huebl, M. Weiler)
- Seminar: Advances in Solid-State Physics (with R. Gross, H. Hübl, A. Marx, M. Opel)
- Seminar: Modern Topics in Magneto and Spin Electronics (with H. Hübl, M. S. Brandt, M. Weiler)

SS 2017
- Seminar: Spin Caloritronics and Spin Pumping (with H. Hübl, M. Weiler)
- Spin Electronics
- Übungen zu Spin Electronics (Exercises to Spin Electronics)
- Seminar: Modern Topics in Magneto and Spin Electronics (with M. Brandt, H. Hübl, M. Weiler)
- Seminar: Advances in Solid-State Physics (with R. Gross, H. Hübl, A. Marx, M. Opel, M. Weiler)

WS 2017/2018
- Seminar: Spin Caloritronics and Spin Pumping (with H. Hübl, M. Weiler)
- Seminar: Advances in Solid-State Physics (with R. Gross, H. Hübl, A. Marx, M. Opel, M. Weiler)
- Seminar: Modern Topics in Magneto and Spin Electronics (with H. Hübl, M. S. Brandt, M. Weiler)

Frank Deppe

WS 2016/2017
- Seminar: Superconducting Quantum Circuits (with R. Gross, A. Marx, K. Fedorov)

SS 2017
- Seminar: Superconducting Quantum Circuits (with R. Gross, A. Marx, K. Fedorov)

WS 2017/2018
- Seminar: Superconducting Quantum Circuits (with R. Gross, A. Marx, K. Fedorov)

Dietrich Einzel

WS 2016/2017
- Mathematische Methoden der Physik I (Mathematical Methods of Physics I)
- Übungen zu Mathematische Methoden der Physik I (Mathematical Methods of Physics I, Problem Sessions)

SS 2017
- Mathematische Methoden der Physik II (Mathematical Methods of Physics II)
- Übungen zu Mathematische Methoden der Physik II (Mathematical Methods of Physics II, Problem Sessions)

WS 2017/2018
- Mathematische Methoden der Physik I (Mathematical Methods of Physics I)
- Übungen zu Mathematische Methoden der Physik I (Mathematical Methods of Physics I, Problem Sessions)

Kirill Fedorov

SS 2016/2017
- WMI Seminar on Modern Topics of Low Temperature Solid State Physics (with R. Gross, R. Hackl, A. Marx, M. Opel)

SS 2017
- Angewandte Supraleitung: Josephson Effekte, supraleitende Elektronik und supraleitende Quantenschaltkreise (Applied Superconductivity: Josephson Effects, Superconducting Electronics and Superconducting Quantum Circuits, with R. Gross)
- WMI Seminar on Modern Topics of Low Temperature Solid State Physics (with R. Gross, R. Hackl, A. Marx, M. Opel)

SS 2017/2018
- WMI Seminar on Modern Topics of Low Temperature Solid State Physics (with R. Gross, R. Hackl, A. Marx, M. Opel)

Rudolf Gross

WS 2016/2017
- Physik der Kondensierten Materie I (Condensed Matter Physics I)
- Übungen zu Physik der Kondensierten Materie I (Condensed Matter Physics I, Problem Sessions, with S. Geprägs)
- WMI Seminar on Modern Topics of Low Temperature Solid-State Physics (with R. Hackl, H. Hübl, A. Marx, M. Opel)
- Seminar: Advances in Solid-State Physics (with H. Hübl, A. Marx, M. Opel)
- Seminar: Superconducting Quantum Circuits (with F. Deppe, K. Fedorov, A. Marx)
- Festkörperkolloquium (Colloquium on Solid-State Physics, with D. Einzel)

SS 2017
- Physik der Kondensierten Materie II (Condensed Matter Physics II)
- Übungen zu Physik der Kondensierten Materie II (Condensed Matter Physics II, Problem Sessions, with S. Geprägs)
- Seminar: Advances in Solid-State Physics (with H. Hübl, A. Marx, M. Opel)
- WMI Seminar on Modern Topics of Low Temperature Solid-State Physics (with R. Hackl, H. Hübl, A. Marx, M. Opel)
- Seminar: Superconducting Quantum Circuits (with F. Deppe, K. Fedorov, A. Marx)
- Festkörperkolloquium (Colloquium on Solid-State Physics, with D. Einzel)
- Ferienakademie: Course 3 “Physics and Electronics in Everyday Life”

WS 2017/2018
- Physik der Kondensierten Materie I (Condensed Matter Physics I)
- Übungen zu Physik der Kondensierten Materie I (Condensed Matter Physics I, Problem Sessions, with S. Geprägs)
- WMI Seminar on Modern Topics of Low Temperature Solid-State Physics (with R. Hackl, H. Hübl, A. Marx, M. Opel)
- Seminar: Advances in Solid-State Physics (with H. Hübl, A. Marx, M. Opel)
- Seminar: Superconducting Quantum Circuits (with F. Deppe, K. Fedorov, A. Marx)
- Festkörperkolloquium (Colloquium on Solid-State Physics, with D. Einzel)

Rudi Hackl

WS 2016/2017
- WMI Seminar on Modern Topics of Low Temperature Solid-State Physics (with R. Gross, H. Hübl, A. Marx, M. Opel)

SS 2017
- WMI Seminar on Modern Topics of Low Temperature Solid-State Physics (with R. Gross, H. Hübl, A. Marx, M. Opel)

WS 2017/2018
- Supraleitung und Tieftemperaturphysik I (Superconductivity and Low Temperature Physics I)

- Übungen zu Supraleitung und Tieftemperaturphysik I (Superconductivity and Low Temperature Physics I, Problem Sessions)
- WMI Seminar on Modern Topics of Low Temperature Solid-State Physics (with R. Gross, H. Hübl, A. Marx, M. Opel)

Hans Hübl

WS 2016/2017
- Supraleitung und Tieftemperaturphysik I (Superconductivity and Low Temperature Physics I)
- Übungen zu Supraleitung und Tieftemperaturphysik I (Superconductivity and Low Temperature Physics I, Problem Sessions)
- Seminar: Spin Caloritronics and Spin Pumping (with M. Althammer, M. Weiler)
- Seminar: Advances in Solid-State Physics (with R. Gross, A. Marx, M. Opel)
- WMI Seminar on Modern Topics of Low Temperature Solid State Physics (with R. Gross, R. Hackl, A. Marx, M. Opel)
- Seminar: Modern Topics in Magneto and Spin Electronics (with M. S. Brandt, M. Althammer, M. Weiler, S. Geprägs)

SS 2017
- Supraleitung und Tieftemperaturphysik II (Superconductivity and Low Temperature Physics II)
- Übungen zu Supraleitung und Tieftemperaturphysik II (Superconductivity and Low Temperature Physics II, Problem Sessions)
- Seminar: Spin Caloritronics and Spin Pumping (with M. Althammer, M. Weiler)
- Seminar: Advances in Solid-State Physics (with R. Gross, A. Marx, M. Opel)
- WMI Seminar on Modern Topics of Low Temperature Solid State Physics (with R. Gross, R. Hackl, A. Marx, M. Opel)
- Seminar: Modern Topics in Magneto and Spin Electronics (with M. S. Brandt, M. Althammer, M. Weiler)

WS 2017/2018
- Seminar: Spin Caloritronics and Spin Pumping (with M. Althammer, M. Weiler)
- Seminar: Advances in Solid-State Physics (with R. Gross, A. Marx, M. Opel)
- WMI Seminar on Modern Topics of Low Temperature Solid State Physics (with R. Gross, R. Hackl, A. Marx, M. Opel)
- Seminar: Modern Topics in Magneto and Spin Electronics (with M. S. Brandt, M. Althammer, M. Weiler, S. Geprägs)

Mathias Weiler

WS 2016/2017
- Seminar: Spin Caloritronics and Spin Pumping (with M. Althammer, H. Hübl)
- Seminar: Modern Topics in Magneto and Spin Electronics (with M. Althammer, M. S. Brandt, S. Geprägs, H. Hübl)

SS 2017
- Seminar: Spin Caloritronics and Spin Pumping (with M. Althammer, H. Huebl)
- Seminar: Modern Topics in Magneto and Spin Electronics (with M. Althammer, M. S. Brandt, S. Geprägs, H. Hübl)

WS 2017/2018
- Magnetismus (Magnetism)
- Übungen zu Magnetismus (Magnetism, Problem Sessions)
- Seminar: Spin Caloritronics and Spin Pumping (with M. Althammer, H. Hübl)
- Seminar: Modern Topics in Magneto and Spin Electronics (with M. Althammer, M. S. Brandt, S. Geprägs, H. Hübl)

Seminars and Colloquia

A. Walther-Meißner-Seminar on Modern Topics in Low Temperature Physics WS 2016/2017, SS 2017 and WS 2017/2018

WS 2016/2017:

1. **Spin injection and tuneable spin-to-charge conversion at $LaAlO_3/SrTiO_3$ oxide interfaces**
   Dr. Hiroshi Naganuma, Unité Mixte de Physique, CNRS, Palaiseau, France
   04. 10. 2016
2. **Integrated optomechanics and linear optics quantum circuits**
   Prof. Dr. Menno Poot, Yale University, New Haven, Connecticut, USA
   19. 10. 2016
3. **Atomic layer deposition for spin electronic devices**
   Dr. Andy Thomas, IFW Dresden, Germany
   11. 11. 2016
4. **Spin dynamics and transport in complex oxides and heterostructures**
   Prof. Dr. Georg Schmidt, Martin-Luther-University Halle-Wittenberg, Halle, Germany
   18. 11. 2016
5. **Higgs mode and magnon interactions in 2D quantum antiferromagnets from Raman scattering**
   Simon Weidinger, Physik-Department, Technical University of Munich, Germany
   16. 12. 2016
6. **Models of light-matter interaction: Symmetries and Solutions**
   Dr. Daniel Braak, Institut für Physik, University of Augsburg, Germany
   19. 12. 2016
7. **Ultrafast Spintronics with Terahertz Radiation**
   Dr. Tobias Kampfrath, Fritz-Haber Institute, Berlin, Germany
   13. 01. 2017
8. **Microstructuring single-crystalline quantum materials**
   Dr. Toni Helm, Max-Planck-Institute for Chemical Physics of Solids, Dresden, Germany
   20. 01. 2017
9. **Magnon transport in spin textures**
   Dr. Helmut Schultheiss, Helmholtz-Zentrum Dresden-Rossendorf, Dresden, Germany
   27. 01. 2017
10. **Long-range mutual synchronization of spin Hall nano-oscillators**
    Dr. Ahmad Awad, University of Gothenburg, Göteborg, Sweden
    14. 02. 2017
11. **X-Ray and neutron scattering studies of iridate thin films**
    Dr. Dany Mannix, Institut Neél, CNRS Grenoble, France
    10. 03. 2017

SS 2017:

12. **Nonlinear effects and parametric amplification in thin NbN superconducting films**
    Daria Gusenkova, Quantum Metamaterial Lab, National University of Science and Technology "MISIS", Moscow, Russia
    27. 04. 2017
13. **Non-integer-spin magnonic excitations in untextured magnets**
    Dr. Akashdeep Kamra, Fachbereich Physik, University of Konstanz, Germany
    09. 06. 2017
14. **Growth and physical property studies of large area piezoelectric thin films**
    Prof. Dr. M.S. Ramachandra Rao, Department of Physics, Nano Functional Materials Technology Centre, IIT Madras, Chennai, India
    22. 06. 2017
15. **Point defects in GaSb studied by positron annihilation spectroscopy**
    Dr. Natalie Segercrantz, Department of Applied Physics, Aalto University, Finland

28. 07. 2017

16. **Microwave photonics: from ultrastrong coupling to scattering tomography**
Prof. Juan José García Ripoll, Instituto de Física Fundamental IFF-CSIC, Quantum Physics Department, Madrid, Spain
24. 08. 2017

WS 2017/2018:

17. **Quenching the stripes: ultrafast dynamics of emergent electronic and vibrational order**
Dr. Robert Kaindl, E.O. Lawrence Berkeley National Laboratory, Berkeley, USA
18. 10. 2017
18. **Growth of $GdBa_2Cu_3O_{7-\delta}$ films on hastelloy metal substrates**
Oleksiy Troshyn, Theva Dünnschichttechnik GmbH, Ismaning, Germany
20. 10. 2017
19. **Heat transport in insulating powder materials**
Matthias Demharter, Bayerisches Zentrum für Angewandte Energieforschung, Garching, Germany
10. 11. 2017
20. **A transmon quantum annealer: decomposing many-body ising constraints into pair interactions**
Dr. Martin Leib, University of Innsbruck, Innsbruck, Austria
14. 12. 2017
21. **Applications and readout of metallic magnetic calorimeters**
Priv.-Doz. Dr. Sebastian Kempf, University of Heidelberg, Heidelberg, Germany
19. 01. 2018

B. Seminar: Advances in Solid State Physics WS 2016/2017, SS 2017 and WS 2017/2018

WS 2016/2017:

1. **Preliminary discussion and assignment of topics**
R. Gross, Walther-Meißner-Institute
18. 10. 2016 and 25. 10. 2016
2. **Quasiparticle mass enhancement approaching optimal doping in a high-T_c superconductor**
Ulrike Zweck, Technical University of Munich
13. 12. 2016
3. **Superconducting spintronics**
Michael Renger, Technical University of Munich
20. 12. 2016
4. **Coherent coupling between a ferromagnetic magnon and a superconducting qubit**
Min-Xing Xu, Technical University of Munich
10. 01. 2017
5. **Detection of zeptojoule microwave pulses using electrothermal feedback in proximity-induced josephson junctions**
Patrick Schnierle, Technical University of Munich
17. 01. 2017
6. **Superconductivity above 100 K in single-layer FeSe-films on doped $SrTiO_3$**
Jan-Robin Scholz, Technical University of Munich
07. 02. 2017

SS 2017:

7. **Preliminary discussion and assignment of topics**
R. Gross, Walther-Meißner-Institute
25. 04. 2017 and 02. 05. 2017

8. **Tunnel junction thermometry down to millikelvin temperatures**
   Simon Mejia, Technical University of Munich
   23. 05. 2017
9. **Electron attraction mediated by Coulomb repulsion**
   Anne-Sophie Walter, Technical University of Munich
   30. 05. 2017
10. **Nanomechanical detection of the spin hall effect**
    Lukas Stelzer, Technical University of Munich
    20. 06. 2017
11. **Snell's law for spin waves**
    Zhang Wentao, Technical University of Munich
    27. 06. 2017
12. **Effective mass near the mott-insulator transition**
    Paul Weinbrenner, Technical University of Munich
    04. 07. 2017
13. **Finite-size effects of anisotropic magnetoresistance**
    Manuel Müller, Technical University of Munich
    11. 07. 2017
14. **Dynamics of simultaneously measured non-commuting observables**
    Ivan Verschueren, Technical University of Munich
    18. 07. 2017
15. **Solving systems of linear equations with a superconducting quantum processor**
    Alexander Ulanowski, Technical University of Munich
    25. 07. 2017

WS 2017/2018:

16. **Preliminary discussion and assignment of topics**
    R. Gross, Walther-Meißner-Institute
    17. 10. 2017 and 24. 10. 2017
17. **Demonstration of an ac Josephson junction laser**
    Lucas Hollender, Technical University of Munich
    05. 12. 2017

C. Seminar: Spin Caloritronics and Spin Pumping WS 2016/2017, SS 2017 and WS 2017/2018

WS 2016/2017:

1. **Preliminary discussion and assignment of topics**
   Mathias Weiler, Matthias Althammer, Stephan Geprägs, Hans Hübl, Walther-Meißner-Institute
   20. 10. 2016 and 27. 10. 2016
2. **Direct detection of pure ac spin current by X-ray pump-probe measurements**
   Johannes Gröbmeyer, Technical University of Munich
   19. 01. 2017

SS 2017:

3. **Preliminary discussion and assignment of topics**
   Mathias Weiler, Matthias Althammer, Stephan Geprägs, Hans Hübl, Walther-Meißner-Institute
   27. 04. 2017 and 04. 05. 2017
4. **Interface optimization for spin Hall magnetoresistance experiments**
   Saki Matsuura, Walther-Meißner-Institute
   01. 06. 2017

5. **Broadband magnetic resonance in Cu_2OSeO_3**
   Lukas Liensberger, Walther-Meißner-Institute
   08. 06. 2017
6. **Antiferromagnetic Spin Seebeck Effect**
   Ezra Nabila, Technical University of Munich
   29. 06. 2017
7. **Anisotropic tunneling magnetoresistance**
   Michaela Schleuder, Walther-Meißner-Institute
   06. 07. 2017
8. **Sensitive broadband magnetic resonance spectroscopy with magnetic field modulation**
   Jonathan Zerhoch, Walther-Meißner-Institute
   20. 07. 2017
9. **Spin dynamics in coupled YIG/Co heterostructures**
   Stefan Klingler, Walther-Meißner-Institute
   27. 07. 2017

WS 2017/2018:

10. **Preliminary discussion and assignment of topics**
    Mathias Weiler, Matthias Althammer, Stephan Geprägs, Hans Hübl, Walther-Meißner-Institute
    19. 10. 2017 and 26. 10. 2017
11. **Kittens on the rise**
    Natalie Segercrantz, Walther-Meißner-Institute
    16. 11. 2017
12. **Magnetoelasticity in nanostrings**
    Daniel Schwienbacher, Walther-Meißner-Institute
    23. 11. 2017
13. **Magnon-Phonon Coupling in Nanostructures**
    Thomas Luschmann, Walther-Meißner-Institute
    11. 01. 2018
14. **TBA**
    Luis Flacke, Walther-Meißner-Institute
    25. 01. 2018
15. **Non-local magnetoresistance**
    Birte Cöster, Walther-Meißner-Institute
    01. 02. 2018
16. **Thermoelectric and thermomagnetic effects**
    Nynke Vlietstra, Walther-Meißner-Institute
    01. 02. 2018

D. Seminar: Superconducting Quantum Circuits WS 2016/2017, SS 2017 and WS 2017/2018

WS 2016/2017:

1. **Preliminary discussion and assignment of topics**
   F. Deppe, A. Marx, R. Gross, Walther-Meißner-Institute
   18. 10. 2016 and 25. 10. 2016
2. **Single-shot read-out of a superconducting qubit using a Josephson parametric oscillator**
   Stefan Pogorzalek, Walther-Meißner-Institute
   22. 11. 2016
3. **A Schrödinger cat living in two boxes**
   Edwar Xie, Walther-Meißner-Institute
   29. 11. 2016

4. **Ultra-coherent nanomechanical resonators via soft clamping and dissipation dilution**
   Daniel Schwienbacher, Walther-Meißner-Institute
   06. 12. 2016
5. **Resolving magnon number states in quantum magnonics**
   Stefan Weichselbaumer, Walther-Meißner-Institute
   13. 12. 2016
6. **Extending the lifetime of a quantum bit with error correction in superconducting circuits**
   Jan Goetz, Walther-Meißner-Institute
   10. 01. 2017
7. **Superconducting Switch for Fast On-Chip Routing of Quantum Microwave Fields**
   Peter Eder, Walther-Meißner-Institute
   17. 01. 2017
8. **Imaging photon lattice states by scanning defect microscopy**
   Michael Fischer, Walther-Meißner-Institute
   24. 01. 2017
9. **Observation of strong radiation pressure forces from squeezed light on a mechanical resonator**
   Philip Schmidt, Walther-Meißner-Institute
   31. 01. 2017

SS 2017:

10. **Preliminary discussion and assignment of topics**
    F. Deppe, A. Marx, R. Gross, Walther-Meißner-Institute
    25. 04. 2017 and 02. 05. 2017
11. **Mid-term report on Master Thesis**
    Christian Besson, Technical University of Munich
    16. 05. 2017
12. **Enhanced qubit readout using locally generated squeezing and in-built Purcell-decay suppression**
    Stefan Binder, Technical University of Munich
    23. 05. 2017
13. **Nonreciprocal Microwave Signal Processing with a Field-Programmable Josephson Amplifier**
    Daniel Arweiler, Technical University of Munich
    30. 05. 2017
14. **Mid-term reports on Bachelor Theses**
    Stephan Trattnig & Stefan Binder, Technical University of Munich
    06. 06. 2017
15. **Faithful conversion of propagating quantum information to mechanical motion**
    Christoph Utschick, Technical University of Munich
    13. 06. 2017
16. **Experimental demonstration of a resonator-induced phase gate in a multiqubit circuit-QED system**
    Alexander Huber, Technical University of Munich
    20. 06. 2017
17. **Strong coupling cavity qed with gate-defined double quantum dots enabled by a high impedance resonator**
    Stephan Trattnig, Technical University of Munich
    27. 06. 2017
18. **Mid-term report on Master Thesis**
    Behdad Ghaffari, Technical University of Munich
    25. 07. 2017

WS 2017/2018:

19. **Preliminary discussion and assignment of topics**

F. Deppe, A. Marx, R. Gross, Walther-Meißner-Institute
17. 10. 2017 and 24. 10. 2017

20. **Approaching ultrastrong coupling in transmon circuit QED using a high impedance resonator**
Philip Schmidt, Walther-Meißner-Institute
19. 12. 2017
21. **Strain coupling of a mechanical resonator to a single quantum emitter in diamond**
Daniel Schwienbacher, Walther-Meißner-Institute
16. 01. 2018
22. **Converting quasiclassical states into arbitrary fock state superpositions in a superconducting circuit**
Edwar Xie, Walther-Meißner-Institut
23. 01. 2018
23. **Observation of a dissipative phase transition in a one-dimensional circuit QED lattice**
Michael Fischer, Walther-Meißner-Institute
30. 02. 2018
24. **Coherent Rabi dynamics of a superradiant spin ensemble in a microwave cavity**
Stefan Weichselbaumer, Walther-Meißner-Institute
06. 02. 2018
25. **Intracity quantum communication via thermal microwave networks**
Stefan Pogorzalek, Walther-Meißner-Institute
13. 02. 2018

E. Solid State Colloquium

The WMI has organized the Solid-State Colloquium of the Faculty of Physics in WS 2016/2017, SS 2017, and WS 2017/2018. The detailed program can be found on the WMI webpage: http://www.wmi.badw-muenchen.de/teaching/Seminars/fkkoll.html.

Staff

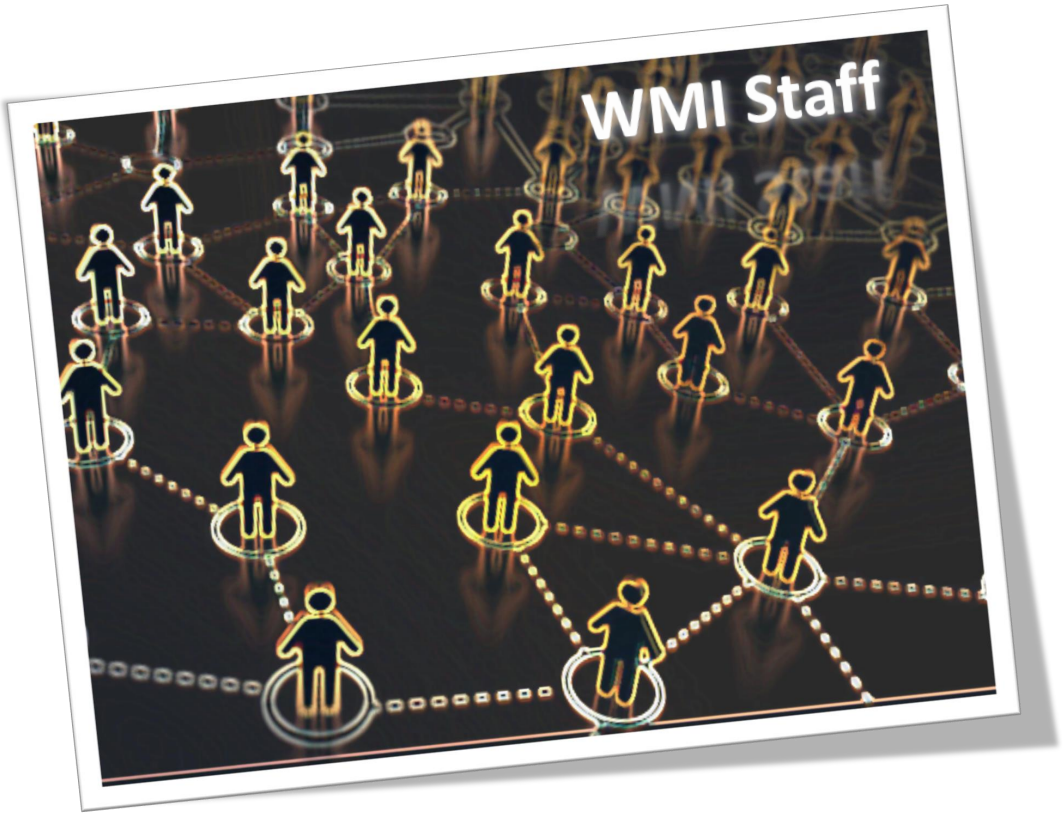

Staff of the Walther-Meißner-Institute

Director
Prof. Dr. Rudolf Gross

Deputy Director
Priv.-Doz. Dr. habil. Hans Hübl

Technical Director
Dr. Achim Marx

The deputy director, the technical director and the elected representative of the scientific staff (Dr. Matthias Opel) are members of the WMI Executive Committee and support the director in the management of WMI.

Administration/Secretary's Office
Ludwig Ossiander
Emel Dönertas

Scientific Staff
Dr. Matthias Althammer
Priv.-Doz. Dr. habil. Frank Deppe
Prof. Dr. Andreas Erb
Dr. Kirill Fedorov
Dr. Stephan Geprägs
Priv.-Doz. Dr. habil. Rudolf Hackl
Dr. Mark Kartsovnik
Dr. Matthias Opel
Dr. Natalie Segercrantz
Dr. Nynke Vlietstra
Dr. Mathias Weiler
Dipl.-Phys. Peter Eder
M. Sc. Michael Fischer
M. Sc. Daniel Jost
M. Sc. Stefan Klingler
M. Sc. Stefan Pogorzalek
M. Sc. Philip Schmidt
M. Sc. Daniel Schwienbacher
M. Sc. Stefan Weichselbaumer
M. Sc. Tobias Wimmer
M. Sc. Eduard Xie

Technical Staff
Peter Binkert
Thomas Brenninger, M.Sc.
Dieter Guratzsch
Astrid Habel
Karen Helm-Knapp
Dipl.-Ing. (FH) Josef Höss
Sebastian Kammerer
Christoph Kastl
Robert Müller
Jan Naundorf
Georg Nitschke
Christian Reichlmeier
Alexander Rössl
Andreas Russo
Harald Schwaiger
Helmut Thies

Assistants
Sybilla Plöderl
Maria Botta

Permanent Guests
Dr. Werner Biberacher
Prof. Dr. Dietrich Einzel
Prof. Dr. B.S. Chandrasekhar
Dr. Kurt Uhlig

Guest Researchers

1. Dr. Werner Biberacher
   permanent guest
2. Prof. Dr. B.S. Chandrasekhar
   permanent guest
3. Prof. Dr. Dietrich Einzel
   permanent guest
4. Dr. Kurt Uhlig
   permanent guest
5. Dr. Toni Helm, Max-Planck-Institut für Chemische Physik fester Stoffe, Dresden, Germany
   19. 01. - 22. 01. 2017
6. Dr. Ahmad Awad, University of Gothenburg, Göteborg, Sweden
   13. 02. - 17. 02. 2017
7. Dr. Nedad Lazarevic, University of Belgrade, Belgrade, Serbia
   17. 04. - 01. 05. 2017, 15. 07. - 01. 08. 2017, 10. 10. - 19. 10. 2017, 01. 12. - 10. 12. 2017
8. Prof. Vladimir Zverev, Institute of Solid Physics, Chernogolovka, Russia
   14. 05. - 05. 06. 2017
9. Dr. Brain Moritz, Stanford Institute of Materials and Energy Science (SIMES), Stanford University, Stanford, USA
   22. 05. - 17. 06. 2017
10. Dr. Akashdeep Kamra, University of Konstanz, Germany
    06. 06. - 11. 06. 2017
11. Prof. Dr. M.S. Ramachandra Rao, Materials Science Research Centre, IIT Madras, Chennai, India
    18. 06. - 24. 06. 2017
12. Dr. Tomas Ramos, Instituto de Fisica Fundamental, Madrid, Spain
    23. 08. - 31. 08. 2017
13. Prof. Juan Jose Garcia Ripoll, Instituto de Fisica Fundamental, Madrid, Spain
    23. 08. - 25. 08. 2017
14. MSc. Ana Milosavljevic, University of Belgrade, Belgrade, Serbia
    10. 10. - 19. 10. 2017
15. Prof. Enrique Solano, Instituto de Fisica Fundamental, Madrid, Spain
    16. 10. - 20. 10. 2017
16. Dr. Mike Sanz, Instituto de Fisica Fundamental, Madrid, Spain
    16. 10. - 20. 10. 2017
17. Adrian Parra, Instituto de Fisica Fundamental, Madrid, Spain
    16. 10. - 20. 10. 2017
18. Prof. Zoran Popovic, University of Belgrade, Belgrade, Serbia
    01. 12. - 10. 12. 2017

Scientific Advisory Board & Executive Committee

Scientific Advisory Board

According to the statutes of the Bavarian Academy of Sciences and Humanities (BAdW) the Scientific Advisory Board evaluates the quality of the scientific work of Walther-Meißner-Institute (WMI) and gives advice to its Executive Committee to provide scientific quality assurance. The Scientific Advisory Board regularly reports to the Research Committee of BAdW.

The members of the Scientific Advisory Board include members of BAdW with appropriate scientific background, representatives of the two Munich universities (TUM and LMU), as well as leading national and international scientists. They are appointed by the Section III "Naturwissenschaften, Mathematik, Technikwissenschaften" of BAdW for five years. The director of WMI is a consultive member of the WMI Scientific Advisory Board. The Scientific Advisory Board is headed by a chairperson and deputy chairperson. They are elected by the Section III "Naturwissenschaften, Mathematik, Technikwissenschaften" of BAdW for five years at the suggestion of the members of the WMI Scientific Advisory Board. The chairperson of the Scientific Advisory Board must be a member of BAdW.

The present members of the WMI Scientific Advisory Board are:

- **Vollhardt, Dieter**, chairman (BAdW, University of Augsburg)
- **Abstreiter, Gerhard**, deputy chairman (BAdW, Technical University of Munich)
- **Bloch, Immanuel** (LMU Munich and Max-Planck-Institute of Quantum Optics)
- **Bühler-Paschen, Silke** (Technical University of Vienna)
- **Finley, Jonathan** (Technical University of Munich)
- **Gross, Rudolf**, consultive member (BAdW, Technical University of Munich)
- **Hänsch, Theodor** (BAdW, LMU Munich and Max-Planck-Institute of Quantum Optics)
- **Schwoerer, Markus** (BAdW, University of Bayreuth)
- **Wallraff, Andreas** (ETH Zurich)
- **Weiss, Dieter** (University of Regensburg)
- **Zinth, Wolfgang** (BAdW, LMU Munich)

Executive Committee

The Walther-Meißner-Institute is headed by the scientific director who is responsible for the development and implementation of the research program. He holds a full professor position at one of the Munich universities (TUM or LMU). He is appointed in a joint process of the respective university and BAdW. The director is supported by the deputy director, the technical director and an elected representative of the scientific staff. They are appointed by the Section III "Naturwissenschaften, Mathematik, Technikwissenschaften" of BAdW for five years at the suggestion of the members of the WMI Scientific Advisory Board.

The present members of the WMI Executive Committee are:

- **Gross, Rudolf**, director
- **Hübl, Hans**, deputy director
- **Marx, Achim**, technical director
- **Opel, Matthias**, representative of the scientific staff

Contact:

Walther–Meißner–Institut
Bayerische Akademie der Wissenschaften
Walther–Meißner–Str. 8
D - 85748 Garching
GERMANY

Phone: +49 – (0)89 289 14201
Fax: +49 – (0)89 289 14206
E–mail: Sekretariat@wmi.badw.de

www.wmi.badw.de

Published by:

Walther–Meißner–Institut
Walther–Meißner–Str. 8, D - 85748 Garching
December 2017